SYNERGISTIC TRIPLE COMBINATION OF siRNAs TO KNOCKDOWN KEY GROWTH FACTORS AND RECEPTORS THAT REGULATE CORNEAL HAZE IN RABBITS

By

SRINIWAS SRIRAM

A DISSERTATION PRESENTED TO THE GRADUATE SCHOOL
OF THE UNIVERSITY OF FLORIDA IN PARTIAL FULFILLMENT
OF THE REQUIREMENTS FOR THE DEGREE OF
DOCTOR OF PHILOSOPHY

UNIVERSITY OF FLORIDA

2013

To Mom and Dad

ACKNOWLEDGMENTS

I thank the chair and members of my supervisory committee for their mentoring, The National Eye Institute and the Department of Defense for its financial support, and my parents for the love and support they have provided me.

TABLE OF CONTENTS

page

LIST OF TABLES

LIST OF FIGURES

LIST OF ABBREVIATIONS

CTGF	Connective tissue growth factor
DAPI	4',6-diamidino-2-phenylindole, a fluorescent stain that can be used to stain both live and fixed cells
DMEM	Dulbecco's Modified Eagle Medium, a cell culture medium
ELISA	Enzyme-linked immune-adsorbent assay, an assay for quantifying the presence of a particular protein.
GAPDH	Glyceraldehyde 3-phosphate dehydrogenase, used as a housekeeping gene in Reverse transcription polymerase chain reaction
PRK	Photoreactive Keratectomy, one of many methods for reshaping the cornea with an excimer laser.
RbCF	Rabbit corneal fibroblasts
siRNA	Short interfering RNA, a class of double stranded RNA, 20-25 base pairs in length that interferes with the expression of specific genes with complimentary nucleotide sequence.
TGFB1	Transforming growth factor beta-1
TGFBR2	Transforming growth factor beta receptor 2

Abstract of Dissertation Presented to the Graduate School
of the University of Florida in Partial Fulfillment of the
Requirements for the Degree of Doctor of Philosophy

SYNERGISTIC TRIPLE COMBINATION OF siRNAs TO KNOCKDOWN KEY GROWTH FACTORS AND RECEPTORS THAT REGULATE CORNEAL HAZE IN RABBITS

By

Sriniwas Sriram

December 2013

Chair: Benjamin Keselowsky
Co-chair: Gregory Schultz
Major: Biomedical Engineering

Purpose

The Transforming Growth Factor β1 (TGFB1), TGFB receptor (TGFBR2) and Connective Tissue Growth Factor (CTGF) are key regulators of fibrosis in the cornea and in other tissues, including liver, skin and kidney. In this study, an anti-fibrotic drug targeting these three critical scarring genes was developed using a synergistic combination of siRNAs, and its effect on downstream scarring genes, Collagen-I (Col-I) and alpha smooth muscle actin (SMA) was assessed in rabbit corneal fibroblasts (RbCFs). The efficacy of this synergistic triple siRNA combination was tested for its effects on reducing alpha smooth muscle actin (SMA) and corneal scarring (haze) in *ex vivo* organ cultured corneas and *in vivo* in rabbits.

Methods

Initially for *in vitro* experiments, up to six individual siRNAs for each of the three-target gene mRNAs were transfected into cultures of RbCFs at concentrations from 15 to 90nM. The knock down of target gene proteins were measured by ELISA and the two most effective siRNAs were tested in dual combinations. Knockdown percentages of

both individual and dual siRNA combinations were analyzed for synergy using Combination Index to predict ‘effective’ and ‘ineffective’ triple siRNA combinations. Effects of both triple siRNA combinations on target and downstream mRNAs were measured using qRT-PCR and levels of SMA protein were assessed by immunohistochemistry.

In *ex vivo* experiments, the central 6 mm diameter region of fresh rabbit globes was ablated to a depth of 155 microns with an excimer laser. Corneas were excised, cultured at the air-liquid interface in defined culture medium supplemented with TGFB1, and treated with either 1% prednisone acetate or with 22.5 μM cationic histidine-lysine nanoparticles complexed with the effective triple siRNA combination. Scar formation was measured using image analysis of digital images and levels of smooth muscle actin (SMA) were assessed in ablated region of corneas using qRT-PCR and immunostaining.

Finally in animals, two different scarring models were utilized to assess the effects of the triple siRNA combination on corneal scarring. In the first model, rabbit corneas were unevenly ablated creating a mesh pattern then treated immediately with the triple siRNA combination. After 1 day the ablated areas of corneas were collected and levels of mRNAs for TGFB1, TGFBR2 and CTGF were measured. After 14 days, levels of mRNA for SMA were measured and SMA protein immunolocalized in frozen sections. In the second model, rabbit corneas were uniformly ablated to a depth of 155 microns followed by three daily doses of the triple combination of siRNA. After 14 days, corneas were photographed and images were analyzed using ImageJ software to assess corneal scarring. Corneas were also analyzed for levels of SMA mRNA.

Results

Single and dual siRNA combinations in *in vitro* experiments produced a wide range of protein knockdown of target genes (5% to 80%). The effective triple siRNA significantly reduced mRNA levels of target genes (>80%) and downstream scarring genes (>85%), and SMA protein (>95%), and significantly reduced cell migration without reducing cell viability.

Excimer ablated *ex vivo* cultured corneas developed intense haze-like scar in the wounded areas and levels of mRNAs for pro-fibrotic genes were significantly elevated 3 to 8 fold in wounded tissue compared to unablated corneas. Treatment with NP-siRNA or steroid significantly reduced quantitative haze levels by 55% and 68%, respectively, and reduced SMA mRNA and immunohistostaining.

In the first *in vivo* therapeutic experiment with a single siRNA dose, two of three rabbits showed substantial reductions of all three target genes after 1 day with a maximum knock down of 80% of TGFB1, 50% reduction of TGFBR2 and 40% reduction of CTGF mRNA levels and reduced SMA mRNA at day 14. In the second *in vivo* therapeutic experiment with multiple doses of siRNA treatment, both rabbits showed a ~22% reduction in scar formation at day 14 as calculated by image analysis. There was also a corresponding 70% and 60% reduction of SMA RNA expression.

Conclusion

These results demonstrate that simultaneous targeting of TGFB1, TGFBR2, and CTGF genes by the effective triple siRNA combination produced high knock down of target and downstream scarring genes *in vitro*. Furthermore, treatment of the effective triple siRNA combination on *in vivo* and *ex vivo* excimer ablated rabbit corneas reduced

levels of SMA, leading to reduced corneal scarring at 14 days. The *ex vivo* corneal culture system also reproduced key molecular patterns of corneal scarring and haze formation generated in rabbits. The results from this study pave the way towards developing a multi-target approach for the reduction of corneal haze and perhaps of other scarring processes affecting the body.

CHAPTER 1
INTRODUCTION

Molecular Mechanism of Corneal Scarring

Corneal scarring remains a serious complication that can ultimately lead to functional vision loss. The Transforming growth factor beta1 (TGFB1) system, has emerged as a key component of the fibrogenic response to wounding by regulating the transformation of quiescent corneal keratocytes into activated fibroblasts that synthesize ECM and into myofibroblasts that contract corneal matrix (C. Chen et al. 2000; Jester, Petroll, and Cavanagh 1999) (Blalock et al. 2003; Grotendorst 1997; Massague 1990). The TGFB1 system has also been implicated in regular scarring of other fibrotic tissues like lung (Westergren-Thorsson et al. 1993), liver (Perkett 1995), kidney (Border et al. 1992), skin (Bullard et al. 1997) and pancreas (Vogelmann et al. 2001) that are correlated with increased expression of type I and type III collagen, integrins, SMA and fibronectin (C. Chen et al. 2000; Penn, Grobbelaar, and Rolfe 2012).

Connective tissue growth factor (CTGF is upregulated in both fibroblasts and epithelium after corneal wound healing (Blalock et al. 2003). Although it participates in the regulation of diverse biological processes related to growth and development, the overexpression of CTGF is correlated with severe fibrotic disorders, including fibrosis in skin, kidney, liver, lung, and vasculature. CTGF was initially identified as a growth factor, then classified as a matricellular protein, and most recently appreciated as a matrix component (Grotendorst 1997). CTGF acting as a downstream mediator of TGFB1 down-regulates synthesis of corneal crystallin proteins in quiescent keratocytes and up-regulates synthesis of collagen, converting them into activated corneal fibroblasts. Furthermore, CTGF directly stimulates transformation of activated

fibroblasts into myofibroblasts, which are filled with alpha smooth muscle actin that forms microfilaments that are the major source of light scattering in corneal scars (Blalock et al. 2003) (Ivarsen, Laurberg, and Møller-Pedersen 2003; Møller-Pedersen 2004; Tiemann and Rossi 2009). Keratocytes also transform into myofibroblasts under the influence of TGFB1. (Desmoulière et al. 1993) (Jester et al. 1996; Sasaki et al. 1996) Thus, the excessive scattering of light that is clinically described as corneal scar and haze results from the combination of collagen laid down in irregular pattern in the wound and opaque activated fibroblasts and myofibroblasts that no longer synthesize the corneal crystallin proteins that keep their cytoplasm transparent .

Current Treatments

There currently are no FDA approved drugs that selectively reduce the expression of genes causing corneal scarring and haze. Mitomycin C is used during some ocular surgeries, but it may have very damaging side effects, including death of endothelial cells (Sihota, Sharma, and Agarwal 1998), stromal melting, and conjunctival thinning (la Fuente, Seijo, and Alonso 2008; Raviv et al. 2000; Tong et al. 2007). They have also shown to block TGFB-induced cell proliferation and myofibroblast differentiation in cultured quiescent keratocytes while altering the transcriptional regulation of macrophage chemotactic protein-1 (MCP-1) and alpha smooth muscle actin (αSMA). Overall these findings suggest that there may be long-term and perhaps permanent consequences to the application of MMC as an anti-fibrotic therapy (Jester, Nien, et al. 2012). Anti- inflammatory steroids have also been used as potential anti-fibrotic agents. Steroids have been demonstrated to reduce cell proliferation *in vitro* and stromal collagen synthesis in rabbit refractive surgery models (Nien et al. 2011).

However, additional investigations have found that the efficacy of steroids appears to vary with the method and timing(Sarchahi et al. 2011) of application (Aras et al. 1998).

Thus, there is a need for an effective anti-scarring drug that can be given topically and specifically targets fibrotic genes while also avoiding non-specific serious side effects that threaten vision.

Significance and Impact

The number of patients with complaints of corneal scarring has increased with the increasing population of patients who have undergone refractive surgical procedures. Vision-impairing corneal scarring following injuries caused by trauma, surgery, or infection remains a major clinical problem, accounting for 1.6 million new cases of blindness each year, an additional 2.3 million with bilateral low vision, and 19 million with monocular blindness (Weichel et al. 2008). The public health implications of disabling haze are potentially great especially since no drugs have been FDA approved to effectively reduce corneal scarring because of the risk of serious side effects. Most of the patients seeking refractive surgery now are young to middle-aged, and in 30 to 40 years a certain percentage can be anticipated to develop cataracts or age-related macular changes (Maguire 1994). There are an estimated 20 million refractive surgical procedures performed worldwide each year, mainly consisting of LASIK surgery for myopia. Refractive laser operations have been shown to result in visual problems in darkness, where 38% were classified as mild, while 5% were so serious that patients were unable to drive in darkness (Bull 2008; Fan-Paul et al. 2002). With the population over age 55 expected to increase by 82% between 1980 and 2030, and over 1 million refractive surgical procedures currently performed each year in the United States,

keratorefractive surgery may become an important public health issue (Fan-Paul et al. 2002).

Another important cause for corneal scarring cases are the blast and burn injuries to the eye caused by explosions during combat operations or terrorist attacks that have become increasingly common in modern warfare. The incidence of ocular injuries had increased during combat from 0.6% during the Civil War of 1860–1864 to 13% during Operation Desert Storm in 1991 (Weichel et al. 2008). A study by Heier et al. (Heier et al. 1993) of trauma at a CSH during Operation Desert Shield and Desert Storm showed that ocular injury and/or disease accounted for 14% of all visits to the emergency department. Of these, corneal foreign bodies (17%), ocular burns (13%) and traumatic iritis (7%) were the most common injuries treated. Traumatic blast and burn injuries to the cornea also occur in the civilian population as a result of accidents. Furthermore, it is an unfortunate reality that civilians remain at risk for attacks by domestic and foreign terrorists. Thus, the development of drugs that reduce corneal scarring would find broad and frequent use in treating the numerous corneal injuries.

Since TGFB1 and CTGF are responsible for stimulating scarring in these refractive surgery procedures, the drugs developed in this research project for traumatic corneal wounds would also have direct application in these elective surgical procedures. Also, because scarring in the skin also is regulated by TGFB1 and CTGF systems, these agents would have enormous potential commercial value for plastic and reconstructive surgery applications.

RNA Interference

Post-transcriptional gene silencing (PTGS) is the phenomenon by which introduction of double-stranded RNA (dsRNA) into a diverse range of organisms and

cell types causes degradation of the complementary mRNA (Fire 1999). When the dsRNA is exogenous, the RNA is imported directly into the cytoplasm and cleaved in to short fragments of 20–25 base pairs with a 2-nucleotide overhang at the 3' end by the endoribonuclease Dicer (Bernstein et al. 2001). These short double stranded fragments are called short interfering RNAs (siRNAs), consisting of a guide strand that is perfectly complementary to a target mRNA and a passenger strand (Tiemann and Rossi 2009). These siRNAs are then separated into single stands and incorporated into one or more of the Argonaute proteins in RNA induced silencing complex (RISC), where the guide RNA strand serves as a sequence specific guide for complementary base pairing with the target (Dirk Grimm 2010; Hammond et al. 2001). The target mRNA is then cleaved leading to its subsequent knockdown (Mario Stevenson 2004). The basic schematic of RNA interference is given in Figure 1-1.

There are many advantages of siRNA-based therapy that makes the technology so desirable. Firstly, it has been shown that have a high degree of specificity and gene silencing efficiency (Campochiaro 2006). Recent studies have also shown that molecules less than 30bp in length are generally believed to avoid induction of interferon (IFN) pathways {Kim:2005fz}{Angaji:2010um}. These inherent advantages of RNAi make it a more viable method of altering gene expression than other methods.

Targeting Cell Signaling Pathways with a Multi Component Approach

Most of the published literature on siRNAs have employed a single target system (TGFB1 or CTGF) to reduce fibrosis in liver (Li et al. 2006), skin, kidney and eye (Sugioka et al. 2010). There has not been a multi target siRNA approach in the field of scarring. Multi-target approaches can interrupt or act on the signaling network at multiple points and affect the cell in ways that an individual component cannot. There

are a lot of benefits in targeting three growth factors, especially since each growth factor apart from having its own distinct roles may also be dependent on other growth factors. For example, not only does TGFB1 auto-induce itself, it also combines with TGFBR2 to stimulate the expression of CTGF, which has been shown to up regulate the expression of SMA and Collagen-I. TGFB1 has been show to stimulate the transition of keratocytes to myofibroblasts that are characterized by the production of SMA. Additionally, TGFB1 promotes fibroblast cell proliferation and migration but retards epithelial cell migration. It is difficult to obtain an effect by employing a single target in a complex signaling pathway where the action of one growth factor can be compensated by another. An approach aimed at multiple targets can potentially be more efficacious and less vulnerable to acquired resistance as the system is less able to compensate for the action of two or more drugs simultaneously (Borisy et al. 2003; Keith, Borisy, and Stockwell 2005).

A number of diseases including cancer and infectious diseases have been successfully treated using multi-component therapies (Keith, Borisy, and Stockwell 2005). Separate targets are affected simultaneously by the individual components to create a combination effect. The targets can occupy the same or separate pathways within an individual cell, or even in separate tissues. In combination, the two drugs may produce a result different from the activity of the individual components. This can be attributed to the fact that the components when used in combination can interrupt or act on the complex signaling networks at multiple points, and affect the cell in ways that the individual components cannot. Since, the action of one component can be affected by

the presence of the other component it may be beneficial to systematically screen combinations for potential synergy (Borisy et al. 2003).

siRNA Delivery

siRNA interacts with membrane proteins, and are taken up by the cell through the cell membrane by generally penetrating into a classic endosomal vesicle, and this vesicle is delivered into the cytoplasm (Resnier et al. 2013). siRNAs cannot be injected in systemic circulation as these nucleic acids are rapidly degraded by plasmatic nucleases. Hence, the encapsulation of siRNA into a delivery system serves to enhance their cellular penetration and delivery into cytoplasm by protecting them from nucleases. Specific tissues or cell types can be selectively targeted using cell type-specific affinity ligands such as antibodies, peptides or aptamers. Finally, the carrier also stabilizes the siRNA to enable sufficient circulation half-life. Although, viral vectors act as efficient delivery systems they can potentially induce accidental gene expression changes following integration to host genome or induce toxic responses. Hence, a safer option would be to use the non-viral delivery system if efficient delivery of exogenous siRNA to the cytoplasm can be achieved (Shim and Kwon 2010).

siRNA can be delivered either exogenously to cells, or expressed endogenously via plasmid transfection or viral siRNA expression vectors. The types of target tissues and cells dictate the optimum administration routes of local versus systemic delivery. For example, siRNA can be directly applied to the eye, skin or muscle via local delivery, whereas systemic siRNA delivery is the only way to reach metastatic and hematological cancer cells. Local delivery offers several advantages over systemic delivery, such as low effective doses, simple formulation, low risk of inducing systemic side effects and facilitated site-specific delivery (Dykxhoorn and Lieberman 2006). Therefore, for drug

delivery to the eye, a more cost-efficient strategy for siRNA delivery would be the local delivery method.

Cationic Polymers

Since, siRNAs are negatively charged and readily bind to cationic molecules, delivery carriers usually consist of cationic polymers, peptides or liposomes that form complex by ionic interactions (Zimmermann et al. 2006). The resulting complex facilitates cellular uptake via the endocytic pathway, providing excellent protection of siRNAs from nuclease attack. Lipid based transfection reagents are the most common approach for nucleic acid delivery to cells in vitro. The cationic lipids in these reagents provide a suitable platform for incorporating the negatively charged siRNA. However, cationic lipid based reagents are considered too toxic for systemic siRNA delivery *in vivo* (Peer et al. 2008). In addition to its toxicity, liposome based transfection reagents are very sensitive to serum in cell culture media, thus require a complicated transfection procedure and are not suitable for high throughput studies. In this study, Mirus TransIT – TKO transfection reagent, a non-liposomal cationic proprietary polymer/lipid formulation, was used for all the transfections *in vitro* experiments.

Similar to liposomes, cationic polymers can also serve as efficient transfection reagents because they can bind and condense nucleic acids into stabilized nanoparticles. Polyethyleneimine (PEI) is a synthetic polymer that has been used in branched or linear forms of different lengths for nucleic acid delivery both locally as well as systemically (Shim and Kwon 2010). However, there is significant concern regarding toxicity of nanoparticles formed from siRNA and unmodified PEI with high molecular masses (e.g., 25 kDa) and doses (Kircheis et al. 2001).

Polylysine was one of the earliest carriers of nucleic acids (Perales et al. 1994). Although these initial studies were promising, the use of polylysine as a carrier was associated with cytotoxicity including complement activation. As yet, unmodified polylysine carriers have not been effective carriers of siRNA but various modifications of the polylysine carriers have yielded effective delivery systems for siRNA (Plank et al. 1996). One such modification that increases the ability of lysine-rich peptides to transport nucleic acids is the addition (or incorporation) of histidines with the lysine peptide.

Endosomal Escape

Once delivered to the right tissue or the right cell, another obstacle that has to be overcome with siRNA delivery systems is the endosome. The siRNAs need to be delivered to the cytoplasm to be effective and most of the delivery systems which use receptor mediated endocytosis or even pinocytosis result in endosomal internalization and eventually elimination via the Golgi network (Figure 1-2). Escape from the endosome is therefore a critical factor for efficient therapeutic applications (Resnier et al. 2013). A few approaches have been made trying to tackle this issue. Some polymers are designed to escape the endosome by the so-called ‘proton-sponge effect’ and direct membrane interaction of polycation and sulphoglucanes which enhances the escape (Russ et al. 2008). Receptor ligands that could also be used as delivery vehicle can be expressed with His-tags that enable the protein–siRNA complex to escape the endosome (Tarwadi et al. 2008). Viruses such as adenoviruses escape the endosome through their ability to lyse lipid bilayer membranes at a certain pH, which is present in the sorting endosome (Wickham et al. 1994). Hence, the endosome escape remains a critical factor for RNAi therapeutics and needs to be carefully addressed (Figure 1-1)

In case of HK polymers, it has been reported that, while lysine is important for binding DNA/RNA, histidine has an important role in buffering acidic endosomes, thereby leading to endosomal disruption and release of nucleic acid (Midoux and Monsigny 1999). Histidines may also have a role in stabilizing the nanoparticle. Furthermore, specific ratios and patterns of histidine and lysine have been found to augment the siRNA delivery (Q. R. Chen et al. 2001). It has also been recently demonstrated that reducible histidine-lysine peptides of lower molecular weight are effective carriers of siRNA (Leng et al. 2009; Mark Stevenson et al. 2008).

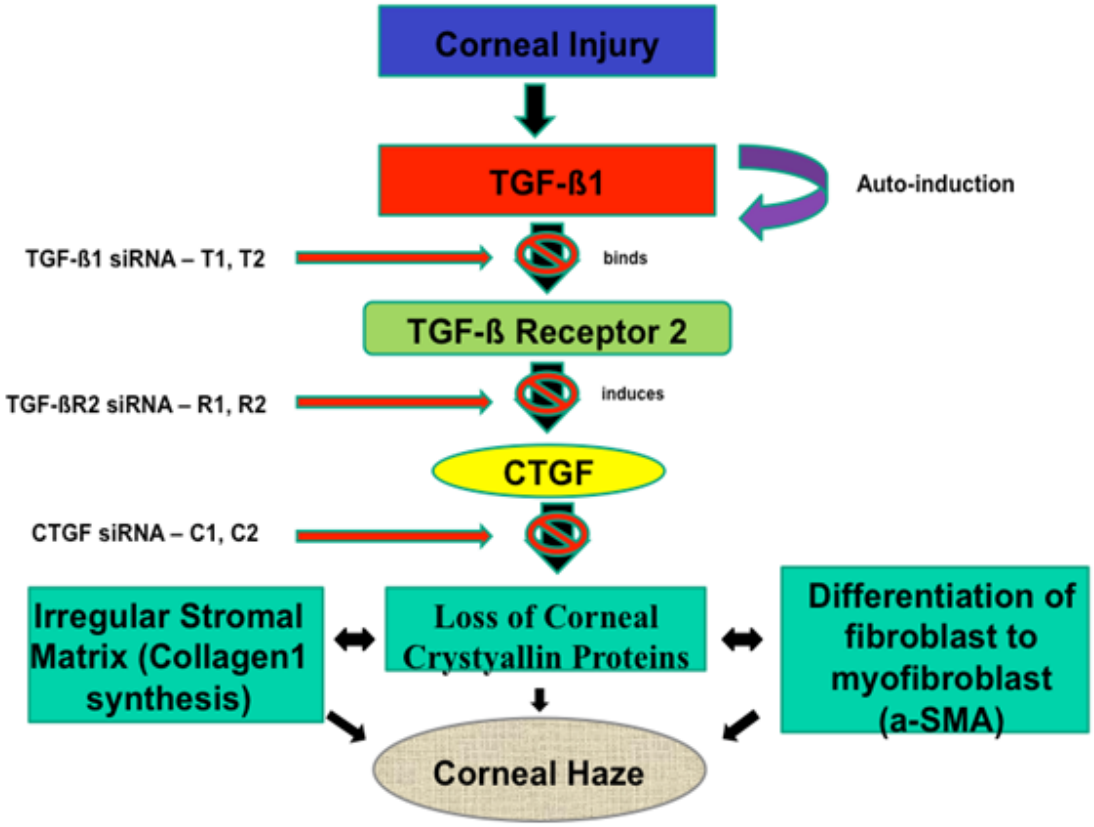

Figure 1-1. Signaling pathway in corneal fibrosis.

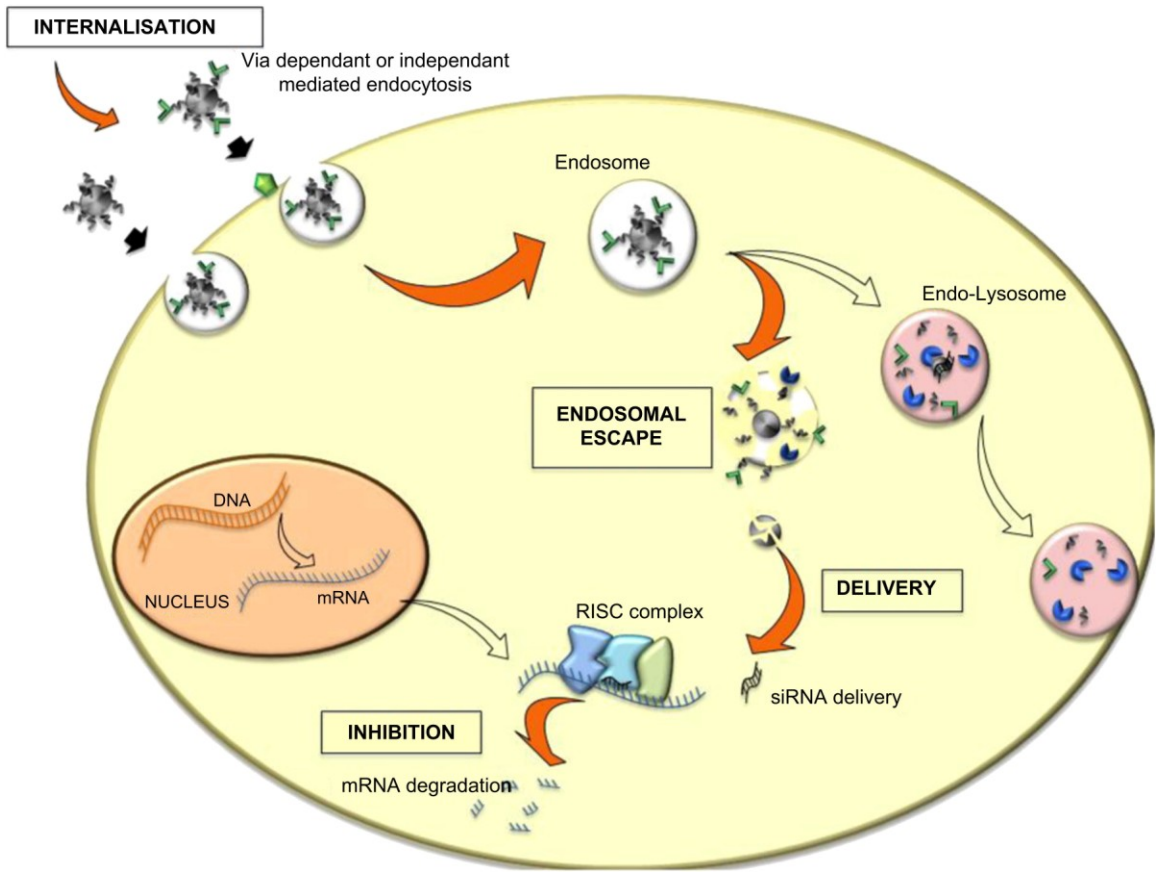

Figure 1-2. Intracellular trafficking of siRNA delivery systems. Two modalities are observed in this phenomenon, a receptor mediated endocytosis and a non-receptor mediated endocytosis. In all these cases, delivery systems are entrapped into endosomal vesicles. These vesicles fuse with lysosome and inevitably lead to siRNA degradation. To avoid this, delivery systems need to escape the endosomal vesicles. Finally, siRNA is delivered into the cytoplasm and produces their inhibitor effect. Source - (Resnier et al. 2013)

CHAPTER 2
GENERATION OF A TRIPLE siRNA COMBINATION AND EVALUATION OF ITS *IN VITRO* EFFICACY

Purpose

To develop an anti-fibrotic treatment targeting three critical scarring genes using a combination of siRNAs and assess its effect on downstream scarring genes, Collagen-I (Col-I) and alpha smooth muscle actin (SMA.

Background

In an injured cornea, a complex signaling cascade of molecular events is initiated by transforming growth factor beta (TGFB1), which binds to the transforming growth factor receptor II (TGFBR2) and induces the synthesis of connective tissue growth factor (CTGF). Addition of neutralizing antibodies to CTGF to cultures of TGFB1stimulated corneal fibroblasts blocked the synthesis of collagen and SMA, indicating that CTGF is the major mediator of TGFB effects on collagen synthesis by corneal fibroblasts. (Desmoulière et al. 1993; Polsky, Armstrong, and Chou 1991) Thus, these *in vitro* data support our hypothesis that the TGFB1/TGFBR2/CTGF system is the major regulator of corneal wound healing and that RNAi agents that selectively inhibit these key genes would reduce formation of corneal scar and haze.

Alternative strategies such as antibodies (Mead 2003) and antisense oligonucleotides (ASOs) (Cordeiro et al. 2003) have also been used to block the TGFB1pathway. Since, ASOs do not harness a naturally existing endogenous gene silencing pathway, its effect relies on achieving a high enough concentration in the target tissues over a prolonged period of time so that a sufficient fraction of target mRNA will be recognized. Hence in practice, to achieve the required tissue concentration, patients are given multiple doses. By contrast, siRNAs harnesses an

endogenous and catalytic gene silencing mechanism, which means that once it has been delivered, they are efficiently recognized and stably incorporated into the RISC to achieve prolonged gene silencing (Tiemann and Rossi 2009). Also, use of ASOs can induce an interferon response in some patients. Though mammalian cells are exquisitely sensitive to the introduction of dsRNA, molecules less than 30bp in length are generally believed to avoid induction of interferon (IFN) pathways (Angaji et al. 2010; Kim et al. 2005).

Monoclonal antibody based therapies can lead to the production of auto-antibodies against the antigen binding domain of a monoclonal antibody or the constant region of a non-humanized mouse monoclonal antibody. Other challenges for topical monoclonal antibody therapies to reduce corneal scarring is the very short life time of monoclonal antibodies in tears of patients, which requires multiple doses a day to reduce TGFB1protein in tears. Hence, a RNA interference based approach has many advantages when compared to ASOs or monoclonal antibodies in the treatment of scar formation following injury, surgery or infection.

In this study, we have developed a RNA interference-based treatment to reduce corneal haze by targeting three critical scarring genes – TGFB1, TGFBR2 and CTGF. The RNAi pathway begins with exogenous double stranded RNA (dsRNA) being processed by the RNAse III family member Dicer into small interfering RNA (siRNA) molecules that are 20-25 nucleotides long. (Bagasra and Prilliman 2004) The resulting siRNA is incorporated into the multi-protein complex called RNA-induced silencing complex (RISC) with the degradation of the sense strand of the double-stranded RNA. (Leuschner et al. 2006) The resulting siRNA recognizes the target mRNAs with

sequence complementarity, which is then cleaved by Argonaute 2, within the RISC complex. (Scherer and Rossi 2003)

It is often difficult to achieve a significant therapeutic effect by employing a one-target, one-drug paradigm on such a complex, multi-factorial, amplifying, signaling pathway. Hence, using a multi-target approach that can interrupt a complex, amplifying, signaling network at multiple points should be able to affect the cell in ways that an individual component cannot. In 1983, Chou and Talaly developed the combination index (CI) calculation that can quantify potential synergism or antagonism when two or more drug treatments are combined. (Chou and Talalay 1983; Chou 2006)

In the field of anti-fibrotic research, there have been recent papers published on using multiple siRNAs that target a single mRNA gene target (Matsumoto, Niimi, and Kohyama 2012) or combining siRNA treatment with other drugs. (Zhang et al. 2011) However, there have been no reports of combining multiple siRNAs that target different genes within the same pathway to reduce corneal scarring. We hypothesize that simultaneously targeting three key scarring genes within the same major wound-healing pathway - TGFB1, TGFBR2 and CTGF, would have a cascade effect on reducing the expressions of downstream mediators such as collagen-I and α-smooth muscle actin (SMA) in corneal scarring. Since this wound healing pathway plays a dominant role in wound healing in other tissues, this triple combination of siRNAs may also effectively reduce scarring in other organs including skin, kidney, liver and lung.

Materials and Methods

Cell Culture

Cultures of rabbit corneal fibroblasts (RbCF) were established by outgrowth from rabbit whole eyes, as described previously. (P. M. Robinson et al. 2012; Woost et al.

1992) Briefly, epithelial and endothelial cells were removed from corneas, the stroma was cut into cubes of approximately 1 mm^3, placed in culture medium consisting of equal parts Dulbecco's Modified Eagle Medium (DMEM), with 4.5g/L glucose and 1g/L L-glutamine. Medium was supplemented with 10% heat-inactivated normal calf serum and antibiotic-antimycotic cocktail (Life Technologies, Carlsbad, CA). Cell from cultures between passages 2 and 5 were used for all experiments. To increase the expression of TGFB1, TGFBR2 and CTGF, RbCF were placed in serum-free media for 48 hours, and then the medium was replaced by 8ug/ml of estradiol (Sigma, St. Louis, MO) and 4ng/mL of TGFB1(R&D Systems, Minneapolis, MN) in DMEM. The cells were dosed twice with the estradiol before transfection of the siRNA and then once after. (Takahashi et al. 1994; Wira 2002)

Protein Concentration

Protein levels for all three proteins (TGF- beta1, CTGF and TGF – beta R2) were measured using capture sandwich enzyme-linked immunosorbent assay (ELISA). The levels of TGF-beta1 were determined using the TGF-beta1 ELISA kit from (R&D systems Minneapolis, MN). The assay was performed following the manufacturer's recommended procedure. The level of CTGF protein was analyzed using the CTGF polyclonal antibodies from US biological (Swapscott, MA), following our previously published procedure. (Chou and Martin 2005; P. M. Robinson et al. 2012) TGF- beta R2 levels were determined using the same procedure as the CTGF protein except the capture and detection antibodies were TGF – beta R2 antibodies (R&D systems Minneapolis, MN). Knockdown percentages were calculated by comparing the protein levels of the treated samples to the samples treated with the scrambled siRNA.

Reverse Transcription–Polymerase Chain Reaction

Total RNA was extracted using the Qiagen RNeasy mini isolation kit (Qiagen, Inc., Valencia, CA) and used according to the manufacturer's directions. cDNA was synthesized using the High Capacity cDNA Reverse Transcription Kit (Applied Biosytems, Carlsbad, CA) according to manufacturer's procedure. The level of mRNA for TGFB1, CTGF, TGFBR2, SMA, collagen II, and 18S ribosomal RNA were determined using the Real-Time PCR TaqMan assay. The primers and probes for each gene are described in Table 2-3. The endogenous control, ribosoma18S RNA, was used normalize target genes. Primers, probes and cDNA were combined with TaqMan Universal PCR Master Mix (Applied Biosytems, Carlsbad, CA) and amplification was performed by the Applied Biosystems 7300HT Fast Real Time PCR System. The thermal cycling conditions were as follows: 2 min at 50°C, 10 min at 95°C, 40 cycles of 15 sec at 95°C, and 1 min at 60°C. The relative gene expression of the growth factors was calculated using the 2-ΔΔCt method.

***In Vitro* Knockdown Experiments**

siRNAs targeting the rabbit mRNA sequences of TGFB1, CTGF and TGFBR2 were purchased from Dharmacon (Dharmacon Products, Thermo Fisher Scientific, Lafayette, CO) (Table 2-1). RbCF were transfected with individual siRNA sequences (15nM, 30nM, 60nM and 90nM) using *Trans*IT-TKO® Transfection Reagent (Mirus, Madison, WI) following the manufacturer's instructions. A transfection optimization experiment was performed to ensure maximal transfection of the siRNAs. Six hours after transfection, the medium was changed to full serum growth medium and then it was changed back to serum free medium 24 hours post-transfection.

For the dual siRNA combination transfection, the siRNAs targeting TGFB1(designated T1 and T2), TGFBR2 (designated R1 and R2) and CTGF (C1 and C2) were added at 30 nM for a final combined concentration of 60 nM. For the triple combination, the siRNAs were added at 30 nM for a final combined concentration of 90 nM. A commercially available scrambled siRNA sequence purchased from Dharmacon was used as the negative control. Forty-eight hours after transfection, protein or total RNA samples were collected. Cell lysates were collected with the addition of phosphate buffered saline solution (PBS) supplemented with 0.1% Triton® X-100 with protease inhibitors cocktail III (Calbiochem, Darmstadt, Germany) with the addition of 0.5mM EDTA. The RNA samples were stabilized using an RNAlater RNA Stabilization Reagent (Qiagen, Inc., Valencia, CA). The samples were frozen at -20^{o}C until further use.

Synergism and Generation of Triple siRNA Combination

Combination Index (CI) is a numerical parameter to quantify the degree of synergism between siRNA sequences. At the extremes, synergism is CI = 0 to 1 and antagonism is CI = 1 to infinity. It is given by the following equation. (C. Chen et al. 2000; Chou and Hayball 1996; Chou 2006; Jester, Petroll, and Cavanagh 1999)

$$\frac{(D)_1}{(Dm)_1[f_a/(1-f_a)]^{1/m1}} + \frac{(D)_2}{(Dm)_2[f_a/(1-f_a)]^{1/m2}}$$

f_a – is the fraction affected by siRNA sequences (1/100 * knockdown %)

D – individual concentration of the drug in the combination

Dm – individual drug dose that inhibits system by m %

m – coefficient signifying the shape of the dose-effect relationship

All the data analysis for synergism was performed using the software Compusyn. (Chou and Martin 2005; Westergren-Thorsson et al. 1993)

For each target growth factor, two individual siRNA sequences were tested which led to a total of 8 different dual combinations for each growth factor. The Compusyn software was then used to compute CI values for each combination, which would give the synergy of individual siRNA sequences within dual combinations at 60 nM. The CI values of 24 different combinations were processed to find two dual combinations with maximal synergy for each growth factor that was made up of the same individual siRNA sequences (Table 2-2). These individual siRNA sequences were then combined to generate a triple siRNA combination and were deemed to be 'effective' as they have maximal synergy in knocking down their respective growth factors in the presence of the other two siRNA sequences. The same methodology was repeated again to generate an 'ineffective' triple siRNA combination whose sequences were identified to have poor synergy among the individual siRNA sequences, These two triple siRNA combinations – 'Effective' and 'Ineffective' were further tested in *in vitro* knockdown experiments to confirm their potency.

Cell Viability and Migration Assays

Forty-eight hours after treatment with the siRNAs, cell viability was assessed by MTS assay using Cell Titer 96 Aqueous One Solution Reagent (Promega Corp, Madison, WI) following manufacturer's protocol. Relative absorbance was determined by comparing untreated cells to the siRNA treated cells. For the migration assay, RadiusTM Cell Migration Plate (Cell Biolabs, San Diego, CA) was used according to manufacturer's protocol. Images were taken at 10x magnification and analyzed using Adobe Photoshop.

Immunohistochemistry

To stain for SMA, the siRNA transfection experiment was conducted on a glass slide with four chambers (HLab-Tek, Hatfield, PA). Forty-eight hours after transfection, the chambers were removed, and the cells were fixed in 4% paraformaldehyde for 10 minutes. The slides were then treated with methanol for 15 minutes at -20^{o}C and blocked in goat serum for 1 hour. Finally, they were incubated with SMA antibody-Cy3 (Sigma) for 1hour. The cells were mounted with DAPI and imaged using *in vitro* confocal microscope. ImageJ software was used for analyzing the images.

Image Analysis by ImageJ and Adobe Photoshop

ImageJ software was used for analyzing the images. Briefly, the image was split into its respective red and blue channels. A constant color threshold of 25-255 was set for all the red channel images, which was used for measuring the area of staining. The number of cells stained with DAPI was counted in the blue channel image using a constant color threshold of 18-87 and a size value from 8 to infinity. The percentage area of cells stained with SMA was then normalized to the number of cells in each corresponding image. This value was then used to calculate the reduction in SMA in the treated images with respect to the untreated controls.

For the image analysis in migration assay, Photoshop was used to analyze the images. The magic wand feature was used to carefully select and measure the percent area of cells. This value was used as a measure of the migration of cells.

Statistical Analysis

All experiments were performed in triplicate and all statistical analyses were conducted using GraphPad prism (San Diego, CA). Student's t test or Analyses of Variances (ANOVA) with Tukey's post-hoc assessments were accordingly used to test

for significance between the groups. Results were considered statistically significant where $p<0.05$.

Results

Dual siRNA Combination

Since the TGF-β pathway is a key mediator of the fibrotic response to corneal wounding, we designed and tested a series of individual siRNA sequences targeting three key scarring genes involved in this pathway (Figure 2-1). The goal of these experiments was to identify two effective siRNAs for each of the three targets that were capable of knocking down their expression. Following that, we evaluated the effect of different dual combinations of these siRNA sequences on rabbit corneal fibroblasts following stimulation with TGFB1and estradiol. Figure 1 represents the knockdown efficiency of all possible dual siRNA combinations that can be obtained by combining three individual siRNA sequences – T1, R2 and C1. The knockdown percentages of both single and dual siRNA combinations were then used in combination index calculations to predict a triple siRNA combination with optimal synergism among its individual sequences.

The combination of TGFB1 siRNA-1 and CTGF siRNA-2 (T1C2) produced a ~60% knockdown of TGF- beta1 protein and 79% of CTGF protein (Figure 2-2A & 2-2C). Greater than 75% of TGF- beta R2 protein was reduced when the TGFB1 siRNA-1 and TGFBR2-siRNA-2 (T1R2) were combined. Interestingly, there was a reduction of only ~37% of TGF-beta1 protein in this combination (Figure 2-2A & 2-2B). The combination TGFBR2-siRNA-2 and CTGF siRNA-1 (C1R2) produced a ~58% reduction of CTGF protein and a reduction of ~65% of TGF-beta R2 (Figure 2-2B & 2-2C). A knockdown of CTGF protein of ~60% was observed by combining TGF-beta1 siRNA 1

with CTGF siRNAs -1 (T1C1) while the TGF-beta1 protein knockdown was ~44% (Figure 2-2A & 2-2C). In some cases, we observed negative interaction between specific pairs of siRNAs. For example, TGFBR2 siRNA R2 led to 60% reduction in TGF-beta R2 receptor in combination with CTGF siRNA1 (C1), but less than 10% reduction in the same protein when combined with CTGF siRNA2 (C2). Similarly, CTGF knockdown by siRNA1 (C1) was reduced in combination with TGF-B1 receptor siRNA1 (R1). We believe the reason for this negative interaction may be because of a competition for critical RNAi components like the RISC complex or the preference of Ago2 for a certain configured dsRNA over another as was reported in other experiments. (Castanotto et al. 2007; Dirk Grimm 2010)

Synergism and Generation of a Triple siRNA Combination

For each target growth factor, two individual siRNA sequences were tested which led to a total of 8 different dual combinations for each growth factor. The Compusyn software was then used to compute CI values for each combination, which gave the synergy of the individual siRNA sequences within dual combinations at 60 nM. At the extremes, synergism is defined as CI = 0 to 1 and antagonism is CI = 1 to infinity. Analyzing the computed CI values of 24 different dual combinations, the sequences T1, C1 and R2 were finalized for the 'Effective' siRNA triple combination. This was because the dual combinations involving these siRNA sequences had the maximum synergy based on the computed CI values. Similarly, an 'ineffective' siRNA triple combination was finalized with the sequences T2, C2 and R1 respectively (Table 2-2). It is noteworthy, that each of the individual siRNAs in the low synergy combination was effective against its intended target when used alone (Figure 2-1).

Knockdown of Target Growth Factors by the Effective Triple Combination (T1R2C1)

At a total concentration of 90 nM, the effective combination of TGFB1siRNA1, TGFBR2 siRNA-2 and CTGF siRNA-1 (T1R2C1) resulted in ~80% knockdown in the expression of the three target growth factors: TGFB1, TGFBR2 and CTGF (Figure 2-3A, 2-2B & 2-2C). The knockdown percentages for the triple siRNA combination did not increase linearly with concentration of the treatment. The knockdown percentages were calculated relative to transduction with a scrambled siRNA control and all expression levels were normalized to 18S rRNA. The toxicity of the treatment was tested by adding increasing concentrations (90 nM to 180 nM) of the effective siRNA triple combination (T1R2C1) to low passage cultures of RbCF. There was no significant reduction in the cell viability at a final concentration of 90 nM, indicating minimal toxicity (Figure 2-3D). However, when compared to cells which were not treated with siRNA, there was a 10% decrease in cell viability when the total siRNA concentration was180 nM. It should be noted, that delivery of 180 nM siRNA required twice the level of moderately toxic transfection reagent. Therefore, we conclude that the reduction in levels of target proteins and mRNAs was not caused by the general toxicity of the siRNAs. Therefore, optimal knockdown of target mRNAs without cytotoxicity was achieved at 90 nM siRNA concentration.

The Effective Triple Combination (T1R2C1) is More Potent than Its Corresponding Individual siRNAs and the Ineffective Triple Combination (T2R1C2)

Since the effective triple combination was efficient at reducing the target mRNAs, we next wanted to test the efficacy of this combination on the downstream targets of the TGF-β pathway, which are collagen and SMA. At a total siRNA concentration of 90 nM, the effective triple combination (T1R2C1) was efficient in reducing the mRNA

expression of collagen-I and SMA by ~80% while individual siRNA sequences at 90 nM were able to achieve a maximum knockdown of only ~60% (Figure 2-4A & 2-2B).

At a concentration of 90 nM, the effective triple combination (T1R2C1) also significantly gave a higher knockdown of both the target and downstream mediators when compared to the ineffective triple combination (T2R1C2). The ineffective combination was especially poor (~20%) in reducing the expression of SMA when compared to the high reduction percentage of ~80% by the effective (Figure 2-4C). The knockdown percentages were calculated with respect to a scrambled siRNA control and normalized to 18S rRNA.

The Effective Triple Combination (T1R2C1) Is More Effective In Knocking Down Protein Expression of SMA than the Ineffective Triple Combination (T2R1C2)

To confirm the protein level knockdown of downstream mediators, immunohistostaining for SMA was performed. The RbCF were treated with TGFB1and estradiol to stimulate the expression of SMA. The effect of both effective (Figure 2-5A) and ineffective triple combinations (Figure 2-5B) was compared to the control, which was transfected with a scrambled siRNA (Figure 2-5C). There was dramatic reduction of SMA protein staining when treated with the effective triple combination while the effect of ineffective triple combination was less evident. Image analysis on 12 random images taken from 4 different wells show that the effective triple combination gave a significantly higher reduction of SMA protein staining (~98%) when compared to the ineffective triple combination (~55%)(Figure 2-5D). The percentage area of cells stained with SMA was normalized to the number of cells in each corresponding image. The SMA reduction percentage in the treated images was calculated with respect to the untreated controls.

The Effective Triple Combination (T1R2C1) Inhibits Migration of Rabbit Corneal Fibroblasts

A migration assay was performed to assess the functional effect of the effective triple siRNA combination. RbCF were cultured in 6 well plates provided from the Radius® cell migration kit. After growing it to confluence, a circular region in the middle of the well was removed using a gel removal solution. The migration of cells were imaged (Figure 2-6A to 2-2D) and measured by image analysis using Photoshop. Measured at two days after injury, the effective triple combination (T1R2C1) significantly inhibited the migration of cells into the cell-free area. The percentage of cells that migrates was calculated digitally from the three replicates was used as a measure of migration (Figure 2-6C). Linear regression analysis on data from the first three days (R squared value – 0.8828) was used to predict the time required for complete closure in siRNA treated wells as approximately 4 days, which is twice that of untreated cells.

Discussion

Corneal wound healing is a complex process in which a variety of cytokines, growth factors, and proteases interact to regulate key phases of corneal healing. However, the TGF-β system has emerged as a key component of the fibrogenic response to wounding by regulating the transformation of quiescent corneal keratocytes into activated fibroblasts that synthesize ECM and into myofibroblasts that contract corneal matrix. (C. Chen et al. 2000; Jester, Petroll, and Cavanagh 1999) The TGF-β system has also been implicated in regular scarring of other fibrotic tissues like lung (Border et al. 1992; Westergren-Thorsson et al. 1993), liver (Bullard et al. 1997; Perkett 1995), kidney (Border et al. 1992; Vogelmann et al. 2001), skin (C. Chen et al. 2000; Penn, Grobbelaar, and Rolfe 2012) and pancreas (Abreu et al. 2002; Vogelmann et al.

2001) that are correlated with increased expression of type I and type III collagen, integrins, SMA and fibronectin. (C. Chen et al. 2000; Penn, Grobbelaar, and Rolfe 2012) Apart from scarring, both TGFB1and CTGF have roles in angiogenesis (Abreu et al. 2002), glaucoma (Zee, Langert, and Stubbs 2012) and proliferative diabetic retinopathy (Hatanaka et al. 2012),

Since, TGFB1, TGFBR2 and CTGF are involved in the scarring mechanism of most fibrotic tissues, the system in this study with a multi-target approach can potentially be modified to regulate scarring in different tissues of the body. The significance of such a system is intensified by fact that there are currently no FDA approved drugs to regulate scar formation in any part of the body.

Most of the published literature on siRNAs have employed a single target system to reduce fibrosis in eye (Sugioka et al. 2010), skin, kidney and liver (Li et al. 2006). We previously developed gene specific approaches for single targets using ribozymes and ASOs targeting TGFB1or CTGF. (Blalock et al. 2004; P. M. Robinson et al. 2012) While they were effective *in vitro* – ribozymes tend to be larger and less stable that siRNAs and ASOs tend to be less potent than siRNAs. Though multiple targets in TGF-β system have been targeted in combination (Zhao et al. 2013), there has not been a multi- gene siRNA approach in the field of corneal scarring. Multi-target approaches can interrupt the signaling network at several points and affect the corneal fibroblast in ways that reducing the expression of an individual component cannot. Delivery of multiple siRNAs is also no different than that for single siRNAs, and many of the complex ‘‘*in vivo*’’ drug interactions that occur between traditional pharmaceuticals do not apply to these agents, thereby facilitating their future use in humans. (Bjorge et al. 2011)

There are several benefits in targeting three growth factors, especially since each growth factor apart from having its own distinct roles, may also be dependent on other growth factors. For example, not only does TGFB1auto-induce itself, it also combines with TGFBR2 to stimulate the expression of CTGF, which has been shown to up regulate the expression of SMA and Collagen-I. TGFB1has been show to stimulate the transition of keratocytes to myofibroblasts that are characterized by the production of SMA. Additionally the ability of TGFB1to elicit multiple, and sometimes opposing, cellular responses in different cell types indicate the complexity of signaling in the wound-healing pathway. For example, TGFB1promotes fibroblast cell proliferation and migration but retards epithelial cell migration. It is difficult to obtain an effect by employing a single target in a complex signaling pathway where the action of one growth factor can be compensated by another and thus justifies the need for a triple combination.

Combined siRNA sequences targeting multiple mRNAs can have unexpected antagonistic effects because each siRNA competes with the other to be assembled into the RISC complex. (Straetemans et al. 2005) There are a number of key determinants of RNAi efficacy that can adversely affect the efficiency of mRNA knockdown by a siRNA combination (Castanotto et al. 2007; Dirk Grimm 2010). This may be the reason for the non-linearity observed in the dose effect curves of the combination siRNA knockdown experiments. In this study, the triple siRNA combination with optimal synergy between the individual siRNA sequences had significantly better results than the ineffective triple combination, even though each of the siRNAs in the low synergy group was potent against its intended target mRNA. The effective triple siRNA

combination, apart from knocking down the target growth factors by ~80% (Figure 2-3) through a cascade effect, also knocked down the mRNA level expressions of downstream mediators like collagen-I and SMA, which led to a significant reduction in the SMA protein level as detected by the immunohistochemistry (Figure 2-5).

Another important functional effect achieved by the effective triple siRNA combination was the reduction in cell migration of cells. Following an injury in the cornea, it has been documented that the expressions of TGFB1and CTGF increases in the surrounding tissues and tears. (T.-C. Chen et al. 2012) In this study, we have shown that the effective triple combination significantly reduced migration of corneal fibroblasts and may prevent myofibroblast transformation by beneficially prohibiting the stromal fibroblasts from contacting the TGFB1present in the surrounding tissues and tears. However, if this retardation of corneal fibroblast was permanent, it might lead to reduced stromal cell density resulting in long term safety concerns. The data from our study show that the cells treated with the triple siRNA combination could still migrate. In fact, using regression analysis we estimated that the time required for the triple siRNA treated cells (4 days) to repopulate the wounding region is twice that of untreated cells (2 days). Since, superficial stromal hyper cellularity is associated with corneal haze formation (Gambato et al. 2005), it is possible that this temporal retardation of corneal fibroblast migration can partially result in the reduction of haze formation.

The flipside to such a multi-targeted approach is the likelihood of off-target effects that may arise from targeting three growth factors, which have many important roles in the normal functioning of cells. Apart from wound healing, TFGB1 is involved in growth and differentiation of many cell types and accumulation of matrix proteins such

as collagen and fibronectin. (Massague 1990) CTGF also has important roles in many biological processes, including cell adhesion, migration, proliferation, angiogenesis, skeletal development, and tissue wound repair. The use of short-term delivery (like nanoparticles) as opposed to long-term delivery (like viruses) to deliver the triple combination would help in reducing the impact of such a knockdown, as their supply is limited to a short amount of time and a specific location.

In addition, siRNAs are also well known to suppress the production of unintended target proteins by binding to the 3' UTR of their mRNAs. (Jackson et al. 2006) During the design of siRNAs, it was ensured that a region targeted by the siRNA's does not share a significant homology with other genes or sequences in the genome by using the BLAST design tool from NCBI.

The functional stability of conventional siRNAs in whole animals has been reported to span at least 14–21 days (Bartlett and Davis 2006) and the introduction of chemical modifications has been shown to extend the duration of their effectiveness. (Bjorge et al. 2011; Dykxhoorn and Lieberman 2006) Our initial *in vivo* results obtained from testing the effective triple combination in a rabbit model of corneal scarring were promising. (sriram, Gibson, et al. 2013) The treatment resulted in a reduction in the expression of SMA when compared to the contra lateral control cornea. Some of the parameters like imaging, dose delivery and intensity of scar formation in animals need to be optimized. Once all of these issues are perfected, our siRNA triple combination could prove to be a powerful treatment option for knocking down multiple targets within the same corneal wound healing pathway. This may be the first step towards

developing a multi target approach for the reduction of not only corneal fibrosis but also scarring in the entire body.

Table 2-1. Two siRNA sequences identified for each target growth factor

Growth Factor	Label	Target Sequences
TGFB1	T1	GCUGACACCCAGUGACACA
	T2	GCUGAGAGGUGGAGAGGAA
TGFBR2	R1	GCAGAGAACUUGAAAGCAU
	R2	CCAUAUGCGGUGUGAAAUA
CTGF	C1	GUGAUGAGCCCAAGGACCA
	C2	GCGAGGAGUGGGUGUGUGA

Table 2-2. Generation of an effective and ineffective triple combination using CI values, calculated as described in the Materials and Methods. A value from 0-1 indicates synergism, while a value of 1 and beyond indicates antagonism

	Effective Triple Combination (T1R2C1)		Ineffective Triple Combination (T2R1C2)	
Growth Factors	Groups	CI values	Groups	CI values
TGFB1	T1C1	0.2060	T2C2	3.1394
	T1R2	0.3684	T2R1	1.3926
TGFBR2	R2T1	1.0191	R1T2	2.8760
	R2C1	0.7261	R1C2	3.5837
CTGF	C1T1	1.3384	C2T2	0.9603
	C1R2	0.1410	C2R1	0.8715

Table 2-3. TAQMAN™ RT PCR Primers and probe sequences

Target	Label	Sequences
CTGF	Forward	AGGAGTGGGTGTGTGATGAG
	Reverse	CCAAATGTGTCTTCCAGTCG
	Probe	ACCACACCGTGGTTGGCCCT
TGF-ßR2	Forward	CGTCGAGACTCCATCTCAAA
	Reverse	AAACAGCCCACAAATGTCAA
	Probe	TCAGCTTTGCACAAGGGCCCT
TGFB1	Forward	CCTGTACAACCAGCACAACC
	Reverse	CGTAGTACACGATGGGCAGT
	Probe	CTCCAGCGCCTGTGGCACAC
Collagen-I	Forward	TTCTGCAGGGCTCCAATGAT
	Reverse	TCGACAAGAACAGTGTAAGTGAACCT
	Probe	TTGAACTTGTTGCCGAGGGCAACAG
SMA	Forward	AGAGCGCAAATACTCCGTCT
	Reverse	CCTGTTTGCTGATCCACATC
	Probe	CGGCTCCATCCTGGCCTCTC
18S rRNA	Forward	GCCGCTAGAGGTGAAATTCTTG
	Reverse	CATTCTTGGCAAATGCTTTCG
	Probe	ACCGGCGCAAGACGGACCAG
GAPDH	Forward	GAGACACGATGGTGAAGGTC
	Reverse	ACAACATCCACTTTGCCAGA
	Probe	CCAATGCGGCCAAATCCGTT

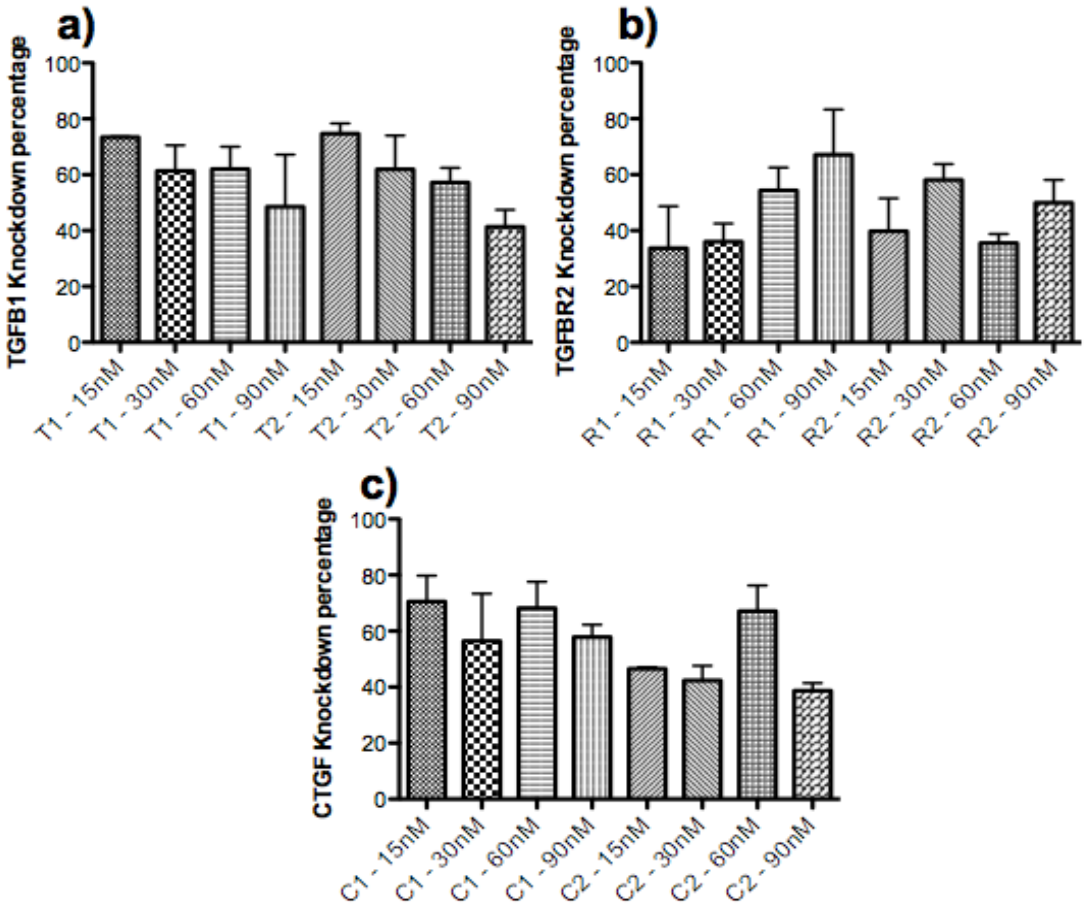

Figure 2-1. Knockdown of target growth factors by individual siRNA sequences. Cultures of Rabbit corneal fibroblasts stimulated with TGFB1and Estradiol were transfected with individual siRNA sequences targeting TGFB1(designated T1 and T2), TGFBR2 (designated R1 and R2) and CTGF (C1 and C2) using Mirus transfection reagent. The siRNA sequences were tested at different concentrations from 15nM to 90nM. Forty-eight hours after transfection, the cell extract was collected using a cell lysis buffer and analyzed using ELISA. The protein level knockdown percentages of - a) TGFB1, b) TGFBR2 and c) CTGF for all individual siRNA sequences were calculated with respect to a scrambled siRNA control.

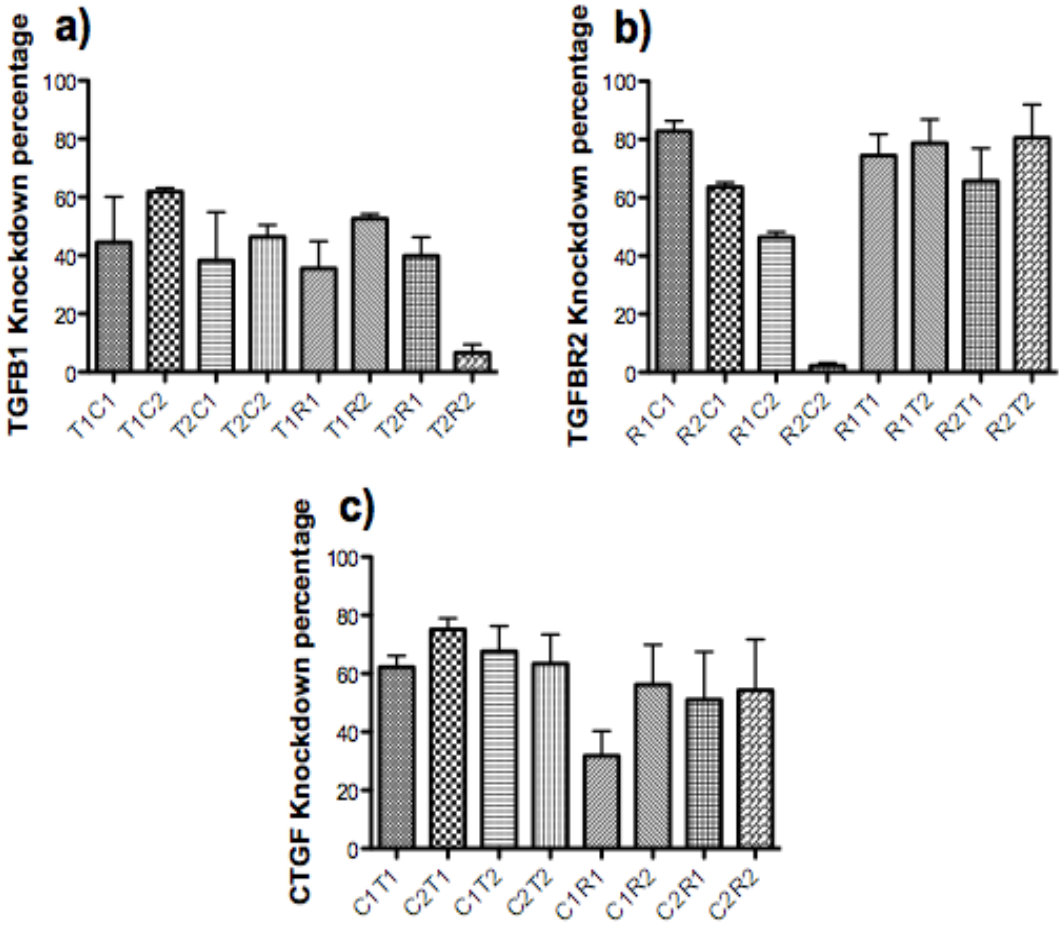

Figure 2-2. Knockdown of target growth factors by different dual siRNA combinations. Cultures of rabbit corneal fibroblasts stimulated with TGFB1and/or Estradiol were transfected with different dual combinations of siRNAs targeting TGFB1(designated T1 and T2), TGFBR2 (designated R1 and R2) and CTGF (C1 and C2). Each siRNA was added at 30nM concentration for a final combined concentration of 60nM. Forty-eight hours after transfection, the cell extract was collected using a cell lysis buffer and analyzed using ELISA. The protein level knockdown percentages of – a) TGF - beta1, b) TGF – beta R2 and c) CTGF for all dual siRNA combinations were calculated with respect to a scrambled siRNA control.

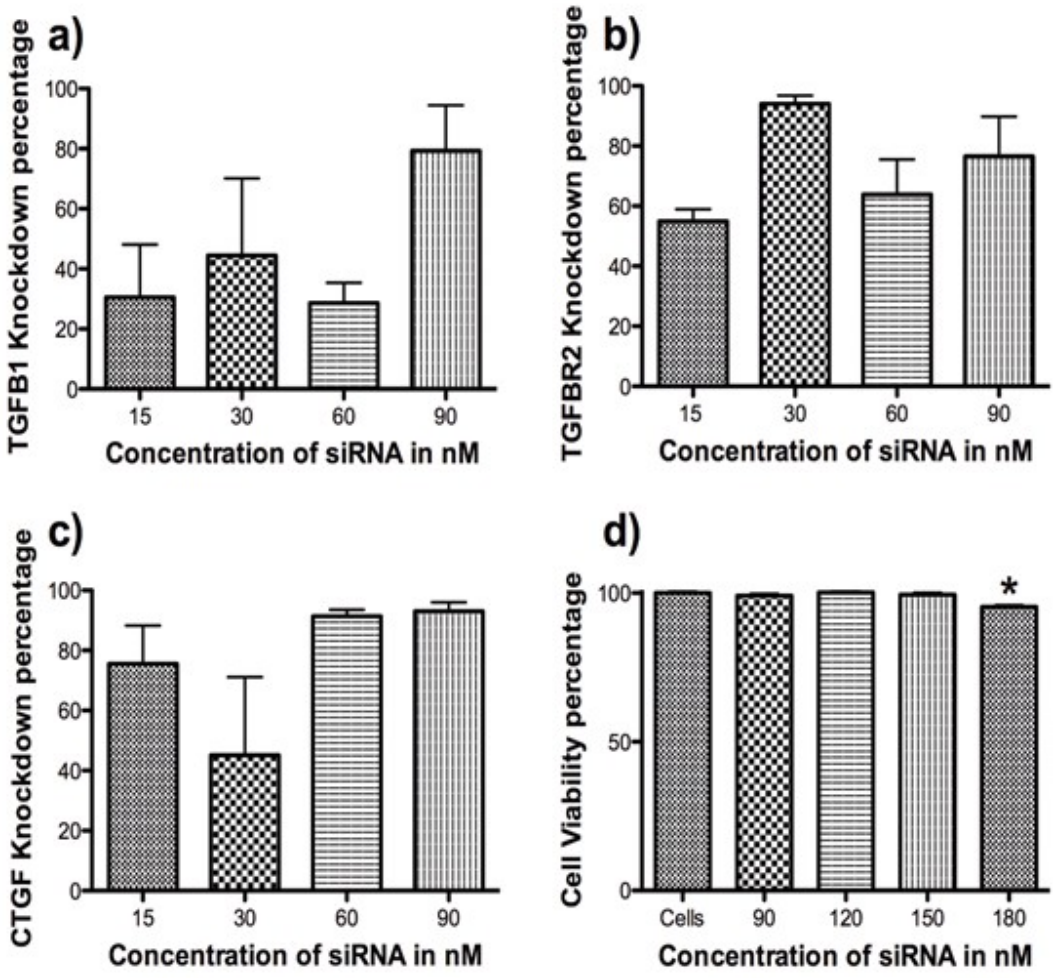

Figure 2-3. Knockdown of target growth factors by Effective Triple combination (T1R2C1). Cultures of rabbit corneal fibroblasts stimulated with TGFB1and Estradiol were transfected with the triple siRNA combination (15nM, 30nM, 60nM and 90nM) using Mirus transfection reagent. The RNA samples were collected 48 hours after transfection and were analyzed using qRT PCR. On a similar experiment, cells were dosed with increasing concentrations of siRNA triple combination (90nM to 180nM) and cell viability was assessed using the MTS assay. The knockdown percentages of a) TGFB1, b) TGFBR2 and c) CTGF are plotted for the identified effective triple combination (T1R2C1). All expressions were normalized to 18S rRNA. The knockdown percentages were calculated with respect to a scrambled siRNA control. d) The percentage of viable rabbit corneal epithelial cells after treating with increasing concentrations of the effective triple combination (T1R2C1). ($p<0.05$).

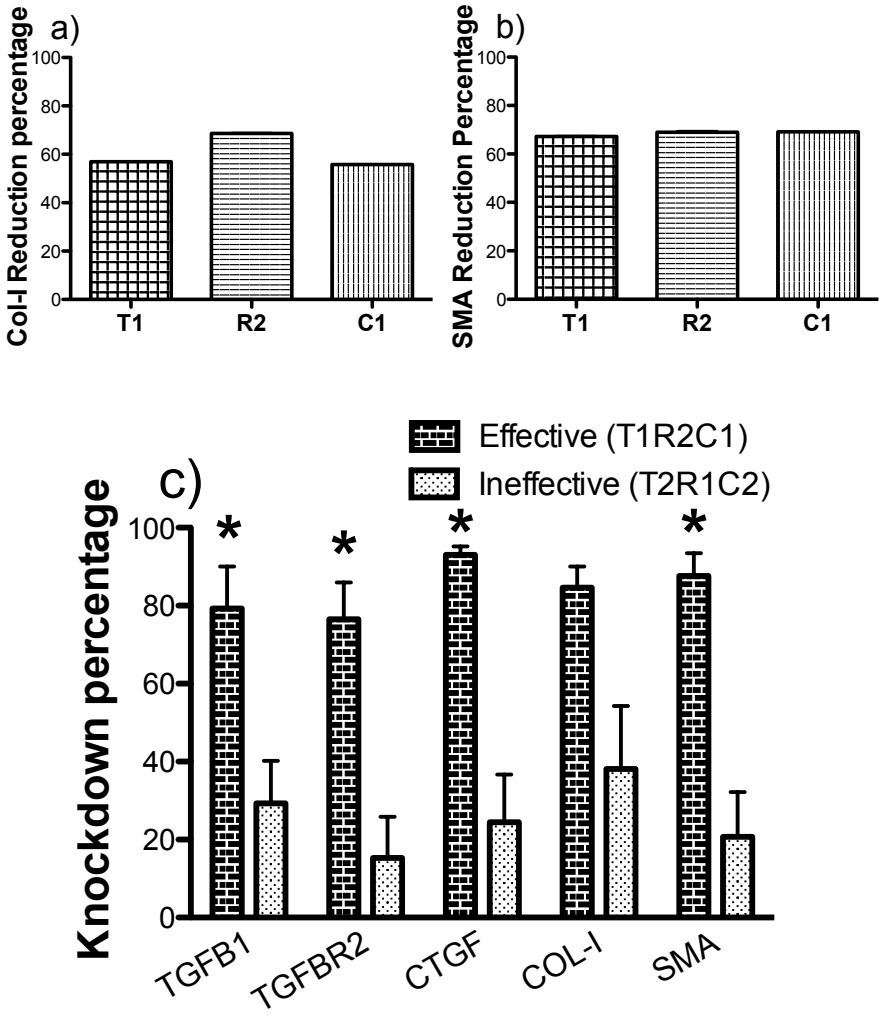

Figure 2-4. The Effective triple combination (T1R2C1) is more potent than single siRNA sequences or Ineffective triple combination (T2R1C2) in blocking downstream mediators. Cultures of rabbit corneal fibroblasts stimulated with TGFB1and estradiol were transfected with effective (T1R2C1), ineffective (T2R1C2) triple siRNA combination and individual siRNA sequences at total siRNA concentration of 90nM using Mirus TransIT-TKO transfection reagent. The RNA samples were collected 48 hours after transfection and were analyzed using qRT PCR. a) & b) Collagen-I and SMA reduction percentages are compared between the effective (T1R2C1) combination and its individual siRNA sequences at 90 nM. c) The RNA level reduction percentages of five genes (target and downstream) are compared between the effective (T1R2C1) and the ineffective triple combination (T2R1C2). All expression levels were normalized to 18S rRNA. The knockdown percentages were calculated with respect to a scrambled siRNA control. ($p<0.05$).

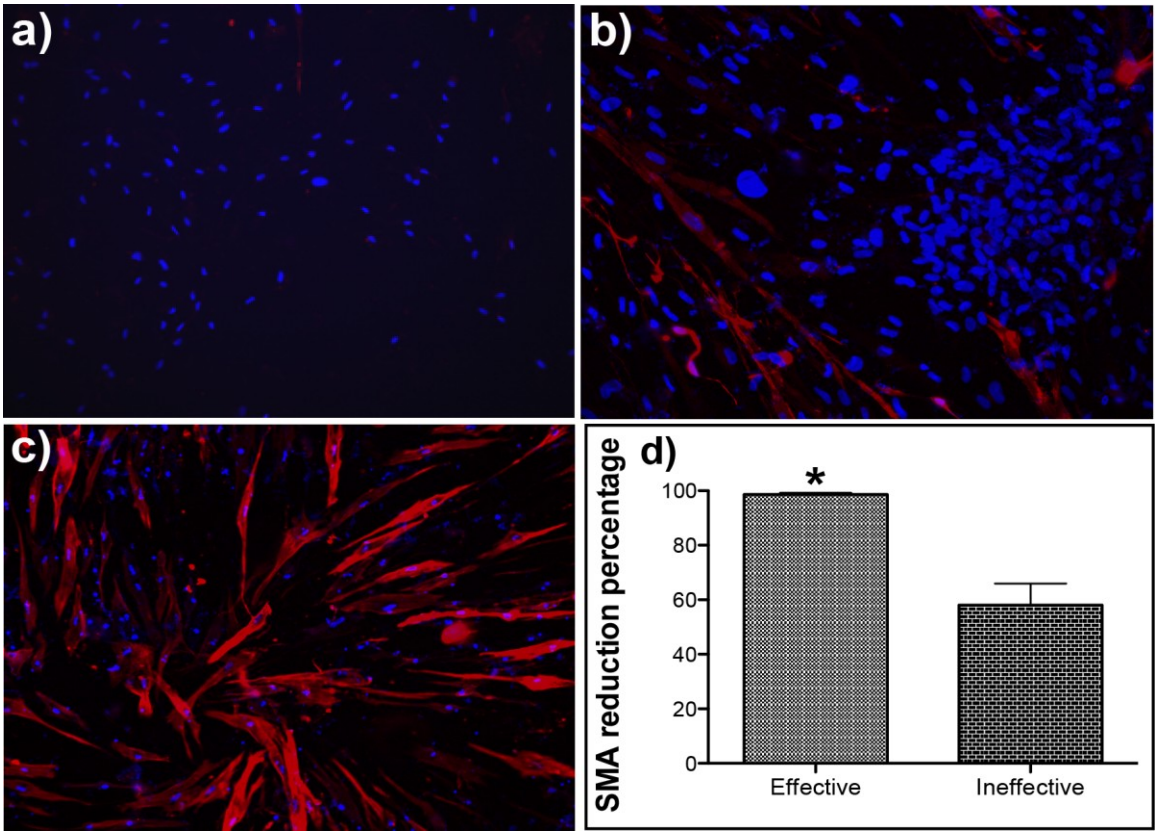

Figure 2-5. Immunohistostaining for SMA shows Effective triple combination (T1R2C1) is more effective in reducing protein expression of SMA than the Ineffective triple combination (T2R1C2). Cultures of rabbit corneal fibroblasts stimulated with TGFB1and estradiol were transfected with effective (T1R2C1) and ineffective (T2R1C2) triple siRNA combination (90 nM) using TransIT-TKO transfection reagent. To stain for SMA, forty-eight hours after transfection, the cells are fixed in 4% paraformaldehyde, blocked in goat serum and then incubated with cy3 labeled SMA antibody. Images of SMA protein immunohistostaining (originally 20X) are shown for: a) effective triple combination (T1R2C1), b) ineffective triple combination (T2R1C2) and c) scrambled control. d) the percentage reduction of SMA staining calculated through image analysis from 4 different areas in 3 replicate wells. The percentage area of cells stained with SMA was normalized to the number of cells in each corresponding image. The SMA reduction percentage in the treated images was calculated with respect to the untreated controls. ($p<0.05$). Images courtesy of Sriniwas Sriram.

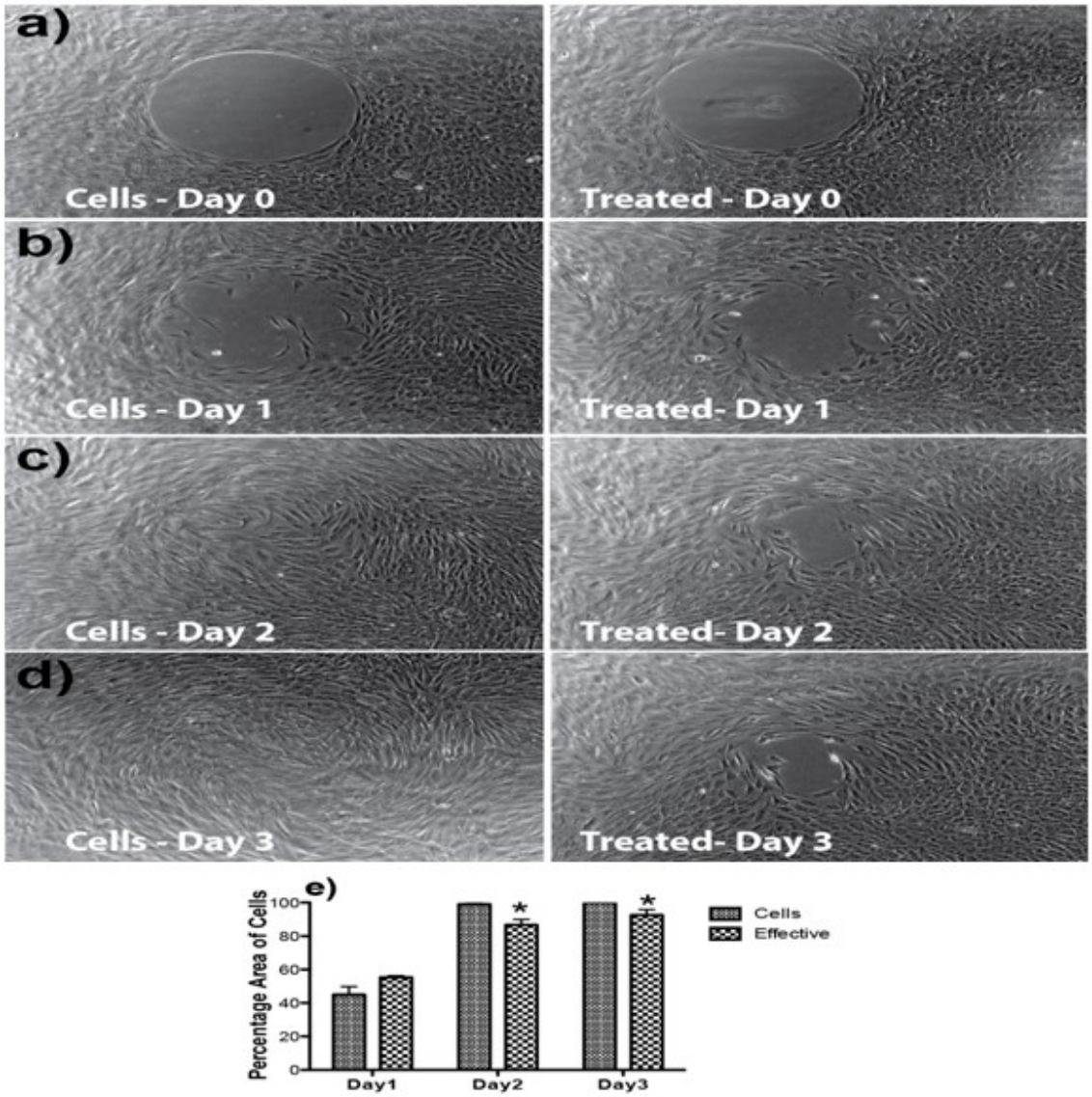

Figure 2-6. The Effective triple combination (T1R2C1) inhibits migration of rabbit corneal fibroblasts. Cultures of rabbit corneal fibroblasts were cultured in 6 well plates provided with the Radius® cell migration kit. After confluence, a circular region in the middle of the well was removed using a gel removal solution. Panels a) – d) show migration assay results comparing cells alone and effective triple combination (T1R2C1) treatment wells. e) the percentage area of cells migrating into the circle based on the migration assays calculated through image analysis from 3 replicate wells. Images courtesy of Sriniwas Sriram.

CHAPTER 3
DEVELOPMENT OF *EX VIVO* CORNEAL ORGAN CULTURE AS A SCARRING MODEL AND EVALUATION OF ITS THERAPEUTIC POTENTIAL

Purpose

To develop an *ex vivo* organ culture model of the rabbit corneal scarring process that is suitable for therapeutic testing and to study the molecular mechanisms involved in haze formation following a laser ablation.

Background

Corneal haze is a common complication that occurs in patients after excimer laser photorefractive keratectomy (PRK). (Sakimoto, Rosenblatt, and Azar 2006) Mechanical, chemical and/or surgical injury to the cornea triggers a complex wound healing response-causing changes in extracellular matrix organization and cellular phenotype and density. (Jester, Petroll, and Cavanagh 1999) There is no fibrotic response in case of epithelial lesions, as stem cells from either the surrounding limbus or other parts of the epithelium migrate into the wounding region and resolve the wound in several days. (Liang et al. 2009; Pellegrini et al. 2009) However, a deeper wound disturbing the basal epithelium and stromal layers stimulate the pathological evolution of the wounding process mainly due to the involvement of fibrogenic growth factors like transforming growth factor beta 1 (TGFB1), TGFB Receptor (TGFBR2) and connective tissue growth factor (CTGF). (Blalock et al. 2003; Tandon et al. 2010) When the quiescent keratocytes come in contact with these growth factors, they become activated and begin to repopulate the resident cells that had undergone apoptosis following the injury. These activated keratocytes then proliferate and undergo phenotypic changes typical of myofibroblasts with increased ability to synthesize extracellular matrix. (Jester et al. 1996; Møller-Pedersen 2004) These myofibroblasts are characterized by their high

concentration of alpha smooth muscle actin (SMA) and elevated expression of cadherins and TGFB1receptors. (Jester, Petroll, and Cavanagh 1999) There are also irregular deposits of collagen; loss of corneal crystallins and the myofibroblasts do not die of apoptosis as expected. (Eraslan and Toker 2009)

There have been several *ex vivo* corneal models reported that have been tested for re-epithelialization after physical (Carrington et al. 2006; Tanelian and Bisla 1992), chemical (Chuck, Behrens, Wellik, Liaw, Dolorico, et al. 2001) and laser wounds (Janin-Manificat et al. 2012). However, most of the models are mainly concerned with the process of re-epithelialization, and only limited studies have been reported with markers on corneal scarring. In particular, none of them have evaluated the therapeutic potential of gene therapy in these culture models.

It is often difficult to achieve a significant therapeutic effect by employing a one-target, one-drug paradigm on a complex, multi-factorial, amplifying, signaling pathway. (Chou and Talalay 1983) An approach aimed at multiple targets can potentially be more efficacious and less vulnerable to acquired resistance as the system is less able to compensate for the action of two or more drugs simultaneously (Borisy et al. 2003; Keith, Borisy, and Stockwell 2005). In this study, we would be using a triple siRNA combination targeting three key scarring genes – TGFB1, TGFBR2 and CTGF, which has been shown to be effective in knocking down the downstream regulators (SMA and Collagen-I) in cell culture experiments (sriram et al. 2012).

Delivery of drugs to the cornea is a major challenge, as the mechanical barriers that protect the cornea (multi-layered epithelium, tight junctions) constrain ocular drug delivery. Protective mechanisms also include lacrimation, solution drainage, diversion of

exogenous chemicals into the systemic circulation, and a highly selective corneal barrier to exclude high molecular weight polyanions, like RNA. Hence, for an effective therapy, a delivery method to target the corneal layer with the maximum post-wounding growth factor localization has to be developed. The principal properties governing absorption of a drug by the cornea are the lipophilicity, partition coefficient and molecular size of that compound. (Lee and Robinson 1986; Sasaki et al. 1996) Nanocarriers provide a potential solution for targeted ocular drug delivery, as they have been shown to be non-immunogenic, to have relatively low toxicity, to be resistant to protein/serum absorption and to be stable in an enzymatic environment. They have also been shown to adhere to the ocular surface and penetrate through the corneal and conjuctival epithelia, after topical administration, making them ideal trial candidates for siRNA delivery (la Fuente, Seijo, and Alonso 2008; Tong et al. 2007). Hence, in this study we are testing the efficacy of a nanoparticle delivery system to deliver siRNAs to the different layers of the cornea.

It has been reported the epithelium is generally the rate limiting barrier to trans-corneal transport. Its barrier favorably depends on the lipophilicity of molecules and almost completely excludes macromolecules (r > 10 Å) (Hämäläinen et al. 1997). For small molecules sufficiently lipophilic to readily cross epithelium, the stroma and endothelium can play a significant role, where endothelium provides a greater barrier than the stroma. This is because stroma is largely aqueous and do not have tight and gap junctions unlike the epithelium and endothelium (Edwards and Prausnitz 2001). Hence, paracellular transport (between cells) is easier for small hydrophilic molecules in the stroma. In this study, we excimer ablate and completely remove the epithelial layer

from the cornea and dose the cornea with siRNA delivered by NP that is both hydrophilic and lipophilic which may aid delivering the drug to different layers of the cornea.

This work aims to characterize scar formation in a corneal organ culture model following a laser ablation and compare it to that of scar formation in animals. We also wanted to evaluate the therapeutic potential of the model by delivering a previously optimized triple siRNA combination to different layers of the cornea and observing its effect on scar formation.

Materials and Methods

Nanoparticles

A commercially available nanoparticle kit called Invivoplex® was purchased from Aparnabio (Rockville, MD) and used according to manufacturer's instructions. They are made up of Histidine-lysine (HK) peptides that have both hydrophilic as well as lipophilic characteristics (soluble in water as well as organic solvents). In addition, the core of the nanoparticle is positively charged. Briefly, siRNA triple combination solution was made at a concentration of 0.9 mg/ml. 600uL of this solution was added with 300uL of the provided cargo buffer. This solution was added drop wise to 900uL of the nanoparticles over a magnetic stirrer. This preparation forms siRNA containing particles of less than 50 nm that are stable for a week at 4°C.

RNA Interference

In a previous paper, we had generated an effective triple siRNA combination targeting TGFB1, TGFBR2 and CTGF with high synergy among its individual siRNA sequences. The effective triple siRNA, in *in vitro* knockdown experiments, significantly reduced mRNA levels of target genes (>80%) and downstream scarring genes (>85%),

SMA protein (>95%), and significantly reduced cell migration without reducing cell viability. This previously optimized effective triple combination was tested for its efficacy in knocking down key scarring genes in this *ex vivo* corneal scarring model. In this study, siSTABLE® siRNAs were ordered Dharmacon (Dharmacon Products, Thermo Fisher Scientific, Lafayette, CO) which are chemically modified to persist in *in vivo* conditions.

Ex Vivo Organ Culture of Rabbit Corneas

Corneas were cultured as previously described in (Castro-Combs et al. 2008; Chuck, Behrens, Wellik, Liaw, Sweet, et al. 2001; Richard et al. 1991; n.d.). The ends of 50ml laboratory test tubes were cut at the indicator lines nearest to the bottom with the help of a saw. These domes were then coated with super glue and aseptically placed firmly concave down into the center of each well of a 12-well tissue culture plate. The plates were then sanitized by placing them under ultraviolet light overnight. Fresh rabbit globes from Pelfreeze were ablated to 155 microns using an excimer laser. Laser ablations were performed with a Summit SVS exicimer laser that is committed to animal vision research. Using the laser in phototherapeutic keratectomy mode, the central 6 mm diameter area of the cornea was be ablated at a dose of 160mJ/cm2 to a total depth of 155 microns. Corneal rims were then surgically extracted from the rabbit globes and using sterile forceps, grasping only the scleral rims and not cornea; each rim was placed over a single dome. Incubations were carried out in 5% CO_2 and 95% air at 37^{o} C for the duration of the experiment. The level of the culture medium was adjusted so the anterior surface of corneas was at the air-liquid interface. Test agents were added to the media as described below.

Experiment 1

Experiment 1 was designed to assess if the excimer laser ablated corneas developed patterns of gene expression that was consistent with scar formation after two weeks of organ culture. Two groups of corneas were analyzed: ablated, and unablated corneas. Four corneas were cultured in each of the two groups in DMEM supplemented with 10% fetal bovine serum containing 1% antibiotic solution (penicillin and streptomycin) and the media was changed every 2 days. After 14 days of culture, mRNA from the four corneas in each treatment group were pooled together and processed for q-RT-PCR measurement of levels of mRNAs for five genes as described below: TGFB1, TGFBR2, CTGF, SMA and Col-I.

Experiment 2

Experiment 2 was designed to assess the delivery of a fluorescently labeled scrambled siRNA sequence using NP (NP-FL-siRNA). The experiment included three groups of corneas: unablated & treated with NP-FL-siRNA, ablated & treated with NP-FL-siRNA and ablated & treated FL-siRNA without NP. Three corneas were cultured in each of the three groups in DMEM supplemented with 10% fetal bovine serum containing 1% antibiotic solution (penicillin and streptomycin) and the media was changed every 2 days. The corneas in the NP-FL-siRNA group (three ablated and three unablated corneas) were topically treated with 50 □L of fluorescently labeled siRNA complexed with nanoparticles for 1 minute using a vacuum trephine while the corneas in FL-siRNA group (three ablated corneas) received an equivalent dose of FL-siRNA without NP. The corneas were cultured for 6 hours and then collected for histology.

Experiment 3

Experiment 3 was designed to assess the relative levels of corneal haze that developed in excimer-ablated corneas, and to determine if the level of corneal haze could be reduced by treatment with a steroid (prednisolone acetate) that is commonly used to reduce corneal inflammation or by treatment with a NP-siRNA formulation that targeted three key scar-stimulating genes (TGFB1, TBRII and CTGF). The experiment included four groups of corneas: unablated, ablated & untreated, ablated & treated with NP-siRNA, and ablated & treated with prednisolone acetate. Six corneas were cultured in each of the four groups. After excimer laser ablation, all the corneas were cultured in DMEM supplemented with 1 ng/ml of TGFB1 and 1% antibiotic solution and the media was changed every 2 days. Furthermore, one group of four corneas were treated with 2 drops of 1%prednisolone acetate ophthalmic suspension (Pacific Pharma) and another set of four corneas were treated with the triple siRNA combination delivered using NP for the first three days after ablation. After 14 days of culture, corneas were photographed then returned to culture, until on day 21, three corneas of each test group were independently processed for qRT-PCR for measurement of SMA mRNA. The remaining three corneas in each group were processed for immunohistostaining of SMA protein.

Reverse Transcription-Polymerase Chain Reaction

Total RNA was extracted using the Qiagen RNeasy mini isolation kit (Qiagen, Inc., Valencia, CA) and used according to the manufacturer's directions. cDNA was synthesized using the High Capacity cDNA Reverse Transcription Kit (Applied Biosytems, Carlsbad, CA) according to manufacturer's procedure. The level of mRNA for TGF-B1, CTGF, TGFBR2, SMA, collagen II, and 18S ribosomal RNA were

determined using the Real-Time PCR TaqMan assay. The primers and probes for each gene are defined in Table 2-3. The endogenous control, ribosoma18S RNA, was used normalize target genes. Primers, probes and cDNA were combined with TaqMan Universal PCR Master Mix (Applied Biosytems, Carlsbad, CA) and amplification was performed by the Applied Biosystems 7300HT Fast Real Time PCR System (Carlsbad, CA). The thermal cycling conditions were as follows: 2 min at 50°C, 10 min at 95°C, 40 cycles of 15 sec at 95°C, and 1 min at 60°C. The relative gene expression of the growth factors was calculated using the 2-ΔΔCt method.

Immunohistochemistry

The corneas from the delivery experiment were collected 6 hours after transfection, while the corneas from the therapeutic experiment were cultured for 21 days before collection and fixing. To stain for SMA, the rabbit corneas from the both the experiments were fixed overnight in 4 % paraformaldehyde. They were then bisected, fixed in Optimal Cutting Temperature medium (OCT) (Sakura Finetek) and then sectioned in 10um slides. The slides were then washed with PBS and blocked in horse serum for 1 hour. Finally, they were incubated with SMA antibody-Cy3 (Sigma) for 1hour at room temperature. The slides were mounted with DAPI and imaged using fluorescence microscope.

Scar Imaging

Nikon D7000, was outfitted with a macro lens capable of native 1:1 reproduction (60mm Nikkor) and the Nikon R1C1 Creative Lighting System (CLS) flash system. The D7000 was set to the “Standard” program, ISO 100, manual exposure with a shutter speed of 1/250 second and f/57. To visualize and measure haze, the lens was outfitted with a circular ring flash whose flash power was set manually (1/6th D7000) and neither

the flash nor lens had a filter. For all images, the lens was set to manual focus and pre-focused to a 1:1 reproduction ratio and the camera was fixed to a tripod and focused by moving the camera closer or further from the subject. Guide lights on the flash heads were used to facilitate haze visualization and focusing.

Image Analysis

To improve the contrast of scar formation in the ablated regions of the cornea, the native full color images were converted to grey scale. This was followed by reducing the background light scattering observed in unablated regions of the cornea to a minimum. All the image-processing steps in this method were performed using the tools in Adobe Photoshop. These steps help in effectively blocking the noise associated with the light scattering of unablated regions, which enables the finer details of the scar to be discerned. The ablation regions in these processed images are then selected with the lasso tool and percent haze is calculated by measuring the pixel intensity in these selected regions.

Statistical Analysis

All experiments were performed in triplicate and all statistical analyses were conducted using GraphPad prism (San Diego, CA). Student's t test or Analyses of Variances (ANOVA) with Tukey's post-hoc assessments were accordingly used to test for significance between the groups. Results were considered statistically significant where $p<0.05$.

Results

Using rabbit corneas cultured at the air-liquid interface, we analysed the ability of a laser ablation to promote corneal scar-like response in corneas *ex vivo*. Scarring was evaluated in terms of specific markers of wound healing (expression of pro fibrotic

genes) and transparency (reduction in pixel intensity of light reflected from a white line beneath the cornea). Further, to evaluate the efficacy of this system as a therapeutic testing model, we evaluated the ability of prednisolone and nanoparticle (NP) derived triple siRNA directed at TGB1 related targets in reducing the formation of these scar-like features.

Ablated Corneas in Culture Develop Scar-Like Features

Freshly obtained rabbit globes were ablated to a depth of 155um and cultured at the air-liquid interface for 21 days in serum free media that was supplemented with 1ng/ml of TGF-B1. The unablated corneas were transparent and showed no signs of any scar-like features while the ablated corneas without any treatment had the most visible scar-like formations in the wounding region (Figure 3-1A & 3-2B). Comparing fluorescein staining of corneas immediately after ablation and subsequently, after 21 days of culturing indicated complete reepithelialisation, resulting in a pluristratified epithelium. *In vivo* confocal images of the ablated corneas at the ends of a laboratory tube show activated epithelial and stromal cells indicative of scar formation (Figure 3-8).

Visual Comparison of Corneas Treated with Therapeutic Agents

To improve the contrast of scar formation in the ablated regions of the cornea, the native full color images were converted to grey scale and the background scattering of light from the unablated regions were reduced to a minimum. Figure 3-2 shows these processed digital images of the corneas from all the treatment groups. The ablated cornea without any treatment (positive scarring control) developed the most robust scar-like features, while the corneas treated with NP-siRNA or treated with steroid developed markedly less scar-like features that were readily apparent by simple visual

examination. The unablated cornea did not develop any haze-like features and was used as a negative control.

Comparison of RNA Level Expression of Pro-Fibrotic Genes in Ablated and Unablated Corneas.

Levels of expression of pro-fibrotic genes in unablated and ablated corneas cultured in full serum conditions without any treatment. RNA from the scar-like tissue was collected using a 8mm punch biopsy, and the expression levels of 5 pro-fibrotic genes were analyzed using qRT PCR. The RNA level expression of all five pro-fibrotic genes was higher in the ablated corneas when compared to the unablated corneas (Figure 3-3). In particular, the expression of TGFB1and SMA were 8 and 4 times higher, respectively, in injured corneas.

Nanoparticles Deliver siRNA to all Layers of the Cornea in Organ-Culture

The efficacy of the delivery of nanoparticles complexed with siRNA to different layers of the cornea was assessed by detecting the presence of a fluorescently labelled scrambled siRNA sequence in histology sections of treated corneas. In ablated corneas treated with nanoparticle complexed fluorescently labelled siRNA (NP-FL-siRNA), a fluorescence gradient was observed. The anterior stromal layers directly beneath the area where NP-FL-siRNA was applied using a vacuum trephine had a high fluorescence intensity. The intensity of fluorescence progressively decreased with increasing distance from the anterior surface. However, there was an increase in the fluorescence intensity in the Descemet's membrane and endothelial cell layers. Higher magnification images of the sections show uptake of siRNA by the cells (Figure 3-4A - 3-4D). Importantly, no fluorescence was observed in the stroma of excimer-ablated corneas when FL-siRNAs alone were applied indicating the "naked siRNAs" did not effectively penetrate into the

corneal tissue (Figure 5e). Also, only a few superficial epithelial cells were fluorescent when FL-NP- siRNAs were applied to the intact unablated cornea (Figure 5f). Neither the stroma layers nor the endothelial cell layer and Descemet's membrane were fluorescent. These results suggest that the fluorescence pattern observed in corneas when FL-NP-siRNA nanoparticles were applied topically to corneas in the area of epithelial ablation was due to penetration of the FL-NP-siRNA nanoparticles into the stroma and not to absorption from the media.

Evaluating the Reduction in Haze Formation

The corneas in the experimental groups were imaged with a digital camera to calculate the reduction in transparency due to formation of corneal haze. Percent haze was calculated by the reduction in pixel intensity of a white line reflecting light through ablated corneas (Image 3-6B) when compared the same image reflected through unablated corneas (Image 3-6A). The pixel intensity of the white line would be higher in the unablated corneas due to its higher transparency while the intensity of the white line would be reduced depending on the severity of the haze. Laser injury to the cornea with no treatment reduced the intensity of the image by 12% when compared to the unablated corneas; while treatment with NP-siRNA (5% reduction) and steroids (3% reduction) improved the transparency of the corneas when compared to the unablated corneas. Treatment with NP-siRNA therefore reduced haze formation by 58%, while treatment with steroids reduced haze formation by 78%.

In an alternate method, the contrast-enhanced images of three replicate corneas from all the four treatment groups were used to measure the percentage of haze formed. The ablation regions in these processed images are selected with the lasso tool and percent haze is calculated by measuring the pixel intensity in these selected

regions (Image 3-5A & 3-5B). The pixel intensity in this selected region should be lower in the unablated corneas due to their relatively high transparency, while the intensity of these regions in ablated corneas should be higher in corneas with ”scar” depending on the severity of the haze. The percentage of haze in ablated & untreated corneas with no treatment was 22% when compared to the unablated corneas. In contrast, treatment of ablated corneas with NP-siRNA improved the transparency of the corneas, resulting in a haze percentage of 9.6% when compared to the unablated corneas. Similarly, treatment of ablated corneas with steroid also improved the transparency of the corneas, resulting in a haze percentage of 7% when compared to the unablated corneas. Therefore, treatment of the ablated corneas with NP-siRNA reduced haze formation by 55%, while treatment with steroids reduced haze formation by 68% compared to ablated corneas that received no treatment.

Treatment with NP-siRNA or steroid reduce mRNAs for scarring genes

RNA from the scar-like tissue was collected using a 8mm punch biopsy, and the expression levels of SMA were analyzed with qRT PCR. The SMA expression in the treated corneas (NP-siRNA and steroids) was significantly lower than that of the ablated and untreated corneas (Figure 3-6D). Specifically, the NP-siRNA treatment was able to reduce the SMA expression by 77%, while the steroid treatment reduced the SMA expression by 85%.

Immunohistostaining of Corneal Tissues Show Reduction in SMA after Treatment with Steroids and NP-siRNA

To visualize the presence of SMA in the ablated untreated corneas and confirm protein level knockdown of the treatments, immunocytochemistry was performed on three corneas from each of the experimental groups. Rabbit globes that were ablated

and untreated show SMA staining in the basal epithelium and anterior stroma (Figure 3-7A). A similar pattern of myofibroblasts formation was observed in both mice and rabbits after a PTK injury. Corneas that were treated with NP-siRNA and steroids showed no staining for SMA (Figure 3-7E & 3-7F).

Discussion

Using rabbit corneas cultured in organ culture, we were able to reproduce the loss of transparency observed in living rabbits when corneas are subjected to laser injury (Figure 3-1A & 3-1B). Since, this model utilizes freshly obtained intact rabbit globes, it is closer to the *in vivo* situation than the three-dimensional cell culture systems reported in the literature (Janin-Manificat et al. 2012; Karamichos et al. 2010).

Several organ culture methods have been proposed to study the corneal *in vitro* wound healing processes (Møller-Pedersen and Møller 1996; Richard et al. n.d.). However, air/liquid organ cultures have been shown to improve epithelial cell morphology and preserve stromal keratocytes for at least 4 weeks (Castro-Combs et al. 2008). This culture system also decreases the intercellular edema generally observed in conventional submerged models (Chuck, Behrens, Wellik, Liaw, Dolorico, et al. 2001; Collin et al. 1995; Foreman et al. 1996). This model was able to reproduce corneal scarring in terms of stromal disorganization and differentiation to myofibroblasts. There was a marked increase in the RNA expression of five pro-fibrotic genes. In particular, SMA, a key marker of scarring tissue showed significant increase when compared to the unablated corneas (Figure 3-2).

In this culture system, corneal scar formation develops in the absence of an intact immune system; tear secretion and corneal innervation, all known to be important participants in the wound healing process. This makes it an interesting model to

observe and study the various molecular pathways that regulate haze formation. It would also make it an ideal model to test therapeutic agents targeting molecular pathways to reduce haze formation. In this study, we have used a triple siRNA combination targeting TGFB1, TGFBR2 and CTGF all of which have been shown to play an important role in corneal scarring. (Blalock et al. 2003; C. Chen et al. 2000; Jester, Petroll, and Cavanagh 1999)(Triple paper) This effective triple siRNA, in *in vitro* knockdown experiments, significantly reduced mRNA levels of target genes (>80%) and downstream scarring genes (>85%), SMA protein (>95%), and significantly reduced cell migration without reducing cell viability.

In the cornea it has been shown that fundamental behaviors of epithelial and stromal cells, including proliferation, adhesion, and migration, are modulated by substratum topography (Pot et al. 2010). A previous study by Netto et al. (Netto et al. 2006) indicated that larger-scale topographic irregularities caused by corneal surgical intervention contribute to myofibroblast generation and haze formation *in vivo*. It has also been shown that nanoscale topographic features modulate TGFB1-induced myofibroblast differentiation and αSMA expression, possibly through upregulation of Smad7. It is therefore possible that in the wound environment, native nanotopographic cues assist in stabilizing the keratocyte/fibroblast phenotype while pathologic microenvironmental alterations may be permissive for increased myofibroblast differentiation and the development of fibrosis and corneal haze (Myrna et al. 2012). Hence, studying anti-fibrotic therapies in excimer laser ablated *ex vivo* corneas is a better system than in cell culture experiments as they provide pathologic

microenvironmental alterations similar to *in vivo* conditions that may stimulate the fibroblasts to change to the myofibroblast phenotype.

One of the main challenges in the use of siRNA has been the delivery. In this study, we have used a histidine and lysine based commercially available nanoparticle kit. In ablated corneas treated with nanoparticle complexed fluorescently labelled siRNA (NP-FL-siRNA), a fluorescence gradient was observed. The anterior stromal layers directly beneath the area where NP-FL-siRNA was applied using a vacuum trephine had a high fluorescence intensity. The intensity of fluorescence progressively decreased with increasing distance from the anterior surface. However, there was an increase in the fluorescence intensity in the Descemet's membrane and endothelial cell layers. Higher magnification images of the sections show uptake of siRNA by the cells (Figure 5 a-d). These results suggest that Descemet's membrane may reduce the penetration of FL-NP-siRNA complex, leading to an increased concentration of the FL-NP-siRNA nanoparticles in the matrix of the basement membrane. Importantly, no fluorescence was observed in the stroma of excimer ablated corneas when FL-siRNAs alone were applied (Figure 5e). Also, only a few superficial epithelial cells were fluorescent when FL-NP- siRNAs were applied to the intact unablated cornea (Figure 5f). Neither the stroma layers nor the endothelial cell layer and Descemet's membrane were fluorescent. These results suggest that the fluorescence pattern observed in corneas when FL-NP-siRNA nanoparticles were applied topically to corneas in the area of epithelial ablation was due to penetration of the FL-NP-siRNA nanoparticles into the stroma and not to absorption from the media. Overall, these results demonstrated the importance of the cationic nanoparticle carrier system to enhance deep penetration of

the FL-siRNAs into the cornea and uptake by stroma keratocytes and endothelial cells. However, the intact epithelium is an effective barrier to even the FL-NP-siRNA nanoparticles.

There is no standard imaging methodology for evaluating corneal haze formation. The accepted method to evaluate corneal haze is visual grading by a masked ophthalmologist. However, this method fails to give a definitive quantifiable measurement and also suffers from subjective bias of the observer. Hence, in this study, we have tried to establish a standard method for quantifying haze formation as a function of transparency of the corneas (Figure 3-4A & 3-4B). The known pixel intensity of a standard white marker line - through unablated corneas and through ablated corneas was measured to determine the reduction in pixel intensity due to haze formation. In this study we were able to show that, when compared to unablated transparent corneas, the ablated/untreated corneas reduced transparency of the corneas by 11% while the NP-siRNA (5% opacity) and steroids (3% opacity) were successful in improving the transparency of the corneas by reducing haze formation. The results from image analysis were similar to that of the visual grading by an ophthalmologist. The delivery of the triple siRNA combination affected a marked decrease in the scar formation comparable to that of the current clinical treatment of steroids (Figure 3-1C & 3-1D). Analyzing RNA from the scar tissues show that NP-siRNA reduced the SMA expression by 78% while the steroids reduced the expression by 85% (Figure 3-4D).

To visualize the presence of SMA in the ablated untreated corneas and confirm protein level knockdown of the treatments, immunohistostaining was performed on three

corneas from each of the experimental groups. Rabbit globes that were ablated and untreated show SMA staining in the basal epithelium and anterior stroma (Figure 3-5A). A similar pattern of myofibroblasts formation was observed in both mice and rabbits after a PTK injury. (Mohan et al. 2008; 2011; Nakamura et al. 2001; Netto et al. 2006). In addition, when severe haze develops in human corneas after PRK, it is nearly always localized immediately beneath the epithelium and in the anterior stroma (Shah et al. 1998; Siganos, Katsanevaki, and Pallikaris 1999) - in the same location that myofibroblasts are noted in the corneas ablated *ex vivo*. Corneas that were treated with NP-siRNA and steroids show no staining for SMA, which confirmed the protein level knockdown of both the treatments (Figure 3-5E & 3-5F).

Results from this study show that the development of corneal haze in cultured corneas in terms of markers of corneal scarring is very similar to that observed in animals. Studies have also shown eunucleated rabbit eyes sustained in culture retain wound healing dynamics and are comparable to live rabbit eye model in terms of laser radiation exposure (Fyffe 2005; Kabosova et al. 2003; McCally and Bargeron 2000; McCally, Farrell, and Bargeron 1992).

Animal models have been used for corneal scarring studies post excimer laser surgery (Mohan et al. 2008; 2011; Netto et al. 2006). However, their use in large scale is limited for practical reasons. Corneal drug delivery experiments require sacrification of animals at each time point in the drug concentration profile, and the use of organ culture therefore help reduce our need for animals in such experiments (Toropainen 2007). Hence, an initial *ex vivo* organ culture screen followed by *in vivo* experiments would make the most efficient use of animals.

Development of an organ culture model for corneal scarring is an important middle ground between cell culture and animal experiments, especially since many of the main features in the formation of corneal scarring in animals were reproduced in the organ culture. The *ex vivo* scarring model can be an important screen for the testing and optimization of new anti-scarring drugs in addition to it being an important tool to study and understand the molecular pathways of the corneal wound healing process.

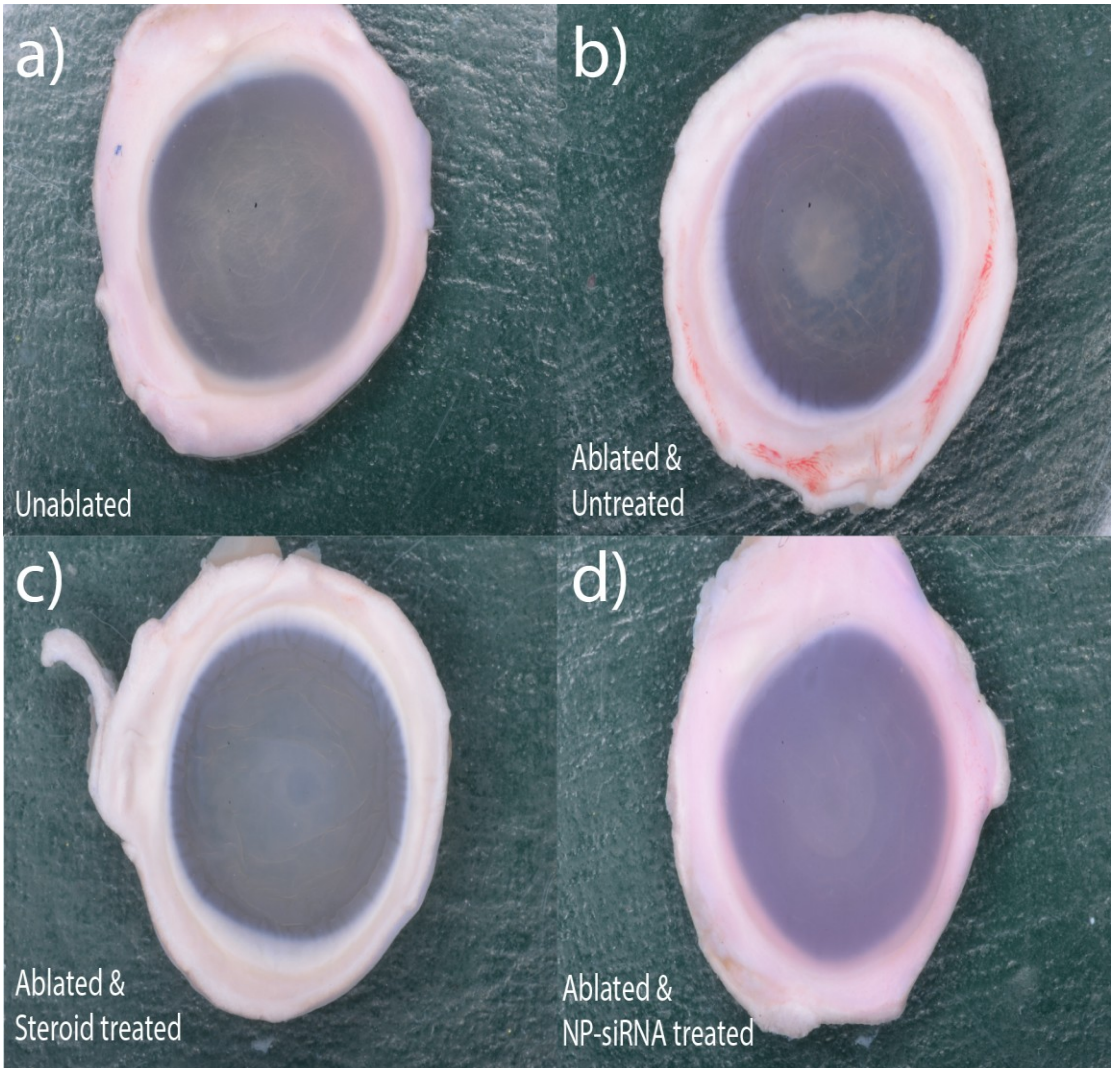

Figure 3-1. Visual comparison of ablated, unablated and treated corneas. Freshly obtained rabbit globes were ablated to a depth of 155um and cultured at the air-liquid interface for 21 days in serum free media. Four groups with six corneas each were tested experimentally – a) Unablated corneas, b) Lazer Ablated with no treatment, c) Lazer ablated and treated with Steroids, d) Lazer ablated and treated with triple siRNA complexed with nanoparticles. Images a-d were obtained after 13 days in culture. Images courtesy of Sriniwas Sriram.

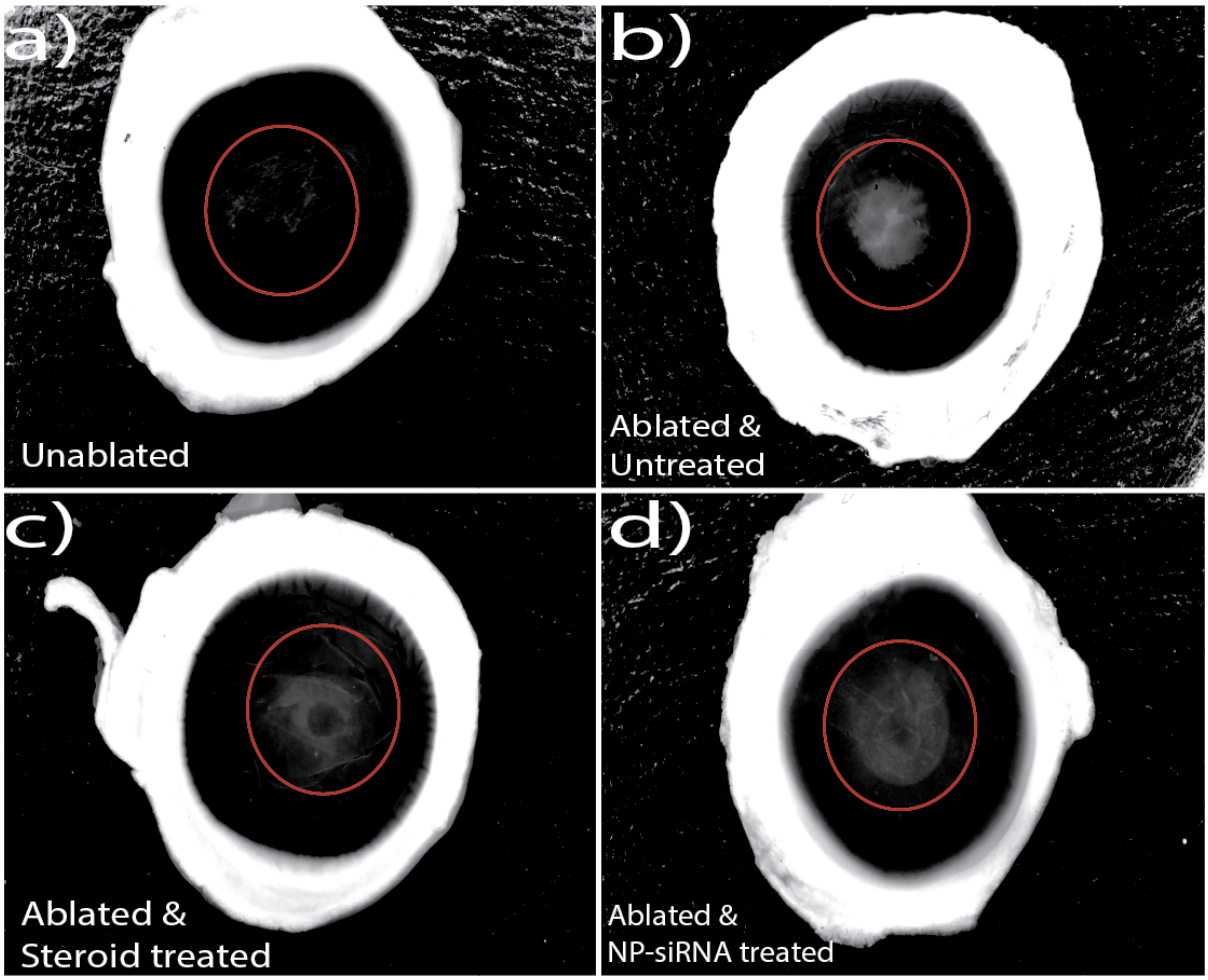

Figure 3-2. Image analysis of ablated, unablated and treated corneas. The images of corneas from the four groups of the above experiment – a) Unablated corneas, b) Laser ablated with no treatment, c) Laser ablated and treated with Steroids, d) Laser ablated and treated with triple siRNA complexed with nanoparticles were processed with Adobe photoshop to increase the visual contrast of haze. All the images were initially converted to grey scale, which was then followed by background correction to reduce the noise associated with the light scattering of unablated regions. The red circles in the image pick out the haze formation in the ablated corneas. Images courtesy of Sriniwas Sriram.

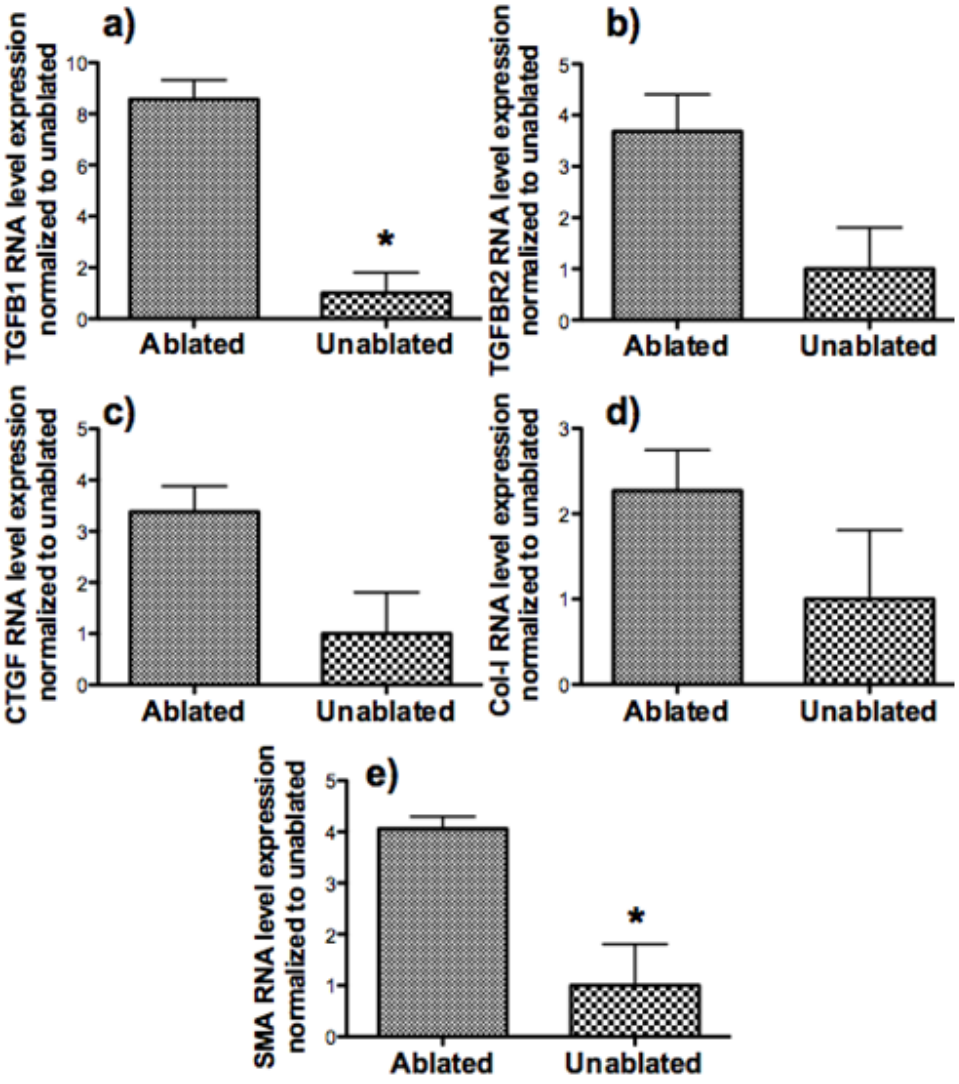

Figure 3-3. Comparison of RNA level expression of pro-fibrotic genes in ablated and unablated corneas. Freshly obtained rabbit globes were ablated to a depth of 155um and cultured at the air-liquid interface for 14 days in full serum media. RNA from the scar-like tissue was collected using a 8mm punch biopsy and the expression levels of 5 profibrotic genes were analyzed using qRT PCR. 18S rRNA was used as the housekeeping gene. All RNA expressions were normalized to their respective levels in unablated corneas.

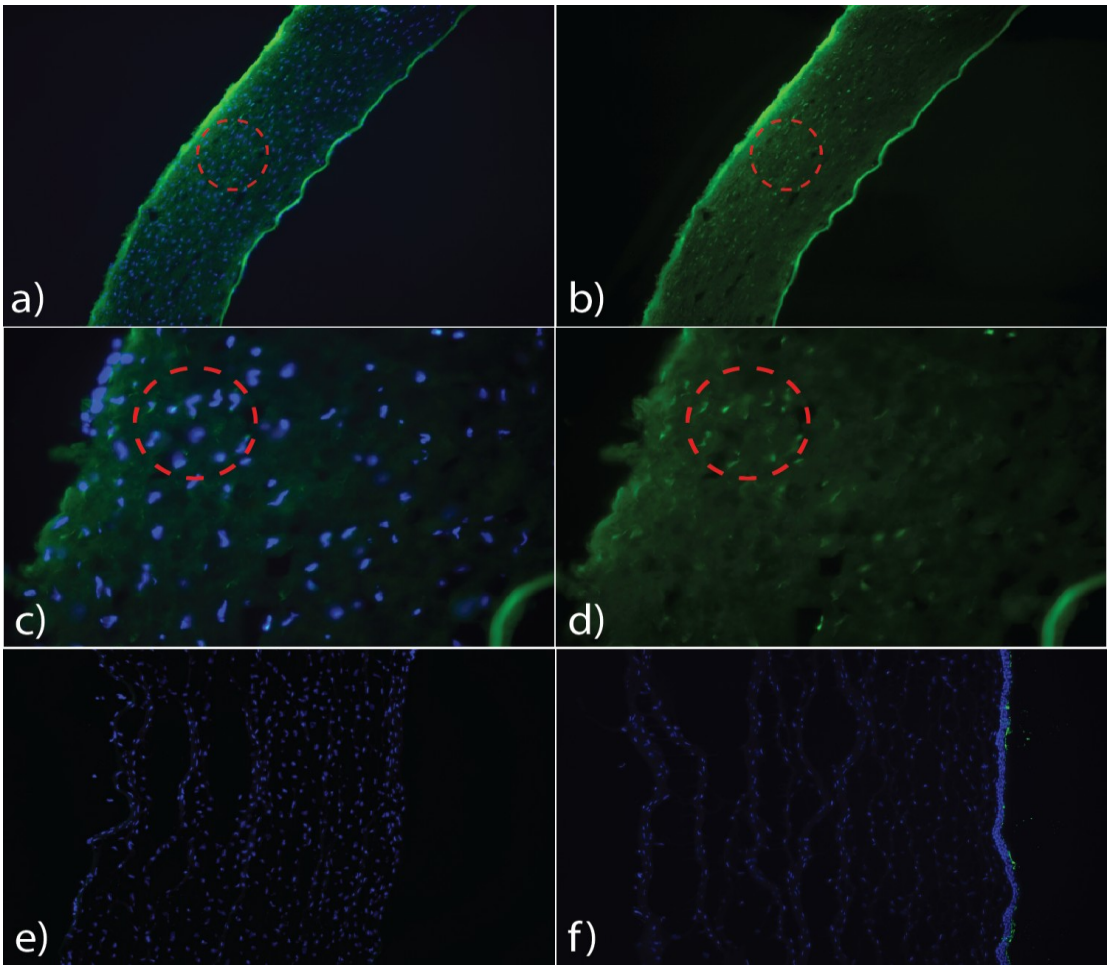

Figure 3-4. Nanoparticles deliver siRNA to all layers of the cornea in organ-culture. Whole rabbit globes were ablated to 125 microns using an excimer laser and treated with fluorescently labeled scrambled siRNA complexed with a nanoparticle for 1 minute. 6 hours after transfection, the corneas were fixed overnight in 4 % paraformaldehyde. They were then bisected, fixed in OCT and then sectioned in 10um slides. The blue color shows the cell nuclei, which were stained with DAPI, and the green shows the fluorescence of the delivered scrambled siRNA. Delivery of siRNA by nanoparticles after ablation is shown at 20x [a) DAPI and FITC, b) FITC] and 40x [c) DAPI and FITC, d) FITC]. Red circles show uptake of fluorescently labeled siRNA by the cells. No fluorescence is observed when - e) globes were treated with siRNAs alone without nanoparticles after ablation, f) globes were treated with nanoparticles complexed with siRNAs without ablating the epithelium. Images courtesy of Sriniwas Sriram.

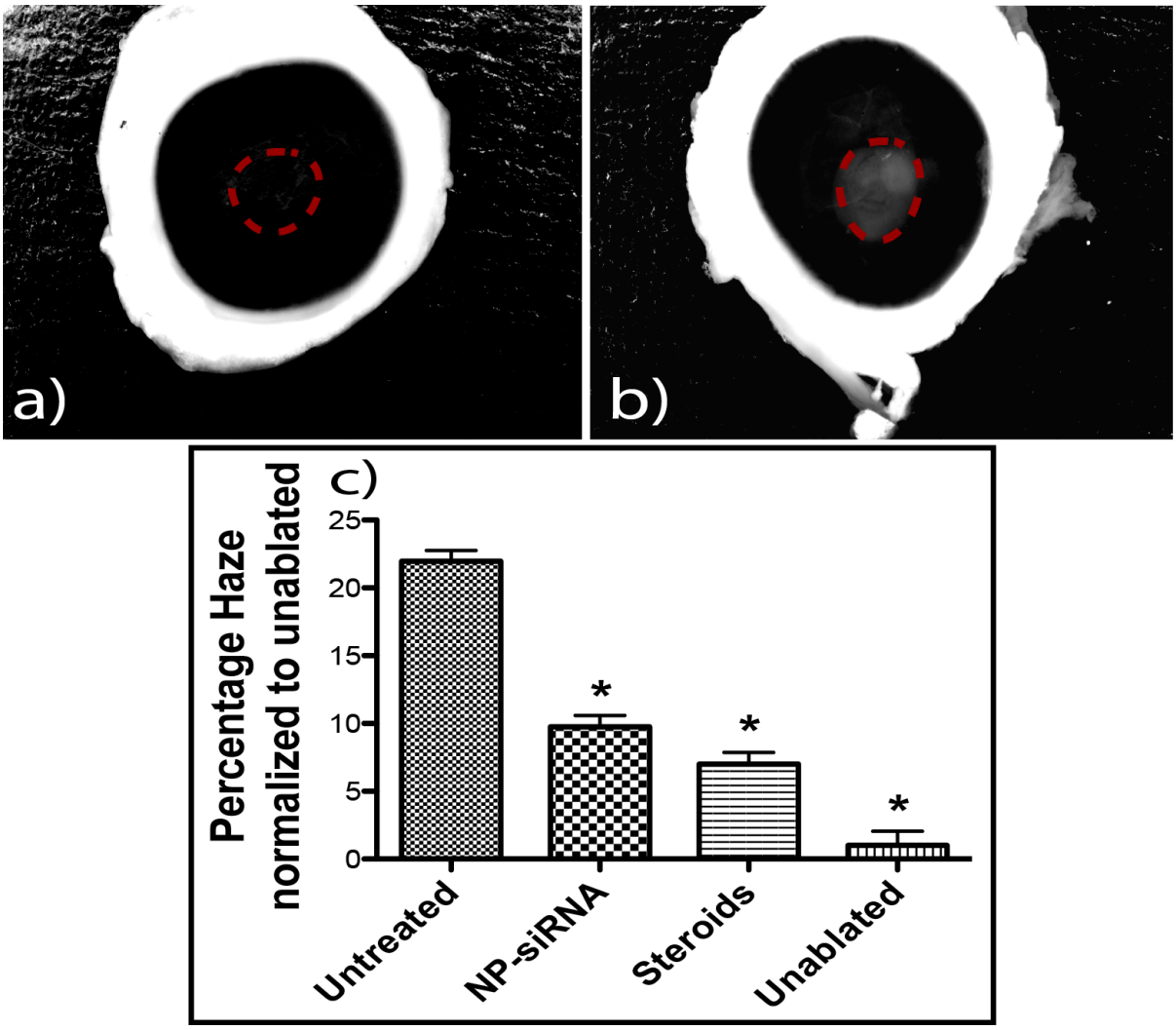

Figure 3-5. Evaluating the reduction in haze formation. The processed images from Figure 2 were analyzed using Adobe Photoshop to quantify the amount of haze formation. The lasso tool in Photoshop was used to trace the area of the scarring region as shown in images a) and b). Percent haze is calculated by measuring the pixel intensity in these selected regions and normalizing it to area of the selected regions. Image c shows the percentage of haze expressed in the ablated corneas in terms of the unablated corneas. Asterisks indicate significant differences ($p<0.05$) of the experimental group compared to untreated corneas, calculated using ANOVA with Tukey's HSD with n=3 in each experimental group.

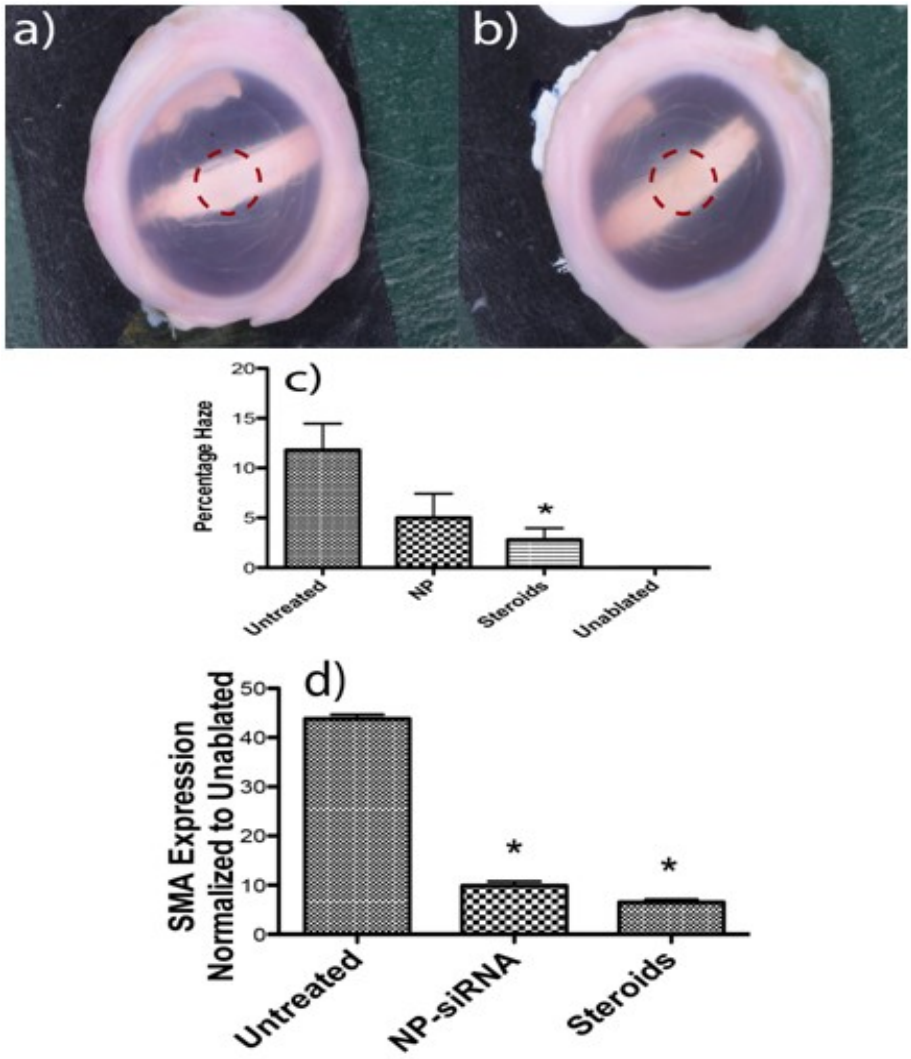

Figure 3-6. Evaluating the reduction in haze formation. The corneas in the experimental groups were imaged with a digital camera to calculate the reduction in transparency due to formation of scar-like features. Percent haze is calculated by finding the reduction in pixel intensity of a white marker line in ablated corneas (Image b) when compared to unablated corneas (Image a). Image analysis was used to quantify the degree of haze formation in these corneas when normalized to unablated corneas. RNA from the scar-like tissue was collected using a 8mm punch biopsy and the expression levels of SMA were analyzed with qRT PCR. 18S rRNA was used as the housekeeping gene and all expression levels were normalized to their respective levels in unablated corneas. Image d shows the reduction in SMA expression in treated corneas when compared to the ablated corneas.

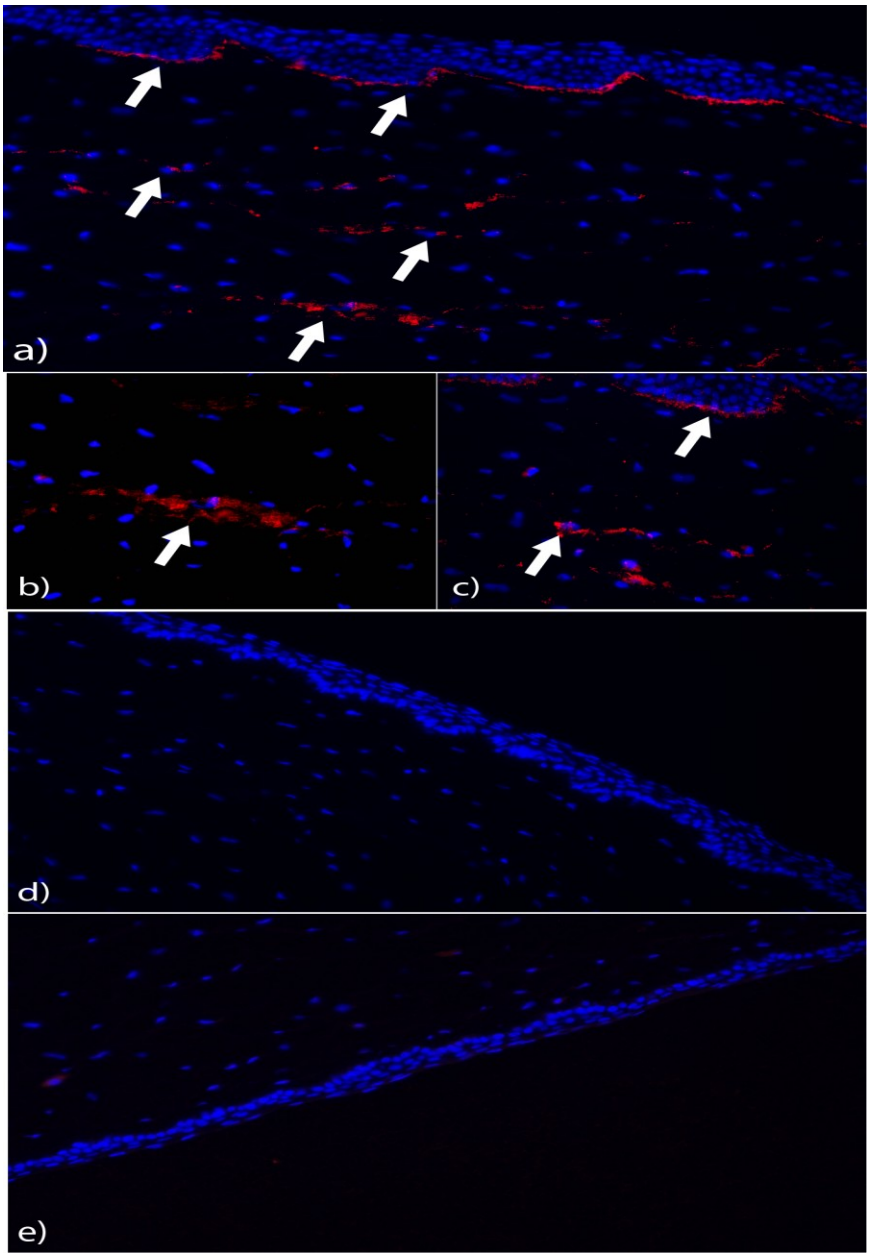

Figure 3-7. Immunohistostaining of corneal tissues show reduction in SMA after treatment with steroids and NP-siRNA. Corneas from the experimental groups were fixed overnight in 4 % paraformaldehyde. They were then bisected, fixed in OCT and then sectioned in 10um slides. To stain for SMA, slides were blocked in horse serum and then incubated with cy3 labeled SMA antibody. Rabbit globes that were ablated and untreated show SMA staining in the basal epithelium and stroma (Figure a). Figure b) and c) show higher magnification of areas with myofibroblasts. Globes that were ablated and treated with NP-siRNA and steroids show no SMA staining (Figures d and e). Images courtesy of Sriniwas Sriram.

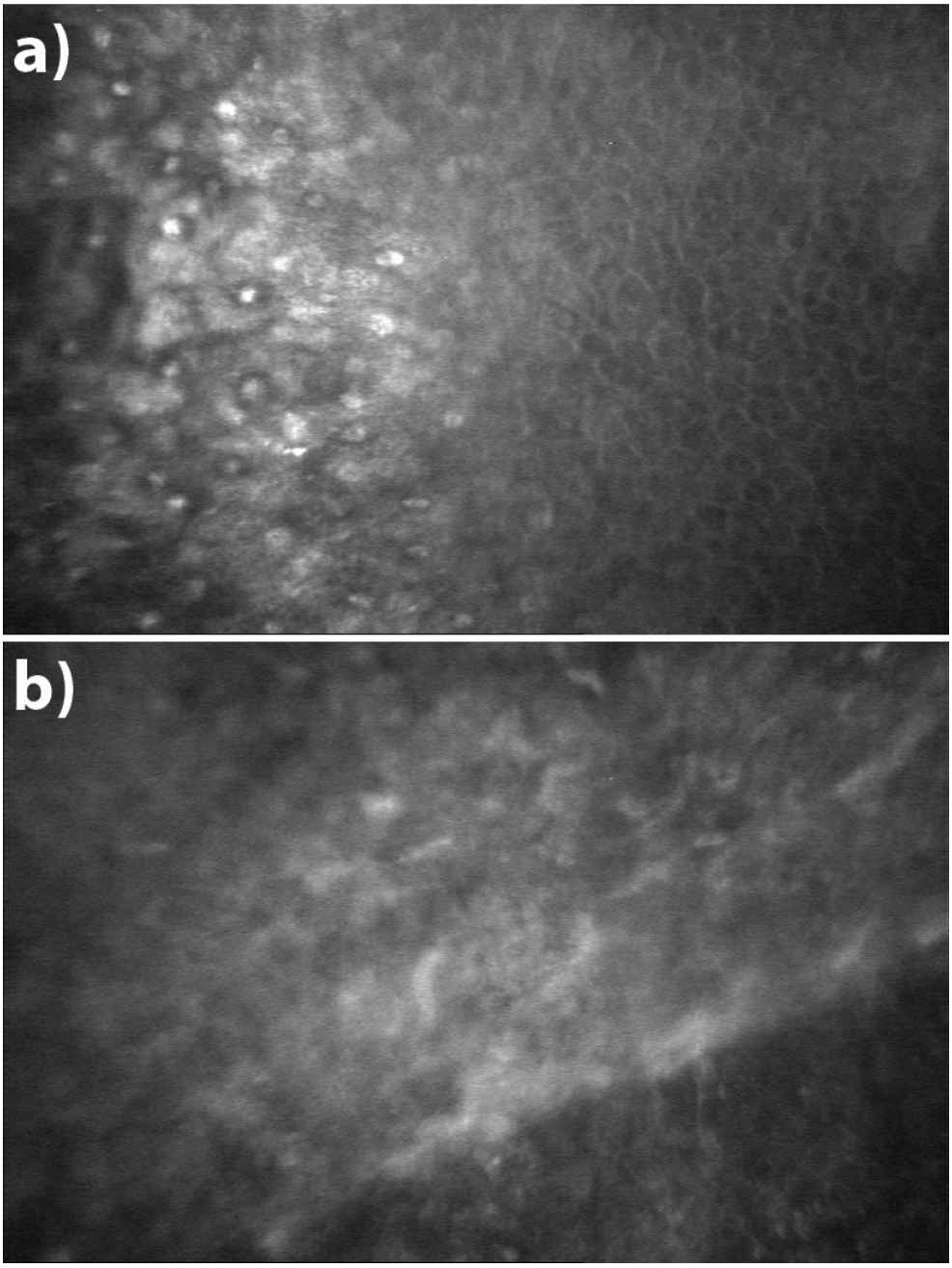

Figure 3-8. *In vivo* confocal images of ablated *ex vivo* corneas. Freshly obtained rabbit globes were ablated to a depth of 155um and cultured at the air-liquid interface for 21 days in complete cell culture medium. To visualize the presence of cells in the scarring region, the ablated corneas at the ends of a 50ml tube were imaged using an *in vivo* confocal microscope. Images a, b show activated epithelial and stromal cells. Images courtesy of Sriniwas Sriram.

CHAPTER 4
REDUCTION OF CORNEAL SCARRING IN RABBITS BY TARGETING THE TGFB1 PATHWAY WITH A TRIPLE SIRNA COMBINATION

Purpose

To test and deliver a previously optimized effective triple siRNA combination to the appropriate corneal layer with high post wounding localization of TGFB1 and CTGF so that there is maximal reduction of scar formation in rabbits.

Background

Corneal scarring remains a serious complication that can ultimately lead to functional vision loss. In an injured cornea, a cascade of molecular events is initiated by prolonged, elevated levels of transforming growth factor beta (TGFB1) which then combines with the Transforming Growth Factor Receptor II (TGFBR2) inducing the synthesis of Connective Tissue Growth Factor (CTGF) causing excessive scarring (corneal haze) that impairs vision. The TGF-β system, has emerged as a key component of the fibrogenic response to wounding by regulating the transformation of quiescent corneal keratocytes into activated fibroblasts that synthesize ECM and into myofibroblasts that contract corneal matrix (Chen et al. 2000; Jester, Petroll, and Cavanagh 1999). These myofibroblasts are filled with alpha smooth muscle actin (SMA) that forms microfilaments that are the major source of light scattering in corneal scars (Blalock et al. 2003). CTGF acting as a downstream mediator of TGFB1, down-regulates synthesis of corneal crystallin proteins in quiescent keratocytes and up-regulates synthesis of collagen. Thus, the excessive scattering of light that is clinically described as corneal scar and haze results from the combination of collagen laid down in irregular pattern in the wound and opaque activated fibroblasts and myofibroblasts

that no longer synthesize the corneal crystallin proteins that keep their cytoplasm transparent (Jester, Brown, et al. 2012).

We have previously shown the effect of PRK on CTGF levels in rat and mouse corneas and found that CTGF was present in all cell layers of the cornea. The levels of CTGF were found to continually rise from the time of wounding up through 28 days post wounding (Blalock et al. 2003). However, in order to completely understand the role of TGFB1 in tissues repair and scarring, it is essential to understand the timing and site of synthesis of these growth factors so that the appropriate cell layer is targeted for nucleic acid therapies. The experiments in this study are expected to reveal when and where TGFB1 and CTGF are synthesized after a corneal injury so that the best mode of action for an anti-fibrotic therapy can be chosen.

There currently are no FDA approved drugs that selectively reduce the expression of genes causing corneal scarring and haze. At present, the methods used to decrease corneal haze are topically applied steroids or anti-metabolite drugs that target the cells capacity to respond to signaling. Mitomycin C is used during some ocular surgeries, but it may have very damaging side effects, such as epithelial defects, stromal melting, endothelial damage, and conjunctival thinning (Azar and Jain 2001). Hence, there is a need to develop a targeted approach that can nullify the specific molecular pathways that give rise to a scar.

It is however difficult to achieve significant therapeutic effect by employing a one-target, one-drug paradigm on such a complex, multi-factorial signaling pathway. Hence, using a multi-target approach can interrupt or act on the complex signaling network at multiple points, and affect the cell in ways that an individual component cannot (Chou

2006). In this study, we have tested a siRNA triple combination targeting TGFB1, TGFBR2 and CTGF. This triple siRNA combination was shown to be effective in reducing the expression of target (TGFB1, TGFBR2 and CTGF) and downstream mediators like Collagen-I and α-Smooth Muscle Actin (SMA) in both *in vitro* cell culture system and *ex vivo* organ cultures (sriram et al. 2012).

Additionally, it is important to deliver these siRNA combinations to the corneal layer where there is high localization of the target growth factors after wounding. Although most of the targeted anti-fibrotic approaches target the stromal fibroblasts due to the eventual presence of myofibroblasts in this region, there has not been any research on the post-wounding localization of TGFB1 and CTGF in the epithelium and the endothelium. A delivery method that targets the corneal layer with maximum post-wounding growth factor localization is critical for an effective therapy.

Delivery of drugs to the cornea is a major challenge, as the mechanical barriers that protect the cornea (multi-layered epithelium, tight junctions) constrain ocular drug delivery (Hao et al. 2010). The principal properties governing corneal drug absorption are its lipophilicity, partition coefficient and molecular size (Lee and Robinson 1986). Nanocarriers is a potential solution for targeted ocular drug delivery as they have been shown to be non-immunogenic, have relatively low toxicity, be resistant to protein/serum absorption and are stable in an enzymatic environment (la Fuente, Seijo, and Alonso 2008). We have previously showed the high efficacy of the nanoparticle kit used in this study in delivering fluorescently labeled siRNA to all layers of the cornea including the endothelium in an *ex vivo* organ culture model (sriram, Robinson, et al. 2013).

The overall goal of this study is to test and deliver a previously optimized effective triple siRNA combination to the appropriate corneal layer with high post wounding localization of TGFB1 and CTGF so that there is maximal reduction of scar formation in rabbits.

Materials and Methods

Laser Ablation of Rabbits

Adult New Zealand Rabbits free of disease were used and treated according to ARVO Statement for the Use of Animals in Ophthalmic and Vision Research. Excimer ablation and collection of corneas was performed as previously described (Netto et al. 2006). Briefly, rabbits were anesthetized with isoflurane inhalation, and proparacaine eye drops provided topical anesthesia. Laser ablations were performed to both eyes of each rabbit with a Summit SVS eximer laser that is committed to animal vision research. In this study, two different approaches were tested to obtain the most intense scarring in the rabbits. In the first approach, using the laser in phototherapeutic keratectomy mode, the central 6 mm diameter area of the cornea was ablated at a dose of 160mJ/cm2 to an initial depth of 80 microns to remove the epithelium and then the final 45 microns were ablated by placing a mesh over the cornea to make an uneven ablation. In the second approach, using the same laser parameters, the central 6 mm diameter area of the cornea was ablated to an even depth of 155 microns.

The eyes were then pretreated with 50uM EDTA for 10 minutes. A total of 150ul of the nanoparticle complexed with the siRNA triple combination was added to one of the eyes while the other was treated with the vehicle control and was considered as a paired negative control. The eyes were held open for 3 minutes to allow the nanoparticle to penetrate the stroma before being disturbed. No postoperative topical

steroid was used to ensure that the wound healing process is not altered with anti-inflammatory agents. Corneas were collected at different time points according to the experiment, homogenized in a pestle with liquid nitrogen and then transferred to TRIzol. The RNA was then extracted using a hybrid RNA extraction protocol with RNeasy spin columns (Rodriguez-Lanetty 2007).

Gross Corneal Dissection

Rabbits without observable corneal wounds were anesthetized, excimer ablated to 125 microns and euthanized at the designated time points as described before. A scalpel was used to immediately scrape the epithelium off with care taken to ensure that the scraped mass was retained on the blade. The scraped epithelial mass was then transferred to 350 µl of tissue lysis buffer (Qiagen, buffer RLT) and the blade was rinsed with 250 µl of additional lysis buffer. The cornea was then excised from the globe by cutting with a fresh scalpel and scissors at the corneal/scleral boundary. The cornea was placed face down and yet another fresh scalpel was used to scrape off and retain the endothelium as was done with the epithelium. The endothelial mass was transferred to 350 µl of lysis buffer and the blade rinsed with an additional 250 µl of lysis buffer. Each grossly isolated cellular layer was then subjected to ultrasonication on ice for further tissue disruption. The probe was rigorously washed, rinsed and dried in between each sample. The homogenates were then immediately loaded onto Qiagen gDNA removal columns and the RNA was purified in accordance with the manufacturer's provided protocol (Qiagen RNAeasy, Qiagen, Inc., Cat. #74104).

The purified RNA was quantified via ultra-violet absorbance using a Nanodrop ND-1000 spectrophotometer set for RNA quantification.

Preparation of siRNA-Nanoparticles

A commercially available nanoparticle kit called Invivoplex® was purchased from Aparnabio (Rockville, MD) and used according to manufacture's instructions. Briefly, siRNA triple combination solution was made at a concentration of 0.9 mg/ml. 600uL of this solution was added with 300uL of the provided cargo buffer. This solution was added drop wise to 900uL of the given nanoparticles over a magnetic stirrer. This preparation forms siRNA nanoparticles <50 nm that are stable for a week.

Reverse Transcription-Polymerase Chain Reaction

Total RNA was extracted using the Qiagen RNeasy mini isolation kit (Qiagen, Inc., Valencia, CA) and used according to the manufacturer's directions. cDNA was synthesized using the High Capacity cDNA Reverse Transcription Kit (Applied Biosytems, Carlsbad, CA) according to manufacturer's procedure. The level of mRNA for TGF-B1, CTGF and SMA were determined using the Real-Time PCR TaqMan assay. The primers and probes for each gene are defined in Table 2-3. The endogenous control, ribosoma18S RNA and GAPDH was used normalize target genes. Primers, probes and cDNA were combined with TaqMan Universal PCR Master Mix (Applied Biosytems, Carlsbad, CA) and amplification was performed by the Applied Biosystems 7300HT Fast Real Time PCR System (Carlsbad, CA). A few samples were run without reverse transcriptase to measure the quantity of genomic DNA (gDNA) present in the sample. The thermal cycling conditions were as follows: 2 min at 50°C, 10 min at 95°C, 40 cycles of 15 sec at 95°C, and 1 min at 60°C. The relative gene expression of the growth factors was calculated using the 2-ΔΔCt method.

Immunohistochemistry

The rabbit corneas from the experiments were fixed overnight in 4 % paraformaldehyde. They were then bisected, fixed in OCT and then sectioned in 10um slides. The slides were then washed with PBS and blocked in horse serum for 1 hour. Finally, they were incubated with SMA antibody-Cy3 (Sigma) for 1hour at room temperature. The slides were mounted with DAPI and imaged using fluorescence microscope.

Macrophotography

Prior to general anesthesia, each eye was topically anesthetized with proparacaine and each pupil was dilated with phenylephrine 2.5% and tropicamide eye drops. Each rabbit was then generally anesthetized with inhaled isoflurane as described earlier. The eyelids were held open and out of the way with either an eyelid speculum or a pair of cotton swabs. A Nikon D7000, was outfitted with a macro lens capable of native 1:1 reproduction (either a 100mm Tokina or 60mm Nikkor) and the Nikon R1C1 Creative Lighting System (CLS) flash system. The D40 was set to the “Normal” program, ISO 200, manual exposure with a shutter speed of 1/500 second and f/16. While the 7000 was set to the “Standard” program, ISO 100, manual exposure with a shutter speed of 1/250 second and f/18. To visualize and measure haze, the flash power was set manually (1/16th, D40, 1/6.4th D7000) and neither the flash nor lens had a filter. For all images, the lens was set to manual focus and pre-focused to a 1:1 reproduction ratio and the camera was focused by moving the camera closer or further from the subject. Guide lights on the flash heads were used to facilitate haze visualization and focusing.

Statistical Analysis

All experiments were performed in triplicate and all statistical analyses were conducted using GraphPad prism (San Diego, CA). Student's t test or Analyses of Variances (ANOVA) with Tukey's post-hoc assessments were accordingly used to test for significance between the groups. Results were considered statistically significant where $p<0.05$.

Results

The levels of TGFB1 and CTGF were analyzed at several time points following ablation to find the best time to dose with anti-scarring drugs. Two different models of scarring were tested to find which of the two generated the most intense scaring in rabbits. Also in this study, the *in vivo* efficacy of a previously optimized triple siRNA combination that was effective in reducing downstream scarring genes (SMA and collagen-I) in both *in vitro* culture and *ex vivo* organ cultures was evaluated. The triple siRNA combination targets three critical scarring genes within the same TGFB1 pathway – TGB1, TGFBR2 and CTGF (sriram et al. 2012; sriram, Robinson, et al. 2013).

The Effect of PRK on mRNA Levels of TGFB1 and CTGF

The corneas of 11 rabbits were evenly ablated to 125 microns using an excimer laser. 3 rabbits were sacrificed at 30 mins after ablation, and 4 rabbits each for Day1 and Day2 post-ablation. The corneas of three rabbits were unablated and used as control. At the designated time points, the corneas were collected and the epithelium and endothelial layers were scrapped using a surgical scalpel and collected in separate tubes. The expression levels of TGFB1 and CTGF were analyzed using qRT PCR. As shown in Figure 4-1, there is an initial spike in the levels of TGFB1 and CTGF as early

as 30 minutes after ablation. There is then a decrease in the expressions at Day 1 followed by an exponential increase on Day 2. The expression trend of TGFB1 and CTGF follow a similar trend in both the epithelial and endothelial layers. Figure 4-1E plots the RNA level expressions of TGFB1 and CTGF in terms of the epithelium. The expressions of both TGFB1 and CTGF was consistently higher in the endothelial layer when compared to the epithelium particularly at day1 when the expression of CTGF in endothelium was ~35 times that of the epithelium. All expressions were calculated with respect to the unablated corneas and was normalized using GAPDH as the housekeeping gene.

The Effective Triple Combination (T1R2C1) Inhibits Target mRNA Accumulation in Rabbits

The corneas of 9 rabbits were unevenly ablated to 125 microns using an excimer laser. The right eye was treated with 150 uL of the effective triple combination (T1R2C1) complexed with nanoparticles and the left eye received equal volume of the vehicle control. One day later, 3 rabbits were humanely sacrificed and total RNA was extracted for analysis by RT-PCR.The effective triple combination (T1R2C1) gave an average of knockdown of 57% for TGFB1, 25 % for TGFBR2 and 24% for CTGF (Figure 4-2). One of the rabbits (rabbit 1) had a maximum knockdown of 80% for TGFB1, 57% for TGFBR2 and 46% for CTGF indicating some the siRNA combination was effectively delivered to the corneal stroma in this animal. The knockdown percentages were calculated with respect to the left eye, which received vehicle control without the siRNA.

SMA Immunohistostaining in Triple siRNA Treated Rabbit Corneas

6 out of the 9 treated rabbits from the above experiment were used for a long-term experiment to observe scar formation. After 14 days, the intensity of scarring in

both the treated and the control eyes were graded by a masked ophthalmologist and were also imaged using a digital camera. The rabbits were then humanely sacrificed and three corneas were collected for SMA immunohistostaining. The corneas were fixed overnight in 4 % paraformaldehyde. They were then bisected, fixed in OCT, sectioned in 10um slides and stained for SMA. The treated cornea of two of the three rabbits selected for immunohistostaining had a lower haze grading score when compared to the control cornea. The control eye that was ablated and treated with vehicle control shows SMA staining in the basal epithelium and stroma while the triple siRNA treated right eye shows reduction in SMA staining (Figure 4-3B & 4-3D).

Three corneas from the 6 treated rabbits from the above experiment were collected for RNA level analysis by qRT PCR. SMA knockdown percentage of >40% was observed in 2 out of the 3 rabbits. The untreated left eye in these rabbits had haze-grading scores of 2 and 3 respectively. No knockdown was observed in the other rabbit, which had a haze grading score of one in the untreated left eye. The RNA level knockdown percentage of SMA was calculated with respect to the untreated left eye and all expressions were normalized to 18S rRNA.

Macrophotography Images of Reduction in Scarring by Repeated siRNA Dosing

The corneas of 3 rabbits were evenly ablated to 155 microns using an excimer laser. One of the rabbits had a pre-existing scar and spots of neovascularization on the right eye and hence had to be excluded. The right eye was treated with the effective triple combination (T1R2C1) complexed with nanoparticles for the first three days after ablation while the left eye was left untreated. After 14 days, the corneas of both rabbits were imaged using the macrophotography technique described in the methods section.

The haze grading scores of both the rabbits were similar with Rabbit b showing a slight reduction in scarring after treatment (Figure 4-4).

Quantification of Scar Reduction by the siRNA Treatment

The digital images from the above experiment were subjected to anti-red gray scale conversion by only using the data in the blue channel. The contrast was increased by automatic brightness correction in ImageJ. The wounding region was split into two regions – Top (Region-I) and Bottom (Region-II) (Figure 4-5A & 4-5B). The pixel intensities of the regions of interest were normalized to that of the transparent unwounded regions of the corresponding corneas. The percentage of haze reduction was calculated by the reduction in pixel intensity of the scarring region in the treated eye with respect to that of the untreated eye. The region – I of both the rabbits show an average of ~22% reduction in scarring due to the siRNA treatment (Figure 4-5C). However there was no visible reduction in scar formation in region II of both the rabbits.

After imaging, the wounding region in the corneal tissues was collected with a 8 mm biopsy punch for RNA analysis. In the corneas treated with the triple siRNA combination, both the rabbits show a corresponding reduction of 60% and 40% in the RNA level expression of SMA (Figure 4-5D). The knockdown percentages of SMA in the corneas were calculated with respect to the untreated eye. All expressions were normalized to 18S rRNA.

Discussion

Several papers discuss the importance of the TGFB1 pathway acting through CTGF to activate quiescent corneal keratocytes and transform them into fibroblasts that synthesize collagen and further transform into myofibroblasts (Grotendorst 1997; Jester, Petroll, and Cavanagh 1999; Massague 1990). However, there has been very little

research on which cell layers of the cornea synthesize high levels of TGFB1 and CTGF. Our observation that both TGFB1 and CTGF mRNA levels are highest in the corneal endothelium is novel, and it has reshaped the thinking behind the primary target cells and future delivery methods for corneal anti-fibrotic therapies. The immediate increase in the expressions of TGFB1 and CTGF as early as 30 minutes post ablation highlights also emphasized the importance of an immediate treatment. The nanoparticle delivery system used in this study was able to successfully deliver siRNA to all layers of the cornea including the endothelium in an *ex vivo* organ culture model (sriram, Robinson, et al. 2013).

The results of the initial therapeutic experiment assessing the efficacy of a single application of the triple siRNA combination demonstrated the “proof of principle” that the siRNAs could be effectively delivered into the target corneal cells. However, there was variability in the level of knockdown among the three rabbits, suggesting that the dosing was not optimized for *in vivo* experiments. Factors that could contribute to the variability include the presence of a nictitating membrane in addition to the eyelids and tears that tend to clear the surface of the cornea and reduce drug exposure time. It is also possible that the volume of the siRNA formulation used for the single dose (150 uL) in this experiment may also have been too high, which would have reduced the amount of the siRNAs that penetrated the cornea and were instead washed away once the trephine was removed.

The reduction in scar formation, 14 days after a single dose of triple siRNA treatment, also showed a positive trend. Three out of six rabbits had a reduction in scar formation as observed in the haze grading scores of a masked ophthalmologist. Both

the digital image and the immunohistostaining staining for SMA in Figure 4-3 show a reduction in scarring in the treated corneas when compared to the control. Both of these measurements were, however, qualitative, and we were unable to accurately quantify the exact reduction in scarring due to the lack of a standard imaging technology in the field of corneal scarring for those rabbits.

There was an interesting trend associated with the haze grading scores and the RNA knockdown percentage of SMA. We observed a RNA knockdown of 40% and 50% in the two rabbits that had a haze grading score of 2 and 3 respectively. However, no SMA knockdown was observed in the rabbit with a haze grading score of 1. This suggests that the triple siRNA combination is effective in knocking down SMA expressions in intense scars and is less effective in case of mild scarring.

A key paper in the literature reports that deeper ablations during PRK lead to more intense scarring in animals (Netto et al. 2006). In the second therapeutic experiment, we created a deep corneal ablation of 155 microns and also repeated the dosing of the triple siRNA combination for the first 3 days after ablation. Neither of the two rabbits in this experiment, however, developed an intense scar in the untreated control corneas. The haze grading scores of both the rabbits were similar with one showing a slight reduction in scarring after siRNA treatment. However, the image analysis on the digital images revealed an average of ~22% reduction in scarring in region 1 of both the corneas treated with the siRNA combination (Figure 5). It is interesting to note that the siRNA treatment had an effect in reducing scarring in Region 1, but not in Region - 2. This could be due to the uneven transfection of the siRNA-

nanoparticle complex into the different corneal layers. The RNA level expression of SMA was also reduced in both the rabbits by 60% and 40%, respectively.

In this study, we performed a series of pilot experiments to better understand the dynamics involved in the *in vivo* translation of an effective *in vitro* anti-fibrotic drug. The most immediate problem associated with the testing of an anti-fibrotic drug in the cornea of rabbits is the generation of a consistent and intense scar. We tried two different models of scarring in this study and although the corneas develop mild to average hazing, there is no consistent and intense scarring among animals. Since the variation in intensity of scarring among animals is natural and cannot be controlled, treating the corneas with TGFB1 post ablation for the first two days may help in the intensification of scar formation (Desmoulière et al. 1993).

Finally, the dosing regimen needs to be optimized so that maximum amount of inhibitory RNA can be delivered to the cornea. Lowering the volume and administering the siRNA cocktail for 2-3 days after the surgery along with an agent to increase the viscosity of the drug, so that it sticks to the surface of the cornea for a longer duration, might help increase the drug exposure time (Tani, Katakami, and Negi 2002). Other options could also include iontophoretically driving the drug to different layers of the cornea (Hao et al. 2009; Mohan et al. 2012). Once these parameters are optimized, the effective triple siRNA combination could lead to significant reduction of corneal scarring.

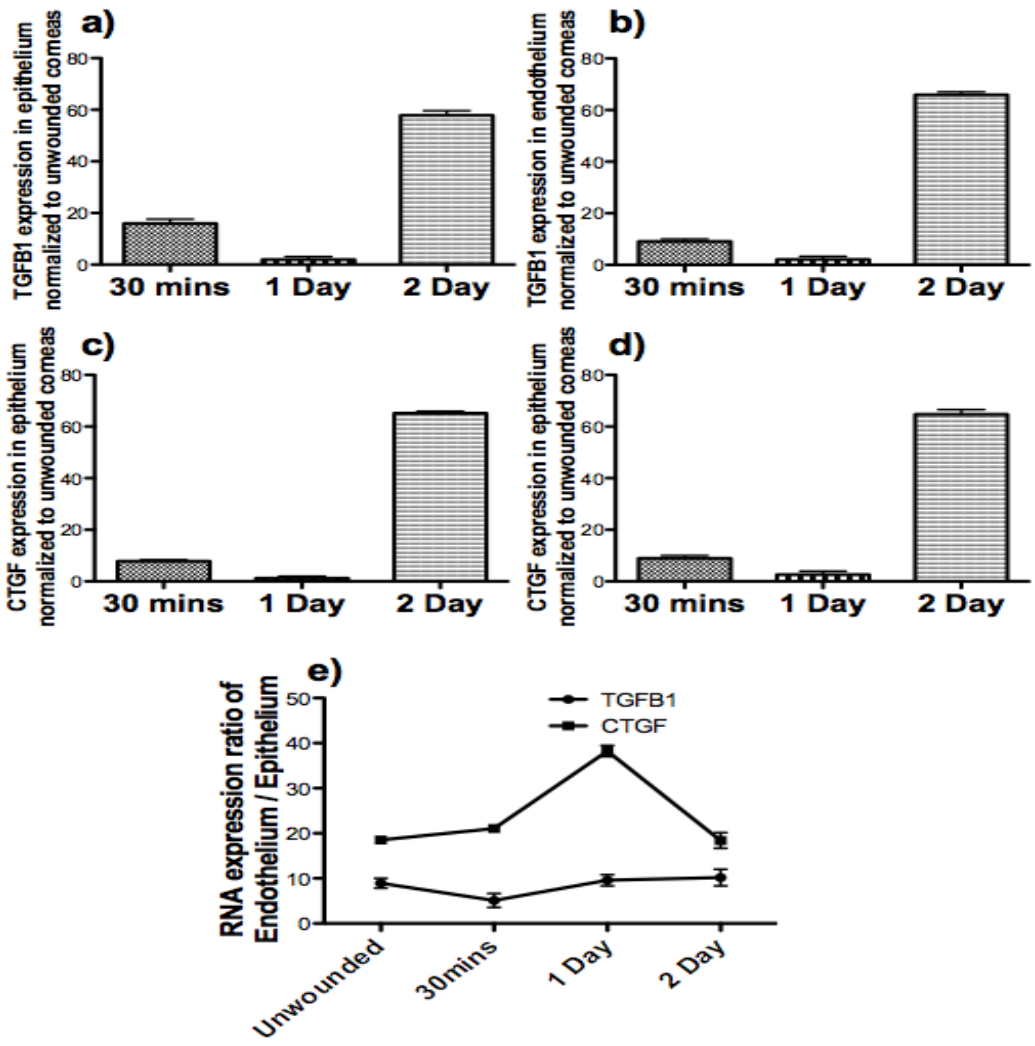

Figure 4-1. Post-ablation expression timeline of TGFB1 and CTGF. The corneas of 11 rabbits were evenly ablated to 125 microns using an excimer laser. 3 rabbits were sacrificed at 30 mins after ablation, and 4 rabbits each for Day1 and Day2 post-ablation. The corneas of three rabbits were unablated and were used as the control. The corneas were collected and the epithelium and endothelial layers were scrapped using a scalpel and collected in separate tubes. The expression levels of TGFB1 and CTGF were analyzed in the epithelial (Images a and b) and endothelial (Images c and d) layers using qRT PCR. All expressions were calculated with respect to the unablated corneas and was normalized using GAPDH as the housekeeping gene. Figure e plots the RNA expressions of TGFB1 and CTGF in endothelium in terms of the epithelium.

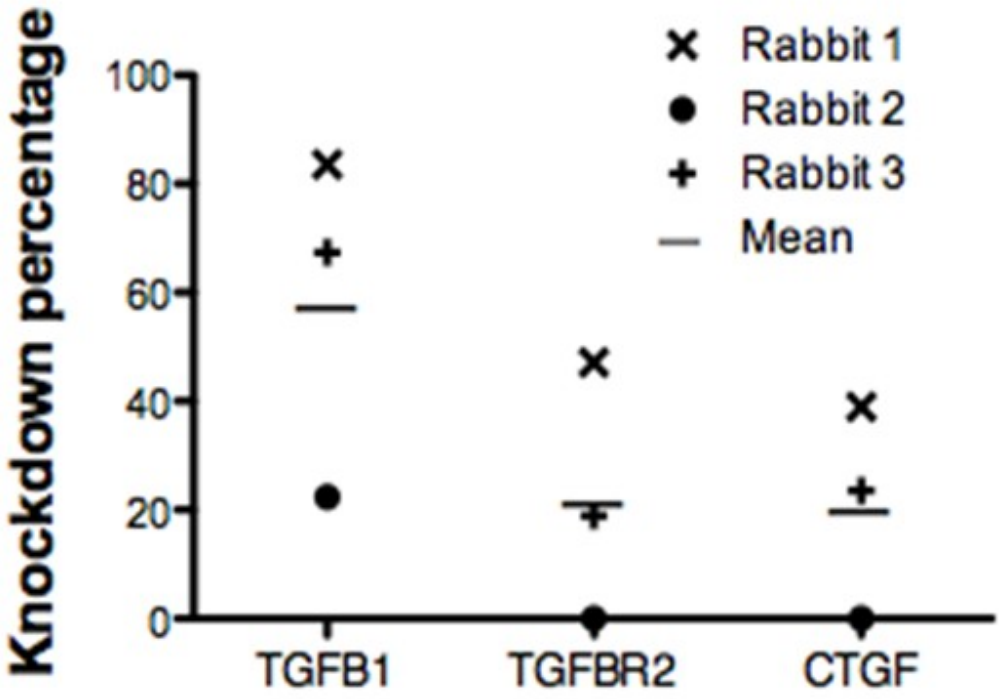

Figure 4-2. Short-term knockdown of target growth factors. The corneas of 3 rabbits were unevenly ablated to 125 microns using an excimer laser. The right eye was treated with the effective triple combination (T1R2C1) complexed with nanoparticles and the left eye received the vehicle control. One day later, the rabbits were sacrificed and RNA was extracted for analysis by qRT PCR. The figure gives the RNA level knockdown percentages of the target growth factors calculated with respect to the left eye. All expressions were normalized to 18S rRNA.

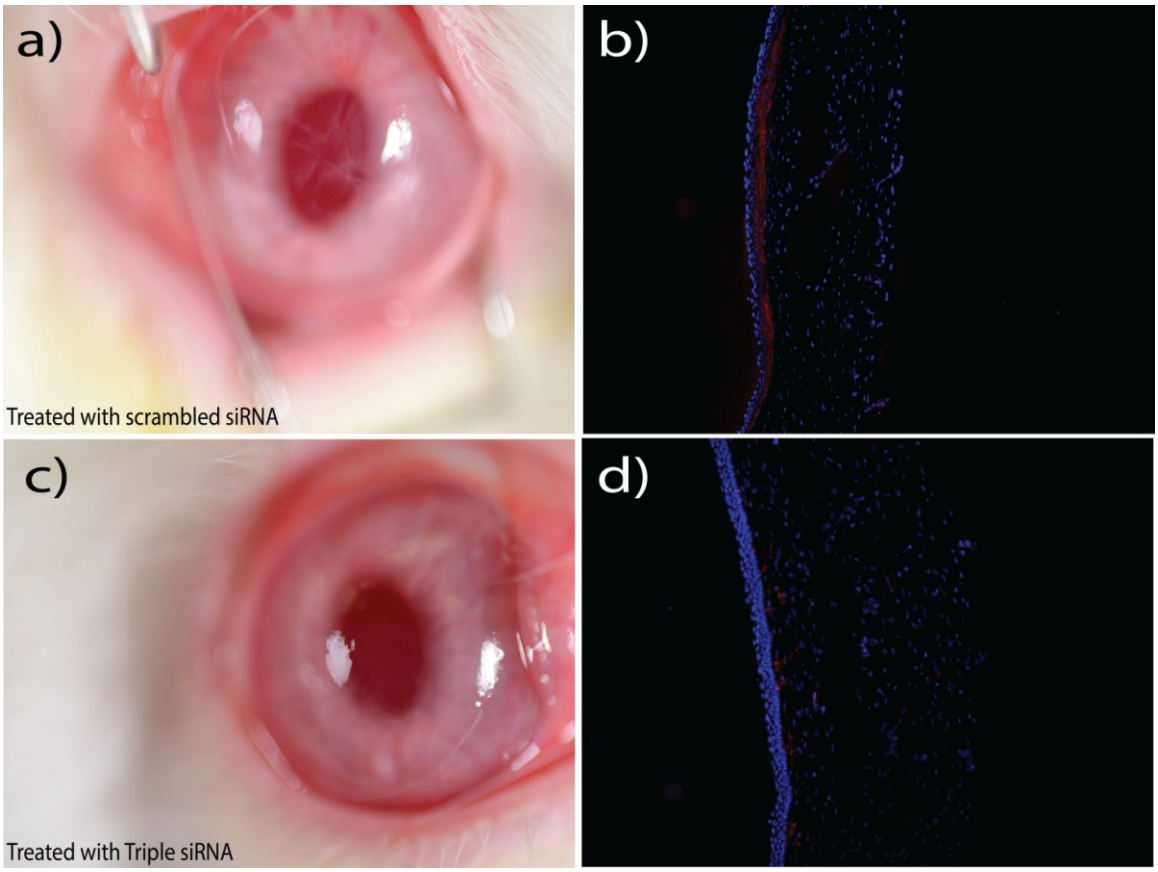

Figure 4-3. SMA immunohistostaining in triple siRNA treated rabbit corneas. The corneas of 6 rabbits were unevenly ablated to 125 microns using an excimer laser. The right eye was treated with the effective triple combination (T1R2C1) complexed with nanoparticles and the left eye received the vehicle control. 14 days later, the rabbits were sacrificed and three corneas were collected for SMA immunohistostaining. The corneas were fixed overnight in 4 % paraformaldehyde. They were then bisected, embedded in OCT and then sectioned in 10um slides. To stain for SMA, slides were blocked in horse serum and then incubated with cy3 labeled SMA antibody (red). The control eye that was ablated and treated with vehicle control shows SMA staining in the basal epithelium and stroma (Image b) while the triple siRNA treated right eye show reduction in SMA staining (Image d). Image a and c show digital camera images of the eyes treated with scrambled siRNA and triple siRNA respectively. Images courtesy of Sriniwas Sriram.

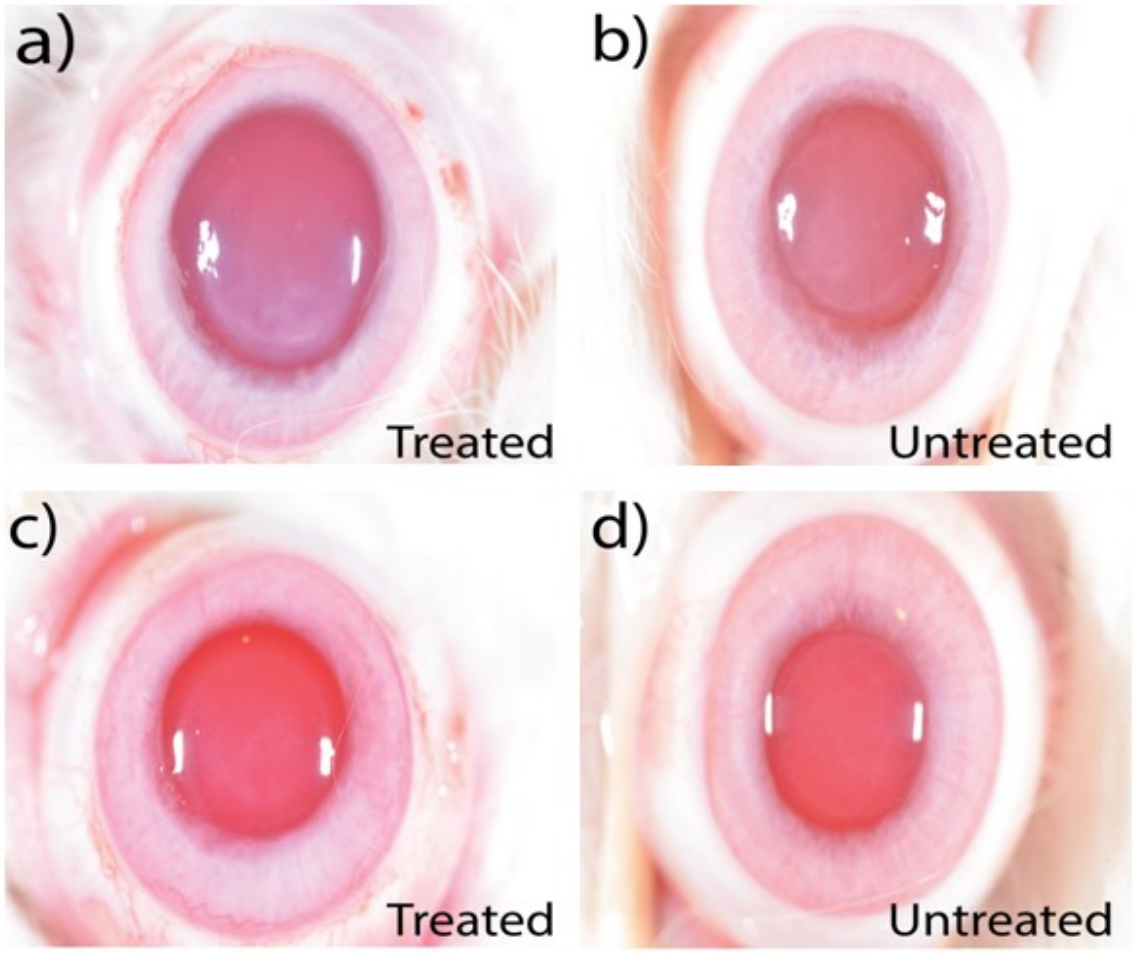

Figure 4-4. Reduction in scarring by repeated siRNA dosing. The corneas of 3 rabbits were evenly ablated to 155 microns using an excimer laser. The right eye was treated with the effective triple combination (T1R2C1) complexed with nanoparticles for the first three days after ablation (Figure a and c) while the left eye was left untreated (Figure b and d). Both eyes were imaged using a digital camera after 14 days. Images courtesy of Sriniwas Sriram.

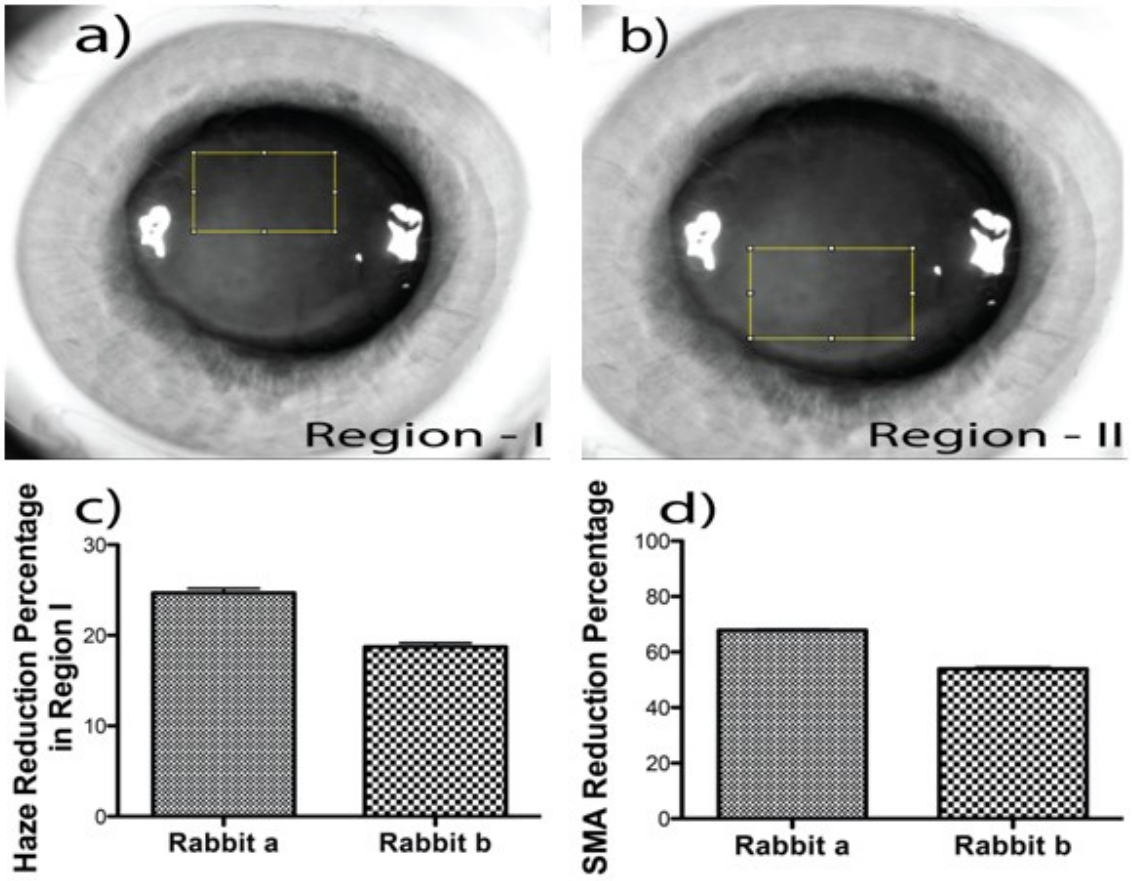

Figure 4-5. Quantification of scar reduction. The digital images from the above experiment were subjected to anti-red grayscale conversion by using the data in the blue channel. The contrast was increased by automatic brightness correction in ImageJ. The wounding region was split into two regions – Top (Region-I) (Figure a) and Bottom (Region-II) (Figure b). The pixel intensities of the regions of interest were normalized to that of the transparent unwounded regions of the corresponding corneas. The percentage of haze reduction was calculated by the reduction in pixel intensity of the scarring region in the treated eye with respect to that of the untreated eye (Figure c). After imaging, the wounding region in the corneal tissues was collected with a 6 mm biopsy punch for RNA analysis. Figure d gives the RNA level knockdown percentage of SMA in the corneas calculated with respect to the untreated eye. All expressions were normalized to 18S rRNA.

CHAPTER 5
CONCLUSIONS AND FUTURE DIRECTIONS

A Multi-Target Anti-Fibrotic Approach Validated

Though multiple targets in TGFB system have been targeted in combination, there has not been a multi-gene siRNA approach in the field of corneal scarring. In the first experiment, starting with *in vitro* results and by using computational analysis, I generated two siRNA triple combinations - an “Effective” with optimal synergy and an “Ineffective” with poor synergy among its individual sequences. The effective triple siRNA outperformed its corresponding individual siRNA sequences and the ineffective triple combination by significantly knocking down the expression of pro-fibrotic genes without affecting cell toxicity. The promising results from this experiment justified our efforts to test the effect of this triple siRNA combination in animals.

Established the Use of *Ex Vivo* Corneal Organ Culture as a Scarring Model

Animal models have been almost been exclusively used for corneal scarring studies post excimer laser surgery. Hence, development of an organ culture model for corneal scarring is an important middle ground between cell culture and animal experiments especially since many of the main features in the formation of corneal scarring in animals were reproduced in the organ culture. In this study, I have characterized scar formation in a corneal organ culture model following a laser ablation and compared it to that of scar formation in animals. I also evaluated the therapeutic potential of the model by delivering the triple siRNA combination to different layers of the cornea using a nanoparticle delivery system and observed its effect on scar formation. In this future, this model can be used as an important screen for testing and

optimizing new anti-scarring drugs in addition to it being an important tool to study and understand different molecular pathways of the corneal wound healing process.

A New Standard for Quantifying Corneal Scar Formation

A major hurdle in evaluating the efficacy of anti-fibrotic drugs in the cornea is the lack of a standard imaging technology to quantify the reduction in scarring. The current clinical method of haze grading with a slit lamp, according to Hanna et al's (Hanna et al. 1992) scale is qualitative and very subjective. Some of the other techniques used to visualize and quantify corneal scarring are confocal microscopy (Møller-Pedersen et al. 1998; Tervo and Moilanen 2003), ultrasound biomicroscopy (UBM) (Foster et al. 2000) and optical coherence tomography (OCT, Humphrey-Zeiss Medical Systems) (Wirbelauer et al. 2002).

Both UBM and OCT use a similar imaging principle, which uses back-scattered signals reflected from different layers of tissues and then reconstructs structural images (S.-Y. Zhou et al. 2013). In general, the resolution of these techniques is not very sensitive to quantify mild haze. It has been reported that haze scores of less than 2 and mild subepithelial haze formation cannot be visualized by Ultrasound biomicroscopy (Nagy et al. 1996) (Foster et al. 2000). Confocal microscopy allows *in vivo* presentation of corneal structure changes on the cellular level (Cavanagh et al. 1993). In the field of cornea scarring, it has been predominantly used to visualize light scattering in the cornea and not for quantifying the reduction of haze because of its fair resolution (white light source) and local perspective of the wounding region. These techniques also require expensive instruments and skilled technicians to image the cornea. The digital camera imaging system to measure corneal haze over the entire ablated region of the cornea described in this study is convenient, accurate, affordable, and can be

performed by essentially any vision researcher. However, there are still aspects of this method that needs refinement and standardization. The dual flash heads creates an unwanted reflection on the cornea due to which we are unable to measure the entire wounding region. Future work will focus on quantifying different intensities of scar formation and comparing it with results from haze grading and macrophotography.

Clinical Impact in the Future

Although, the triple siRNA treatment in this study did not completely eliminate scarring, it did generate a strong positive trend in the reduction of scarring. It is important to understand and resolve the problems associated with the generation of intense scarring, drug delivery optimization and scar imaging before investing in a major *in vivo* experiment with many animals. Once these parameters are optimized, the effective triple siRNA combination could lead to significant reduction of scarring in the cornea and perhaps also in other tissues.

LIST OF REFERENCES

Abreu, José G, Nan I Ketpura, Bruno Reversade, and E M De Robertis. 2002. "Connective-Tissue Growth Factor (CTGF) Modulates Cell Signalling by BMP and TGF-Beta.." *Nature cell biology* 4(8): 599–604.

Angaji, S A, S S Hedayati, R H Poor, S Madani, and S S Poor. 2010. "Application of RNA Interference in Treating Human Diseases." *Journal of genetics*.

Aras, C, A Ozdamar, R Aktunç, and C Erçikan. 1998. "The Effects of Topical Steroids on Refractive Outcome and Corneal Haze, Thickness, and Curvature After Photorefractive Keratectomy with a 6.0-Mm Ablation Diameter.." *Ophthalmic surgery and lasers* 29(8): 621–27.

Azar, D T, and S Jain. 2001. "Topical MMC for Subepithelial Fibrosis After Refractive Corneal Surgery.." *Ophthalmology* 108(2): 239–40.

Bagasra, Omar, and Kiley R Prilliman. 2004. "RNA Interference: the Molecular Immune System.." *Journal of molecular histology* 35(6): 545–53.

Bartlett, Derek W, and Mark E Davis. 2006. "Insights Into the Kinetics of siRNA-Mediated Gene Silencing From Live-Cell and Live-Animal Bioluminescent Imaging.." *Nucleic acids research* 34(1): 322–33.

Bernstein, E, A A Caudy, S M Hammond, and G J Hannon. 2001. "Role for a Bidentate Ribonuclease in the Initiation Step of RNA Interference.." *Nature* 409(6818): 363–66.

Bjorge, Jeffrey D, Andy S Pang, Melanie Funnell, Ke Yun Chen, Roman Diaz, Anthony M Magliocco, and Donald J Fujita. 2011. "Simultaneous siRNA Targeting of Src and Downstream Signaling Molecules Inhibit Tumor Formation and Metastasis of a Human Model Breast Cancer Cell Line." *PLOS ONE* 6(4): e19309.

Blalock, Timothy D, Matthew R Duncan, Juan C Varela, Michael H Goldstein, Sonal S Tuli, Gary R Grotendorst, and Gregory S Schultz. 2003. "Connective Tissue Growth Factor Expression and Action in Human Corneal Fibroblast Cultures and Rat Corneas After Photorefractive Keratectomy.." *Investigative ophthalmology & visual science* 44(5): 1879–87.

Blalock, Timothy D, Rong Yuan, Alfred S Lewin, and Gregory S Schultz. 2004. "Hammerhead Ribozyme Targeting Connective Tissue Growth Factor mRNA Blocks Transforming Growth Factor-Beta Mediated Cell Proliferation." *Experimental eye research* 78(6): 1127–36.

Border, W A, N A Noble, T Yamamoto, J R Harper, Y u Yamaguchi, M D Pierschbacher, and E Ruoslahti. 1992. "Natural Inhibitor of Transforming Growth Factor-Beta Protects Against Scarring in Experimental Kidney Disease.." *Nature* 360(6402): 361–64.

Borisy, Alexis A, Peter J Elliott, Nicole W Hurst, Margaret S Lee, Joseph Lehar, E Roydon Price, George Serbedzija, Grant R Zimmermann, Michael A Foley, Brent R Stockwell, and Curtis T Keith. 2003. “Systematic Discovery of Multicomponent Therapeutics..” *Proceedings of the National Academy of Sciences of the United States of America* 100(13): 7977–82.

Bull, N. 2008. “Time for Revision of Seafarers Vision Testing? Article for Discussion.” *Int Marit Health*.

Bullard, K M, D L Cass, M J Banda, and N S Adzick. 1997. “Transforming Growth Factor Beta-1 Decreases Interstitial Collagenase in Healing Human Fetal Skin..” *Journal of pediatric surgery* 32(7): 1023–27.

Campochiaro, P A. 2006. “Potential Applications for RNAi to Probe Pathogenesis and Develop New Treatments for Ocular Disorders..” *Gene therapy* 13(6): 559–62.

Carrington, Louise M, Julie Albon, Ian Anderson, Christina Kamma, and Mike Boulton. 2006. “Differential Regulation of Key Stages in Early Corneal Wound Healing by TGF-Beta Isoforms and Their Inhibitors..” *Investigative ophthalmology & visual science* 47(5): 1886–94.

Castanotto, D, K Sakurai, R Lingeman, and H Li. 2007. “Combinatorial Delivery of Small Interfering RNAs Reduces RNAi Efficacy by Selective Incorporation Into RISC.” *Nucleic acids ….*

Castro-Combs, Juan, Guillermo Noguera, Marisol Cano, Margaret Yew, Peter L Gehlbach, Jonathan Palmer, and Ashley Behrens. 2008. “Corneal Wound Healing Is Modulated by Topical Application of Amniotic Fluid in an Ex Vivo Organ Culture Model.” *Experimental eye research* 87(1): 56–63.

Cavanagh, H D, W M Petroll, H Alizadeh, Y G He, J P McCulley, and J V Jester. 1993. “Clinical and Diagnostic Use of in Vivo Confocal Microscopy in Patients with Corneal Disease..” *Ophthalmology* 100(10): 1444–54.

Chen, C, B Michelini-Norris, S Stevens, J Rowsey, X Ren, M Goldstein, and G Schultz. 2000. “Measurement of mRNAs for TGFss and Extracellular Matrix Proteins in Corneas of Rats After PRK..” *Investigative ophthalmology & visual science* 41(13): 4108–16.

Chen, Q R, L Zhang, S A Stass, and A J Mixson. 2001. “Branched Co-Polymers of Histidine and Lysine Are Efficient Carriers of Plasmids..” *Nucleic acids research* 29(6): 1334–40.

Chen, Tsan-Chi, Chien-Hsueh Lai, Jie-Ling Chang, and Shu-Wen Chang. 2012. “Mitomycin C Retardation of Corneal Fibroblast Migration via Sustained Dephosphorylation of Paxillin at Tyrosine 118..” *Investigative ophthalmology & visual science* 53(3): 1539–47.

Chou, T C, and M Hayball. 1996. “Chou: CalcuSyn for Windows: Multiple-Drug Dose-Effect... - Google Scholar.” *Biosoft*.

Chou, T C, and N Martin. 2005. “CompuSyn for Drug Combinations.” *A Computer Software for Quantitation of Synergism and Antagonism, and the Determination of IC50, ED50 and LD50 Values.[PC software and user's guide.](ComboSyn, Paramus, NJ)*.

Chou, T C, and P Talalay. 1983. “Analysis of Combined Drug Effects: a New Look at a Very Old Problem.” *Trends in Pharmacological Sciences*.

Chou, Ting-Chao. 2006. “Theoretical Basis, Experimental Design, and Computerized Simulation of Synergism and Antagonism in Drug Combination Studies..” *Pharmacological reviews* 58(3): 621–81. http://eutils.ncbi.nlm.nih.gov/entrez/eutils/elink.fcgi?dbfrom=pubmed&id=16968952&retmode=ref&cmd=prlinks.

Chuck, Roy S, Ashley Behrens, Sarah R Wellik, Lih-Huei Liaw, Paula M Sweet, Kathryn E Osann, Peter J McDonnell, and Michael W Berns. 2001. “Simple Organ Cornea Culture Model for Re-Epithelialization After in Vitro Excimer Laser Ablation.” *Lasers in surgery and medicine* 29(3): 288–92.

Chuck, Roy S, Ashley Behrens, Sarah Wellik, Leacky L H Liaw, Arlene M T Dolorico, Paula Sweet, Lawrence C Chao, Kathryn E Osann, Peter J McDonnell, and Michael W Berns. 2001. “Re-Epithelialization in Cornea Organ Culture After Chemical Burns and Excimer Laser Treatment.” *Archives of Ophthalmology* 119(11): 1637–42.

Collin, H B, J A Anderson, N R Richard, and P S Binder. 1995. “In Vitro Model for Corneal Wound Healing; Organ-Cultured Human Corneas..” *Current eye research* 14(5): 331–39.

Cordeiro, M F, A Mead, R R Ali, R A Alexander, S Murray, C Chen, C York-Defalco, N M Dean, G S Schultz, and P T Khaw. 2003. “Novel Antisense Oligonucleotides Targeting TGF-Beta Inhibit in Vivo Scarring and Improve Surgical Outcome..” *Gene therapy* 10(1): 59–71.

Desmoulière, A, A Geinoz, F Gabbiani, and G Gabbiani. 1993. “Transforming Growth Factor-Beta 1 Induces Alpha-Smooth Muscle Actin Expression in Granulation Tissue Myofibroblasts and in Quiescent and Growing Cultured Fibroblasts..” *The Journal of cell biology* 122(1): 103–11.

Dirk Grimm, Lora Wang Joyce S Lee Nina Schürmann Shuo Gu Kathleen Börner Theresa A Storm Mark A Kay. 2010. “Argonaute Proteins Are Key Determinants of RNAi Efficacy, Toxicity, and Persistence in the Adult Mouse Liver.” *The Journal of clinical investigation* 120(9): 3106.

Dykxhoorn, Derek M, and Judy Lieberman. 2006. “Running Interference: Prospects and Obstacles to Using Small Interfering RNAs as Small Molecule Drugs..” *Annual review of biomedical engineering* 8: 377–402.

Edwards, Aurélie, and Mark R Prausnitz. 2001. “Predicted Permeability of the Cornea to Topical Drugs.” *Pharmaceutical Research* 18(11): 1497–1508.

Eraslan, Muhsin, and Ebru Toker. 2009. “Mechanisms of Corneal Wound Healing and Its Modulation Following Refractive Surgery.” *Marmara Med J* 22: 169–78.

Fan-Paul, Nancy I, Joan Li, Julia Sullivan Miller, and George J Florakis. 2002. “Night Vision Disturbances After Corneal Refractive Surgery..” *Survey of ophthalmology* 47(6): 533–46.

Fire, A. 1999. “RNA-Triggered Gene Silencing.” *algorithms*.

Foreman, D M, S Pancholi, J Jarvis-Evans, D Mcleod, and M E Boulton. 1996. “A Simple Organ Culture Model for Assessing the Effects of Growth Factors on Corneal Re-Epithelialization.” *Experimental eye research* 62(5): 555–64.

Foster, F Stuart, Charles J Pavlin, Kasia A Harasiewicz, Donald A Christopher, and Daniel H Turnbull. 2000. “Advances in Ultrasound Biomicroscopy.” *Ultrasound in Medicine & Biology* 26(1): 1–27.

Fyffe, James G. 2005. “Corneal Injury to Ex-Vivo Eyes Exposed to a 3.8 Micron Laser.”

Gambato, Catia, Alessandra Ghirlando, Erika Moretto, Fabiola Busato, and Edoardo Midena. 2005. “Mitomycin C Modulation of Corneal Wound Healing After Photorefractive Keratectomy in Highly Myopic Eyes..” *Ophthalmology* 112(2): 208–18–discussion219.

Grotendorst, G R. 1997. “Connective Tissue Growth Factor: a Mediator of TGF-Beta Action on Fibroblasts..” *Cytokine & growth factor reviews* 8(3): 171–79.

Hammond, S M, S Boettcher, A A Caudy, R Kobayashi, and G J Hannon. 2001. “Argonaute2, a Link Between Genetic and Biochemical Analyses of RNAi..” *Science (New York, N.Y.)* 293(5532): 1146–50.

Hanna, K D, Y M Pouliquen, G O Waring, M Savoldelli, F Fantes, and K P Thompson. 1992. “Corneal Wound Healing in Monkeys After Repeated Excimer Laser Photorefractive Keratectomy..” *Archives of Ophthalmology* 110(9): 1286–91.

Hao, Jinsong, S Kevin Li, Chia-Yang Liu, and Winston W Y Kao. 2009. “Electrically Assisted Delivery of Macromolecules Into the Corneal Epithelium..” *Experimental eye research* 89(6): 934–41.

Hao, Jinsong, S Kevin Li, Winston W Y Kao, and Chia-Yang Liu. 2010. “Gene Delivery to Cornea..” *Brain research bulletin* 81(2-3): 256–61.

Hatanaka, Hiroki, Noriko Koizumi, Naoki Okumura, Eunduck P Kay, Eri Mizuhara, Junji Hamuro, and Shigeru Kinoshita. 2012. “Epithelial-Mesenchymal Transition-Like Phenotypic Changes of Retinal Pigment Epithelium Induced by TGF-B Are Prevented by PPAR-Γ Agonists..” *Investigative ophthalmology & visual science* 53(11): 6955–63.

Hämäläinen, K M, K Kananen, S Auriola, K Kontturi, and A Urtti. 1997. “Characterization of Paracellular and Aqueous Penetration Routes in Cornea, Conjunctiva, and Sclera..” *Investigative ophthalmology & visual science* 38(3): 627–34.

Heier, J S, R W Enzenauer, S F Wintermeyer, M Delaney, and F P LaPiana. 1993. “Ocular Injuries and Diseases at a Combat Support Hospital in Support of Operations Desert Shield and Desert Storm..” *Archives of Ophthalmology* 111(6): 795–98.

Ivarsen, A, T Laurberg, and T Møller-Pedersen. 2003. “Characterisation of Corneal Fibrotic Wound Repair at the LASIK Flap Margin..” *The British journal of ophthalmology* 87(10): 1272–78.

Jackson, A L, J Burchard, J Schelter, B N Chau, M Cleary, L Lim, and P S Linsley. 2006. “Widespread siRNA ‘Off-Target’ Transcript Silencing Mediated by Seed Region Sequence Complementarity.” *Rna* 12(7): 1179–87.

Janin-Manificat, Hélène, Marie-Rose Rovère, Stéphane D Galiacy, François Malecaze, David J S Hulmes, Catherine Moali, and Odile Damour. 2012. “Development of Ex Vivo Organ Culture Models to Mimic Human Corneal Scarring..” *Molecular vision* 18: 2896–2908.

Jester, J V, P A Barry-Lane, H D Cavanagh, and W M Petroll. 1996. “Induction of Alpha-Smooth Muscle Actin Expression and Myofibroblast Transformation in Cultured Corneal Keratocytes..” *Cornea* 15(5): 505–16.

Jester, J V, W M Petroll, and H D Cavanagh. 1999. “Corneal Stromal Wound Healing in Refractive Surgery: the Role of Myofibroblasts..” *Progress in retinal and eye research* 18(3): 311–56.

Jester, James V, Chyong Jy Nien, Vasilis Vasiliou, and Donald J Brown. 2012. “Quiescent Keratocytes Fail to Repair MMC Induced DNA Damage Leading to the Long-Term Inhibition of Myofibroblast Differentiation and Wound Healing..” *Molecular vision* 18: 1828–39.

Jester, James V, Donald Brown, Aglaia Pappa, and Vasilis Vasiliou. 2012. “Myofibroblast Differentiation Modulates Keratocyte Crystallin Protein Expression, Concentration, and Cellular Light Scattering..” *Investigative ophthalmology & visual science* 53(2): 770–78.

Kabosova, Andrea, Andrei A Kramerov, Annette M Aoki, Gillian Murphy, James D Zieske, and Alexander V Ljubimov. 2003. “Human Diabetic Corneas Preserve Wound Healing, Basement Membrane, Integrin and MMP-10 Differences From Normal Corneas in Organ Culture..” *Experimental eye research* 77(2): 211–17.

Karamichos, Dimitris, Xiaoqing Q Guo, Audrey E K Hutcheon, and James D Zieske. 2010. “Human Corneal Fibrosis: an in Vitro Model..” *Investigative ophthalmology & visual science* 51(3): 1382–88.

Keith, Curtis T, Alexis A Borisy, and Brent R Stockwell. 2005. “Multicomponent Therapeutics for Networked Systems..” *Nature reviews. Drug discovery* 4(1): 71–78.

Kim, Dong-Ho, Mark A Behlke, Scott D Rose, Mi-Sook Chang, Sangdun Choi, and John J Rossi. 2005. “Synthetic dsRNA Dicer Substrates Enhance RNAi Potency and Efficacy..” *Nature biotechnology* 23(2): 222–26.

Kircheis, R, L Wightman, A Schreiber, B Robitza, V Rössler, M Kursa, and E Wagner. 2001. “Polyethylenimine/DNA Complexes Shielded by Transferrin Target Gene Expression to Tumors After Systemic Application..” *Gene therapy* 8(1): 28–40.

la Fuente, de, M, B Seijo, and M J Alonso. 2008. “Bioadhesive Hyaluronan–Chitosan Nanoparticles Can Transport Genes Across the Ocular Mucosa and Transfect Ocular Tissue.” *Gene therapy* 15(9): 668–76.

Lee, V H, and J R Robinson. 1986. “Topical Ocular Drug Delivery: Recent Developments and Future Challenges..” *Journal of ocular pharmacology* 2(1): 67–108.

Leng, Q, M C Woodle, P Y Lu, and A J Mixson. 2009. “Advances in Systemic siRNA Delivery.” *Drugs of the future*.

Leuschner, Philipp J F, Stefan L Ameres, Stephanie Kueng, and Javier Martinez. 2006. “Cleavage of the siRNA Passenger Strand During RISC Assembly in Human Cells..” *EMBO reports* 7(3): 314–20.

Li, Guangming, Qing Xie, Yi Shi, Dingguo Li, Mingjun Zhang, Shan Jiang, Huijuan Zhou, Hanming Lu, and Youxin Jin. 2006. “Inhibition of Connective Tissue Growth Factor by siRNA Prevents Liver Fibrosis in Rats.” *Wound Repair and Regeneration* 8(7): 889–900.

Liang, L, H Sheha, J Li, and S C G Tseng. 2009. “Limbal Stem Cell Transplantation: New Progresses and Challenges..” *Eye (London, England)* 23(10): 1946–53.

Maguire, L J. 1994. “Keratorefractive Surgery, Success, and the Public Health..” *American journal of ophthalmology* 117(3): 394–98.

Massague, Joan. 1990. “The Transforming Growth Factor-Beta Family.” *Annual review of cell biology* 6(1): 597–641.

Matsumoto, Yoh, Naoko Niimi, and Kuniko Kohyama. 2012. “Characterization of Fibrosis-Promoting Factors and siRNA-Mediated Therapies in C-Protein-Induced Experimental Autoimmune Myocarditis..” *Cellular immunology* 279(1): 70–77.

McCally, R L, R A Farrell, and C B Bargeron. 1992. “Cornea Epithelial Damage Thresholds in Rabbits Exposed to Tm:YAG Laser Radiation at 2.02 Microns..” *Lasers in surgery and medicine* 12(6): 598–603.

McCally, Russell L, and C B Bargeron. 2000. “Corneal Damage From Infrared Radiation.”

Mead, A L. 2003. “Evaluation of Anti-TGF- 2 Antibody as a New Postoperative Anti-Scarring Agent in Glaucoma Surgery.” *Investigative ophthalmology & visual science* 44(8): 3394–3401.

Midoux, P, and M Monsigny. 1999. “Efficient Gene Transfer by Histidylated Polylysine/pDNA Complexes.” *Bioconjugate chemistry*.

Mohan, R R, A Tandon, A Sharma, J W Cowden, and J C K Tovey. 2011. “Significant Inhibition of Corneal Scarring in Vivo with Tissue-Selective, Targeted AAV5 Decorin Gene Therapy.” *Investigative ophthalmology & visual science* 52(7): 4833–41.

Mohan, Rajiv R, Jonathan C K Tovey, Ajay Sharma, and Ashish Tandon. 2012. “Gene Therapy in the Cornea: 2005--Present..” *Progress in retinal and eye research* 31(1): 43–64.

Mohan, Rajiv R, W Michael Stapleton, Sunilima Sinha, Marcelo V Netto, and Steven E Wilson. 2008. “A Novel Method for Generating Corneal Haze in Anterior Stroma of the Mouse Eye with the Excimer Laser.” *Experimental eye research* 86(2): 235–40.

Myrna, Kathern E, Rima Mendonsa, Paul Russell, Simon A Pot, Sara J Liliensiek, James V Jester, Paul F Nealey, Donald Brown, and Christopher J Murphy. 2012. “Substratum Topography Modulates Corneal Fibroblast to Myofibroblast Transformation..” *Investigative ophthalmology & visual science* 53(2): 811–16.

Møller-Pedersen, T, and H J Møller. 1996. “Viability of Human Corneal Keratocytes During Organ Culture..” *Acta ophthalmologica Scandinavica* 74(5): 449–55.

Møller-Pedersen, T, H F Li, W M Petroll, H D Cavanagh, and J V Jester. 1998. “Confocal Microscopic Characterization of Wound Repair After Photorefractive Keratectomy..” *Investigative ophthalmology & visual science* 39(3): 487–501.

Møller-Pedersen, Torben. 2004. “Keratocyte Reflectivity and Corneal Haze..” *Experimental eye research* 78(3): 553–60.

Nagy, Z Z, J Németh, I Sûveges, and B Csákány. 1996. “Examination of Subepithelial Scar Formation After Photorefractive Keratectomy with the Ultrasound Biomicroscope.” *Klinische Monatsblätter für Augenheilkunde* 209(5): 283–85.

Nakamura, K, D Kurosaka, H Bissen-Miyajima, and K Tsubota. 2001. “Intact Corneal Epithelium Is Essential for the Prevention of Stromal Haze After Laser Assisted in Situ Keratomileusis..” *The British journal of ophthalmology* 85(2): 209–13.

Netto, Marcelo V, Rajiv R Mohan, Sunilima Sinha, Ajay Sharma, William Dupps, and Steven E Wilson. 2006. “Stromal Haze, Myofibroblasts, and Surface Irregularity After PRK.” *Experimental eye research* 82(5): 788–97.

Nien, Chyong Jy, Kevin J Flynn, Melissa Chang, Donald Brown, and James V Jester. 2011. “Reducing Peak Corneal Haze After Photorefractive Keratectomy in Rabbits: Prednisolone Acetate 1.00% Versus Cyclosporine a 0.05%..” *Journal of cataract and refractive surgery* 37(5): 937–44.

Peer, D, E J Park, Y Morishita, C V Carman, and M Shimaoka. 2008. “Systemic Leukocyte-Directed siRNA Delivery Revealing Cyclin D1 as an Anti-Inflammatory Target.” *Science (New York, N.Y.)*.

Pellegrini, G, P Rama, F Mavilio, and M De Luca. 2009. “Epithelial Stem Cells in Corneal Regeneration and Epidermal Gene Therapy..” *The Journal of pathology* 217(2): 217–28.

Penn, Jack W, Adriaan O Grobbelaar, and Kerstin J Rolfe. 2012. “The Role of the TGF-B Family in Wound Healing, Burns and Scarring: a Review..” *International journal of burns and trauma* 2(1): 18–28.

Perales, J C, T Ferkol, H Beegen, O D Ratnoff, and R W Hanson. 1994. “Gene Transfer in Vivo: Sustained Expression and Regulation of Genes Introduced Into the Liver by Receptor-Targeted Uptake..” *Proceedings of the National Academy of Sciences of the United States of America* 91(9): 4086–90.

Perkett, E A. 1995. “Role of Growth Factors in Lung Repair and Diseases..” *Current opinion in pediatrics* 7(3): 242–49.

Plank, C, K Mechtler, F C Szoka, and E Wagner. 1996. “Activation of the Complement System by Synthetic DNA Complexes: a Potential Barrier for Intravenous Gene Delivery..” *Human gene therapy* 7(12): 1437–46.

Polsky, B, D Armstrong, and T C Chou. 1991. “Synergistic Inhibition of Human Immunodeficiency Virus Type 1 Replication in Vitro by Two-Drug and Three-Drug Combinations of 3‘-Azido-3’-Deoxythymidine, ….” *Antimicrobial agents ….*

Pot, Simon A, Sara J Liliensiek, Kathern E Myrna, Ellison Bentley, James V Jester, Paul F Nealey, and Christopher J Murphy. 2010. “Nanoscale Topography-Induced Modulation of Fundamental Cell Behaviors of Rabbit Corneal Keratocytes, Fibroblasts, and Myofibroblasts..” *Investigative ophthalmology & visual science* 51(3): 1373–81.

Raviv, T, P A Majmudar, R F Dennis, and R J Epstein. 2000. “Mytomycin-C for Post-PRK Corneal Haze..” *Journal of cataract and refractive surgery* 26(8): 1105–6.

Resnier, Pauline, Tristan Montier, Véronique Mathieu, Jean-Pierre Benoit, and Catherine Passirani. 2013. “A Review of the Current Status of siRNA Nanomedicines in the Treatment of Cancer.” *Experimental eye research* 34(27): 6429–43.

Richard, N R, J A Anderson, J L Weiss, and P S Binder. 1991. “Air/Liquid Corneal Organ Culture: a Light Microscopic Study..” *Current eye research* 10(8): 739–49.

Richard, Normand R, Janet A Anderson, Jack L Weiss, and Perry S Binder. “Air/Liquid Corneal Organ Culture: a Light Microscopic Study.” *informahealthcare.com*.

Robinson, Paulette M, Timothy D Blalock, Rong Yuan, Alfred S Lewin, and Gregory S Schultz. 2012. “Hammerhead Ribozyme-Mediated Knockdown of mRNA for Fibrotic Growth Factors: Transforming Growth Factor-Beta 1 and Connective Tissue Growth Factor..” *Methods in molecular biology (Clifton, N.J.)* 820: 117–32.

Rodriguez-Lanetty, Mauricio. 2007. *Trizol/RNeasy Hybrid RNA Extraction Protocol*. http://people.oregonstate.edu/~weisv/Protocols/Molecular/Trizol_RNeasy%20hybrid.pdf.

Russ, V, H Elfberg, C Thoma, J Kloeckner, M Ogris, and E Wagner. 2008. “Novel Degradable Oligoethylenimine Acrylate Ester-Based Pseudodendrimers for in Vitro and in Vivo Gene Transfer..” *Gene therapy* 15(1): 18–29.

Sakimoto, Tohru, Mark I Rosenblatt, and Dimitri T Azar. 2006. “Laser Eye Surgery for Refractive Errors..” *Lancet* 367(9520): 1432–47.

Sarchahi, Ali Asghar, Abdolhamid Meimandi Parizi, Masoomeh Eghtedari, and Salar Keshavarz. 2011. “Effect of Different Treatment Regimen with Dexamethasone and Acetylcysteine on Corneal Wound Healing in Rabbits..” *Iranian journal of medical sciences* 36(3): 188–95.

Sasaki, Hitoshi, Kenzo Yamamura, Koyo Nishida, Junzo Nakamura, and Masataka Ichikawa. 1996. “Delivery of Drugs to the Eye by Topical Application.” *Progress in retinal and eye research* 15(2): 583–620.

Scherer, Lisa J, and John J Rossi. 2003. “Approaches for the Sequence-Specific Knockdown of mRNA..” *Nature biotechnology* 21(12): 1457–65.

Shah, S S, M S Kapadia, D M Meisler, and S E Wilson. 1998. “Photorefractive Keratectomy Using the Summit SVS Apex Laser with or Without Astigmatic Keratotomy.” *Cornea*.

Shim, Min Suk, and Young Jik Kwon. 2010. “Efficient and Targeted Delivery of siRNA in Vivo..” *The FEBS journal* 277(23): 4814–27.

Siganos, D S, V J Katsanevaki, and I G Pallikaris. 1999. “Correlation of Subepithelial Haze and Refractive Regression 1 Month After Photorefractive Keratectomy for Myopia..” *Journal of refractive surgery (Thorofare, N.J. : 1995)* 15(3): 338–42.

Sihota, R, T Sharma, and H C Agarwal. 1998. “Intraoperative Mitomycin C and the Corneal Endothelium..” *Acta ophthalmologica Scandinavica* 76(1): 80–82.

sriram, Sriniwas, Daniel J Gibson, Paulette Robinson, Sonal Tuli, Alfred Lewin, and Gregory Schultz. 2013. “Reduction of Corneal Scarring in Rabbits by Targeting the TGFB1 Pathway with a Triple siRNA Combination (in Press).” Vol.4 (No.10A3).

sriram, Sriniwas, Gregory S Schultz, Alfred Lewin, Paulette M Robinson, Daniel J Gibson, and Sonal S Tuli. 2012. “Combination siRNA Treatment to Knockdown CTGF, TGF-Ss1, TGF-ssR2 and Collagen in Rabbit Corneal Fibroblasts.” *ARVO Meeting Abstracts* 53(6): 2209.

sriram, Sriniwas, Paulette Robinson, Alfred Lewin, and Gregory Schultz. 2013. “Nanoparticle Vectored siRNAs Reduce Profibrotic Gene Expression in Wounded Rabbit Corneas.” *ARVO Meeting Abstracts* 54(6): 3878.

Stevenson, Mario. 2004. “Therapeutic Potential of RNA Interference..” *The New England journal of medicine* 351(17): 1772–77.

Stevenson, Mark, Victor Ramos-Perez, Surjeet Singh, Mahmoud Soliman, Jon A Preece, Simon S Briggs, Martin L Read, and Leonard W Seymour. 2008. “Delivery of siRNA Mediated by Histidine-Containing Reducible Polycations..” *Journal of controlled release : official journal of the Controlled Release Society* 130(1): 46–56.

Straetemans, Roel, Timothy O'Brien, Luc Wouters, Jacky Van Dun, Michel Janicot, Luc Bijnens, Tomasz Burzykowski, and Marc Aerts. 2005. “Design and Analysis of Drug Combination Experiments.” *Biometrical Journal* 47(3): 299–308.

Sugioka, Koji, Koji Yoshida, Aya Kodama, Hiroshi Mishima, Kosuke Abe, and Yoshikazu Shimomura. 2010. “Connective Tissue Growth Factor Cooperates with Fibronectin in Enhancing Attachment and Migration of Corneal Epithelial Cells.” *The Tohoku Journal of Experimental Medicine* 222(1): 45–50.

Takahashi, T, B Eitzman, N L Bossert, D Walmer, K Sparrow, K C Flanders, J McLachlan, and K G Nelson. 1994. “Transforming Growth Factors Beta 1, Beta 2, and Beta 3 Messenger RNA and Protein Expression in Mouse Uterus and Vagina During Estrogen-Induced Growth: a Comparison to Other Estrogen-Regulated Genes..” *Cell growth & differentiation : the molecular biology journal of the American Association for Cancer Research* 5(9): 919–35.

Tandon, A, J C K Tovey, A Sharma, R Gupta, and R R Mohan. 2010. “Role of Transforming Growth Factor Beta in Corneal Function, Biology and Pathology..” *Current molecular medicine* 10(6): 565–78.

Tanelian, D L, and K Bisla. 1992. “A New in Vitro Corneal Preparation to Study Epithelial Wound Healing..” *Investigative ophthalmology & visual science* 33(11): 3024–28.

Tani, Emiko, Chikako Katakami, and Akira Negi. 2002. “[Effects of Various Eye Drops on Corneal Wound Healing After Superficial Keratectomy in Rabbits]..” *Nippon Ganka Gakkai zasshi* 106(3): 135–42.

Tarwadi, Jalal A Jazayeri, Richard J Prankerd, and Colin W Pouton. 2008. “Preparation and in Vitro Evaluation of Novel Lipopeptide Transfection Agents for Efficient Gene Delivery..” *Bioconjugate chemistry* 19(4): 940–50.

Tervo, Timo, and Jukka Moilanen. 2003. “In Vivo Confocal Microscopy for Evaluation of Wound Healing Following Corneal Refractive Surgery..” *Progress in retinal and eye research* 22(3): 339–58.

Tiemann, Katrin, and John J Rossi. 2009. “RNAi-Based Therapeutics-Current Status, Challenges and Prospects..” *EMBO molecular medicine* 1(3): 142–51.

Tong, Yaw-Chong, Shwu-Fen Chang, Chia-Yang Liu, Winston W Y Kao, Chong Heng Huang, and Jiahorng Liaw. 2007. “Eye Drop Delivery of Nano-Polymeric Micelle Formulated Genes with Cornea-Specific Promoters.” *The Journal of Gene Medicine* 9(11): 956–66.

Toropainen, E. 2007. “Corneal Epithelial Cell Culture Model for Pharmaceutical Studies.”

Vogelmann, R, D Ruf, M Wagner, G Adler, and A Menke. 2001. “Effects of Fibrogenic Mediators on the Development of Pancreatic Fibrosis in a TGF-Beta1 Transgenic Mouse Model..” *American journal of physiology. Gastrointestinal and liver physiology* 280(1): G164–72.

Weichel, Eric D, Marcus H Colyer, Spencer E Ludlow, Kraig S Bower, and Andrew S Eiseman. 2008. “Combat Ocular Trauma Visual Outcomes During Operations Iraqi and Enduring Freedom..” *Ophthalmology* 115(12): 2235–45.

Weiss, B, G Davidkova, and L W Zhou. 1999. “Antisense RNA Gene Therapy for Studying and Modulating Biological Processes..” *Cellular and molecular life sciences : CMLS* 55(3): 334–58.

Westergren-Thorsson, G, J Hernnäs, B Särnstrand, A Oldberg, D Heinegård, and A Malmström. 1993. “Altered Expression of Small Proteoglycans, Collagen, and Transforming Growth Factor-Beta 1 in Developing Bleomycin-Induced Pulmonary Fibrosis in Rats..” *The Journal of clinical investigation* 92(2): 632–37.

Wickham, T J, E J Filardo, D A Cheresh, and G R Nemerow. 1994. “Integrin Alpha v Beta 5 Selectively Promotes Adenovirus Mediated Cell Membrane Permeabilization..” *The Journal of cell biology* 127(1): 257–64.

Wira, C R. 2002. “Antigen Presentation by Vaginal Cells: Role of TGF as a Mediator of Estradiol Inhibition of Antigen Presentation.” *Endocrinology* 143(8): 2872–79.

Wirbelauer, Christopher, Jörg Winkler, Gerd O Bastian, Heike Häberle, and Duy Thoai Pham. 2002. “Histopathological Correlation of Corneal Diseases with Optical Coherence Tomography..” *Graefe's archive for clinical and experimental ophthalmology = Albrecht von Graefes Archiv für klinische und experimentelle Ophthalmologie* 240(9): 727–34.

Woost, P G, M M Jumblatt, R A Eiferman, and G S Schultz. 1992. “Growth Factors and Corneal Endothelial Cells: I. Stimulation of Bovine Corneal Endothelial Cell DNA Synthesis by Defined Growth Factors..” *Cornea* 11(1): 1–10.

Zee, Von, Cynthia L, Kelly A Langert, and Evan B Stubbs. 2012. “Transforming Growth Factor-B2 Induces Synthesis and Secretion of Endothelin-1 in Human Trabecular Meshwork Cells..” *Investigative ophthalmology & visual science* 53(9): 5279–86.

Zhang, J, C Gu, N A Noble, W A Border, and Y Huang. 2011. “Combining Angiotensin II Blockade and Renin Receptor Inhibition Results in Enhanced Antifibrotic Effect in Experimental Nephritis.” *AJP: Renal Physiology* 301(4): F723–32.

Zhao, Rui, Qitao Yan, Haili Huang, Jingye Lv, and Wenli Ma. 2013. “Transdermal siRNA-TGFβ1-337 Patch for Hypertrophic Scar Treatment..” *Matrix biology : journal of the International Society for Matrix Biology*.

Zhou, Shi-you, Chun-xiao Wang, Xiao-yu Cai, David Huang, and Yi-zhi Liu. 2013. “Optical Coherence Tomography and Ultrasound Biomicroscopy Imaging of Opaque Corneas..” *Cornea* 32(4): e25–e30.

Zimmermann, Tracy S, Amy C H Lee, Akin Akinc, Birgit Bramlage, David Bumcrot, Matthew N Fedoruk, Jens Harborth, James A Heyes, Lloyd B Jeffs, Matthias John, Adam D Judge, Kieu Lam, Kevin McClintock, Lubomir V Nechev, Lorne R Palmer, Timothy Racie, Ingo Röhl, Stephan Seiffert, Sumi Shanmugam, Vandana Sood, Jürgen Soutschek, Ivanka Toudjarska, Amanda J Wheat, Ed Yaworski, William Zedalis, Victor Koteliansky, Muthiah Manoharan, Hans-Peter Vornlocher, and Ian MacLachlan. 2006. “RNAi-Mediated Gene Silencing in Non-Human Primates..” *Nature* 441(7089): 111–14.

BIOGRAPHICAL SKETCH

Sriniwas Sriram matriculated to the University of Florida after completing his Bachelor of Technology from Sathyabama University, India. An internship in the Carnegie Melon University in the summer of 2010 piqued his interest in the field of RNA interference. Subsequently in the next semester, he joined the lab of Dr. Schultz and began working on a treatment to control excessive corneal scarring. He successfully defended his thesis and earned a Master of Science degree in May 2011. Currently, he is continuing to broaden his scope of knowledge in the field of biomedical sciences where he plans to apply his engineering skills to solve clinical and scientific problems.

On a personal level, Sriniwas loves football and is a passionate fan of Chelsea football club. Watching Chelsea play live still remains one of his unfulfilled dreams.